UCLA/PPG--1135

DE90 001808

THE TITAN REVERSED-FIELD PINCH FUSION REACTOR STUDY

The collection of papers presented at
International Symposium on
Fusion Nuclear Technology
Tokyo, Japan, April 10-19, 1988

UCLA-PPG-1135 **March 1988**

University of California, Los Angeles
Department of Mechanical, Aerospace, and Nuclear Engineering and
Institute for Plasma and Fusion Research
Los Angeles, CA

Los Alamos National Laboratory
Los Alamos, NM

GA Technologies Inc.
San Diego, CA

Rensselaer Polytechnic Institute
Department of Nuclear Engineering
Troy, NY

THE TITAN RESEARCH GROUP

University of California, Los Angeles

Farrokh Najmabadi, Robert W. Conn, Steven P. Grotz, Nasr M. Ghoniem

James P. Blanchard, Yuh-Yi Chu, Patrick I. H. Cooke[1], Mohammad Z. Hasan, Charles E. Kessel, Rodger C. Martin, George E. Orient, Anil K. Prinja[2], Shahram Sharafat, Erik L. Vold

GA Technologies Inc.

Kenneth R. Schultz, Clement P. C. Wong

Edward T. Cheng, R. Leuis Creedon, Otto Fischer[3], Charles G. Hoot, Steven G. Visser

Los Alamos National Laboratory

Robert A. Krakowski

John R. Bartlit[4], Charles G. Bathke, Ronald L. Miller, Richard A. Nebel, Ken A. Werley

Rensselaer Polytechnic Institute

Don Steiner

William P. Duggan, William P. Kelleher

Fusion Engineering Design Center

Ali E. Dabiri[5], George E. Gorker, Don C. Keeton, Dave C. Lousteau, Scott L. Thomson

Argonne National Laboratory

Dai-Kai Sze

Canadian Fusion Fuels Technology Project

Paul J. Gierszewski, O. Kveton

[1] Permanent address: UKAEA Culham Lab., Abingdon, Oxon OX14 3DB, U.K.

[2] Present address: University of New Mexico, Albuquerque, NM 87107.

[3] Permanent address: Swiss Federal Inst. for Reactor Research (EIR), Wurenlingen, Switzerland.

[4] TSTA Program.

[5] Present address: Science Applications International Corp., San Diego, CA.

PREFACE

The TITAN Reversed-Field Pinch (RFP) fusion reactor study is a multi-institutional research effort [1-3] to determine the technical feasibility and key developmental issues of an RFP fusion reactor, especially at high power density, and to determine the potential economics (cost of electricity), operations, safety, and environmental features of high-mass-power-density fusion systems.

The TITAN conceptual designs are DT burning, 1000 MWe power reactors based on the RFP confinement concept. The designs are compact, have a high neutron wall loading of 18 MW/m^2 and a mass power density of 700 kWe/tonne. The inherent characteristics of the RFP confinement concept make fusion reactors with such a high mass power density possible. Two different detailed designs have emerged: the TITAN-I lithium-vanadium design, incorporating the integrated-blanket-coil (IBC) concept; and the TITAN-II aqueous loop-in-pool design with ferritic steel structure. Parametric systems studies have been utilized both to optimize the point designs and to determine the parametric design window associated with each approach. This combination of parametric and point design work is referred to as a "parapoint" study.

Following is a collection of 16 papers on the results of the TITAN study which were presented at the International Symposium on Fusion Nuclear Technology (April 10-19, 1988, Tokyo, Japan). This collection describes the TITAN research effort, and specifically the TITAN-I and TITAN-II designs, summarizing the major results, the key technical issues, and the central conclusions and recommendations.

Overall, the basic conclusions are that high-mass-power-density fusion reactors appear to be technically feasible even with neutron wall loadings up to 20 MW/m^2; that single-piece maintenance of the FPC is possible and advantageous; that the economics of the reactor is enhanced by its compactness; and the safety and environmental features need not be sacrificed in high-power-density designs. The fact that two design approaches have emerged, and others may also be possible, in some sense indicates the robustness of the general findings. Therefore, magnetic fusion systems may well be feasible over a wide range of parameter space than previously considered possible and attractive.

REFERENCES

1. R. W. Conn, F. Najmabadi, N. M. Ghoniem, "The Reversed-Field Pinch as a Compact Fusion Reactor," University of California - Los Angeles, UCLA-PPG-969, May 1985.
2. F. Najmabadi, R. W. Conn, N. M. Ghoniem, S. P. Grotz, J. Blanchard, *et al.*, "The TITAN Reversed-Field Pinch Fusion Reactor Study; The Final Report," UCLA-PPG-1200, Joint Report of University of California - Los Angeles, GA Technologies, Inc., Los Alamos National Laboratory, and Rensselaer Polytechnic Institute, January 1988.
3. F. Najmabadi, N. M. Ghoniem, R. W. Conn, *et al.*, "The TITAN Reversed-Field Pinch Fusion Reactor Study; Scoping Phase Report," UCLA-PPG-1100, Joint Report of University of California - Los Angeles, GA Technologies, Inc., Los Alamos National Laboratory, and Rensselaer Polytechnic Institute, January 1987.

The TITAN Study

Papers Presented at
International Symposium on Fusion Nuclear Technology
Tokyo, Japan, April 10-19, 1988

1. Overview of the TITAN-I Fusion Power Core.
2. Overview of the TITAN-II Reversed-Field Pinch Aqueous Fusion Power Core Design.
3. The Safety Design for The TITAN Reversed-Field Pinch Reactor Study.
4. Activation and Waste Disposal of the TITAN RFP Reactors.
5. Maintenance Procedures for the TITAN-I and TITAN-II Reversed-Field Pinch Reactors.
6. Material Selection for the TITAN Reversed-Field Pinch Reactor.
7. Thermal-Hydraulic and Structural Design for the Lithium-Cooled TITAN-I Reversed-Field Pinch Reactor.
8. An Optimum Rankine Power Cycle for the Lithium-Cooled TITAN-I Reversed-Field Pinch Reactor.
9. Engineering Design of the TITAN-II Divertor.
10. Properties of Concentrated Aqueous Lithium Nitrate Solutions and Applications to Fusion Reactor Design.

OVERVIEW OF THE TITAN-I FUSION-POWER CORE

S. P. Grotz[1], N. M. Ghoniem,[1] and
The TITAN Research Group
J. R. Bartlit,[3,*] C. G. Bathke,[3] J. P. Blanchard,[1] E. T. Cheng,[2] Y. Chu,[1] R. W. Conn,[1]
P. I. H. Cooke,[1,‡] R. L. Creedon,[2] E. Dabiri[6] W. P. Duggan,[4] O. Fischer,[2,**] P. J. Gierszewski,[7]
G. E. Gorker,[6] M. Z. Hasan,[1] C. G. Hoot,[2] D. C. Keeton,[6] W. P. Kelleher,[4] C. E. Kessel,[1]
R. A. Krakowski,[3] O. Kveton,[7] D. C. Lousteau,[6] R. C. Martin,[1] R. L. Miller,[3] F. Najmabadi,[1]
R. A. Nebel,[3] G. E. Orient,[1] A. K. Prinja,[1,‡‡] K. R. Schultz,[2] S. Sharafat,[1] D. Steiner,[4]
D. K. Sze,[5] S. L. Thomson,[6] S. G. Visser,[2] E. L. Vold,[1] K. A. Werley,[3] C. P. C. Wong[2]

Department of Mechanical, Aerospace and Nuclear Engineering
and Institute for Plasma and Fusion Research
University of California, Los Angeles
Los Angeles, CA 90024-1597

ABSTRACT

The TITAN reactor is a compact (major radius of $3.9\,m$ *and plasma minor radius of* $0.6\,m$*), high neutron wall loading (*$\sim$ $18\,MW/m^2$*) fusion energy system based on the reversed-field pinch (RFP) confinement concept. The reactor thermal power is* $2918\,MWt$ *resulting in net electric output of* $960\,MWe$ *and a mass power density of* $700\,kWe/tonne$*. The TITAN-I fusion power core (FPC) is a lithium, self-cooled design with vanadium alloy (V-3Ti-1Si) structural material. The surface heat flux incident on the first wall is* $\sim$ $4.5\,MW/m^2$*. The magnetic field topology of the RFP is favorable for liquid metal cooling. In the TITAN-I design, the first wall and blanket consist of single pass, poloidal flow loops aligned with the dominant poloidal magnetic field. A unique feature of the TITAN-I design is the use of the integrated-blanket-coil (IBC) concept. With the IBC concept the poloidal flow lithium circuit is also the electrical conductor of the toroidal-field and divertor coils. Three dimensional neutronics analysis yields a tritium breeding ratio of 1.18 and a molten salt extraction technique is employed for the tritium extraction system. Almost every FPC component would qualify for Class C waste disposal. The compactness of the design allows the use of single-piece maintenance of the FPC. This maintenance procedure is expected to increase the plant availability. The entire FPC operates inside a vacuum tank, which is surrounded by an atmosphere of inert argon gas to impede the flow of air in the system in case of an accident. The top-side coolant supply and return virtually eliminate the possibility of a complete LOCA occurring in the FPC. The peak temperature during a LOFA is* $991\,^{\circ}C$*.*

---

[1] University of California, Los Angeles.
[2] GA Technologies Inc.
[3] Los Alamos National Laboratory.
[4] Rensselaer Polytechnic Institute.
[5] Argonne National Laboratory.
[6] Fusion Engineering Design Center.
[7] Canadian Fusion Fuels Technology Project.
[*] TSTA program.
[‡] Permanent address: UKAEA Culham Lab., Abingdon, Oxon OX14 3DB, U.K.
[**] Permanent address: Swiss Federal Inst. for Reactor Research (EIR), Wurenlingen, Switzerland.
[‡‡] Present address: University of New Mexico, Albuquerque, NM 87107.

1. INTRODUCTION AND BACKGROUND

The TITAN Reversed-Field Pinch (RFP) fusion reactor research effort [1,2] has been undertaken to determine the technical feasibility and key developmental issues of an RFP fusion reactor, especially at high power density, and to determine the potential economics (cost of electricity), operations, safety, and environmental features of high-mass-power-density fusion systems. Two different detailed designs, TITAN-I and TITAN-II, have emerged and parametric systems studies have been utilized both to optimize the point designs and to determine the parametric design window associated with each approach. This combination of parametric and point design work is referred to as a "parapoint" study. This paper summarizes the engineering efforts of the TITAN research team on TITAN-I, a self-cooled lithium design with vanadium structure. TITAN-II is an aqueous breeder loop-in-pool design which is summarized in Reference 3. Complete details of the TITAN-I and TITAN-II fusion power core designs can be found in the TITAN Final Report [1].

The TITAN conceptual designs are DT burning, ~1000 MWe power reactors based on the RFP confinement concept. The designs are compact, have a high neutron wall loading of 18 MW/m^2 and a mass power density of 700 kWe/tonne. The inherent characteristics of the RFP confinement concept make fusion reactors with such a high mass power density possible.

The reversed-field pinch [4], like the tokamak, belongs to a class of axisymmetric, toroidal confinement systems that utilize both toroidal (B_ϕ) and poloidal (B_θ) magnetic fields to confine the plasma. The fundamental property of the RFP is that the field configuration and toroidal field reversal are the result of the relaxation of the plasma to a near-minimum-energy state, as proposed by Taylor [5-6]; the generation of the reversed toroidal field is the natural consequence of this relaxation process. In the tokamak, stability is provided by a strong toroidal field $B_\phi \gg B_\theta$ such that the safety factor exceeds unity, that is, $q > 1$. In the RFP, on the other hand, strong magnetic shear produced by the radially varying (and

decreasing) toroidal field stabilizes the plasma with $q < 1$ and relatively modest B_ϕ. RFPs, therefore, can operate with a large ratio of plasma current to toroidal field and stability constraints on the aspect ratio are removed. High-current-density operation and ohmic heating to ignition are possible, and the choice of the aspect ratio can be made solely on the basis of engineering considerations. Also, the RFP can operate at a high total beta, thereby allowing operation at high power density. The experimentally measured poloidal beta values are in the range 10-20%. Furthermore, the low magnetic field strength on the external conductors results in a high engineering beta defined as the ratio of the plasma pressure to the magnetic field pressure at the magnets. Low current-density and less massive resistive coils are therefore possible. The TITAN plasma is ohmically heated to ignition using resistive copper ohmic heating (OH) coils. The toroidal-field and divertor coils are also normal-conducting, Integrated-Blanket-Coil (IBC) for TITAN-I and copper coils for TITAN-II. The equilibrium field is produced by a pair of super-conducting coils to reduce the required recirculating power.

Extensive parametric system studies have been performed to select and optimize the design point and then to determine the associated design window for an attractive RFP reactor. These design points were then subjected to detailed engineering analysis and subsystem design. These trade studies pointed to an attractive RFP reactor regime of operation with neutron wall loadings in the range of 10-20 MW/m^2 and mass power densities in the range of 500-700 kWe/tonne in which COE is an insensitive function of the neutron wall loading. Reference design point, corresponding to 18 MW/m^2 of neutron wall loading were chosen for TITAN designs in order to determine the technical feasibility and key developmental issues for the entire design window.

Another feature of these TITAN-class reactors is that the cost of the FPC is a small fraction of the overall plant cost ($<$10%). This makes the economics of the reactor less sensitive to changes in the plasma performance or in the unit cost of FPC

components. Moreover, since the FPC is smaller and cheaper, a rapid development program at lower cost is possible, changes in the FPC design would not introduce large cost penalties, and the economics of learning-curves can be exploited.

2. CONFIGURATION

The general arrangement of the TITAN-I FPC is illustrated in Fig. 1. The entire FPC is contained in a vacuum tank to ease the remote making and breaking of vacuum welds during scheduled and unscheduled maintenance. All of the primary coolant ring-headers are above the torus so that in the event of a break in the primary piping, coolant will remain in the torus and the most severe consequence will be that of a LOFA. The flow paths are aligned with the dominant, poloidal field so that MHD consequences are reduced. The coolant flow paths are illustrated in Fig. 2. The first wall and blanket are made of extruded vanadium alloy tubing and are single-pass, poloidal flow. The shield assembly has two zones, a 30 cm, 30% structure zone immediately behind the blanket and a 15 cm, 90% structure zone at the back to reduce the neutron flux to the OH coils. All of the structural material in the FPC is vanadium alloy. Exclusion of other, high-activation alloys (e.g., HT-9) reduces peak temperature during LOFA's and allows for Class-C waste disposal. Operating characteristics of the FPC are listed in Table 1.

The integrated-blanket-coil (IBC) concept [7] is used in TITAN-I. An electric current passed through the poloidal-flow lithium circuit provides the toroidal field required for the TF and divertor coils. The IBC concept eliminates the need for shielding of the two coils and reduces the number of components needing access during maintenance. All of the magnets are normal conducting with the exception of the two superconducting equilibrium field coils located at the outboard edge of the fusion power core.

TITAN uses three toroidal-field divertors for impurity control. The coils used in the divertors are IBC-type coils similar to those in the blanket. The neutralizer plate

is a lithium cooled structure with vanadium-alloy coolant tubes and a tungsten-rhenium surface. The peak heat flux on the divertor plate is 7.5 MW/m^2.

3. MATERIALS

In high power density, compact fusion reactors such as TITAN, the harsh neutron environment limits the choice of structural, shield and insulator materials. Several loading conditions are addressed such as thermal, chemical, radiation, mechanical and electromagnetic. In particular the response of plasma facing materials to radiation, thermal and pressure stresses, and their compatibility with the coolant are of primary concern. Because of the retention of mechanical strength at high temperatures and good thermal properties, vanadium-base alloys are promising materials for structural components. Relative to austenitic and ferritic steels, the vanadium alloys have much better corrosion resistance. Three alloys, V-15Cr-5Ti, VANSTAR and V-3Ti-1Si have been studied. Irradiation, creep and coolant compatibility issues have been investigated and led to the choice of the V-3Ti-1Si alloy as the primary structural material for the TITAN-I design.

4. NEUTRONICS

Tritium breeding, waste disposal, nuclear heating (both during operation and after shutdown), annual replacement mass of vanadium alloy and protection of all magnets in the fusion power core are among the list of important issues taken into account in the neutronics design optimization. An important finding is that some nuclear performance characteristics such as decay heat, waste disposal rating, and atomic displacement in structural alloys are dramatically improved if the lithium coolant is enriched with ^{6}Li. Therefore, the ^{6}Li enrichment in lithium is chosen to be 30% in the reference design.

The first wall and IBC components have a lifetime of one full power year. The hot shield is replaced every five full power years assuming the maximum atomic displacement in the vanadium alloy structure to be 200 dpa. The ohmic heating

coils are expected to last for the entire 30 full power years plant lifetime. The limiting factor is radiation damage to the spinel electrical insulator in the magnets, estimated in terms of neutron fluence to be about 2×10^{23} n/cm^2 ($E_n > 0.1$ MeV). The global tritium breeding ratio is 1.18 from a 3-dimensional calculation, including the effect of the divertors, while the one-dimensional full coverage calculation gives 1.33. The blanket energy multiplication factor, M is 1.2.

5. THERMAL HYDRAULICS

The major features of the thermal-hydraulic design for the TITAN high wall loading reactor are: (1) alignment of the coolant channels along the dominant poloidal magnetic field, (2) separation of the first wall and blanket coolant circuits thus allowing lower coolant exit temperature for the first wall, and (3) use of MHD turbulent flow heat transfer at the high heat flux first wall, made possible by the low magnetic interaction parameter. A thermal-hydraulic design has emerged that can handle up to 5 MW/m^2 of heat flux on the first wall. The coolant velocity in the first wall tubes is about 20 m/s and in the blanket it is about 0.5 m/s. Material erosion due to high velocity lithium flow in the first wall tubes is estimated to be negligible. The total pressure drop in the first wall tubes is about 10 MPa and the resulting primary stress is 4 to 7 times smaller than the allowable stress (e.g., ~80 MPa at 650°C). A two-stage coolant pump, about 5 MPa per stage, is used for the first wall while a single-stage pump is used for the blanket where the pressure drop is about 2 MPa. The total pumping power requirement for coolant circulation is about 3.6% of the net electric output.

The high velocity required to cool the first wall limits the coolant temperature rise to 100 ^oC (the outlet temperature is 400 ^oC). Two power-cycle options are considered. One, mix the first wall coolant with the hotter blanket coolant (blanket outlet temperature is 700 ^oC) and two, have two steam-turbine power cycles which are optimized for the temperature conditions of the first wall and blanket, respectively. The gross thermal efficiency of the latter option is 44% and

has been chosen for TITAN-I.

6. TRITIUM SYSTEMS

The maximum off-site tritium release is designed to be 10 Ci/d. The tritium flux on the first wall is estimated at 1.5×10^{17} cm^{-2} s^{-1}, and 95% of the tritons have energies below 5 eV. With vanadium susceptible to plasma-driven permeation (PDP) and the triton energies very low, superpermeation of the low-energy tritons may result (reduced tritium re-emission and increased permeation into the coolant). The DIFFUSE [8] code gives a minimum of 110 g/d PDP which can be much larger if superpermeation occurs. Extraction of tritium from Li is based on the molten salt technique, adequate for extracting 420 g/d of bred tritium plus PDP at a cost of \$5 to \$15 million. A tritium concentration of one wppm in Li at equilibrium gives ~200 g soluble tritium inventory in the primary coolant loop. A Li secondary loop has an inventory of about 300 g of tritium; use of sodium in the loop would yield about one gram of inventory and cold-trapping is not required. The divertor tritium inventory and coolant permeation are insignificant despite the large fluxes because of the resistance of the tungsten divertor plate to tritium permeation.

The room air detritiation systems can clean up a 5 kg spill of tritium in three days at a capital cost of \$5 million. Plasma exhaust gas processing will be based on palladium diffusers. DIFFUSE gives a tritium inventory in the FPC structure between 3 and 7 g and release into the vacuum tank which surrounds the FPC of ~6 g/d.

7. SAFETY

During the study, different fusion power core designs were considered that can have the potential of operating at high neutron wall loading of 18–20 MW/m^2. Safety features have been incorporated into this design from the beginning, with the purpose of designing with passive safety, simplicity, high availability, and low cost.

The key safety feature of the TITAN-I lithium/vanadium fusion power core design is the complete enclosure of the lithium primary loop system in an inert gas-filled confinement building. The blanket containers, vacuum vessel, and confinement building form three barriers to prevent lithium fires and protect the public from radioactive materials. All piping connections are located at the top of the torus to prevent the complete loss of first wall/blanket coolant during an accident. Lithium drain tanks are provided to reduce passively the vulnerable blanket lithium inventory. A totally passive system that could drain all the lithium inventory into a fire-safe mode within approximately 30 seconds is possible. Two-dimensional thermal analyses of the loss of coolant and loss of flow accidents (LOCA and LOFA) in the first wall and blanket regions have been performed. Different design features are selected to prevent LOCA's and to minimize the LOFA peak temperature of the first wall during accidents in order to minimize the potential release of radioactivity. To evaluate this design further, lithium fire accident scenarios are studied by using the LITFIRE [9] code developed by MIT and site boundary dose calculations were performed to understand the potential release of radioactivity under major accident and routine release conditions.

The maximum temperature during a first wall LOCA and system LOFA (the most severe accident postulated for TITAN-I) is 991 ^{o}C. Thermal creep-rupture analysis of the vanadium structure indicates that failure will not occur during the temperature excursion period of the accident, about 5 to 6 days. The maximum temperature during a lithium-fire is 747 ^{o}C in the combustion zone. The results from these accident evaluations indicate that the lithium self-cooled design can potentially be passively safe, without reliance on active safety systems.

8. MAINTENANCE

The compact design of the TITAN-I fusion power core reduces the system to a few small and relatively low mass components, making toroidal segmentation of the FPC unnecessary. A single-piece maintenance procedure in which the replaceable

first wall and blanket is removed as a single unit is, therefore, possible. The potential advantages of single-piece maintenance procedures are: 1) shortest period of down time resulting from scheduled and unscheduled FPC repairs, 2) improved reliability resulting from integrated FPC pretesting in an on-site, non-nuclear test facility where coolant leaks, coil alignment, thermal expansion effects, etc., would be corrected prior to committing to nuclear service using rapid, and inexpensive, hands-on repair procedures, 3) no adverse effects resulting from the interaction of new materials operating in parallel to radiation damaged materials, and 4) ability to continually modify the FPC design as may be indicated by reactor performance and technological developments.

The TITAN FPC design provides for top access to the reactor with vertical lifts used to remove the components. The number of remote handling procedures is few and the movements are uncomplicated. The annual torus replacement requires that the reusable ohmic-heating coil set and reflector/shield assembly be removed and temporarily stored in a hot cell. The used first wall and blanket assembly is drained and disconnected from the coolant supply system, then lifted to a processing room where it is cooled and prepared for Class-C waste burial. The new, pre-tested first wall and blanket assembly is then lowered into position and the removal procedure is reversed to complete the replacement process.

9. SUMMARY

The TITAN-I reactor is a compact, high neutron wall loading ($\sim 18\,MW/m^2$) fusion energy system based on the reversed-field pinch (RFP) confinement concept. The reactor thermal power is $2918\,MW$ resulting in net electric output of $960\,MW$ and a mass power density of $700\,kWe/tonne$. The fusion power core is a lithium, self-cooled design with vanadium alloy (V -3Ti -1Si) structural material. The TITAN design utilizes the soft beta limit feature of RFPs and operates with a highly radiative plasma in order to limit the heat flux on the divertor plates to acceptable levels. The surface heat flux incident on the first wall is, therefore,

$\sim 4.5\,MW/m^2$. MHD effects had precluded the use of liquid metal coolants for high heat flux components in previous designs, but the magnetic field topology of the RFP is favorable for liquid metal cooling. In the TITAN-I design, the first wall and blanket consist of single pass, poloidal flow loops aligned with the dominant poloidal magnetic field. The thermal-hydraulic analysis shows a reasonable MHD pressure drop ($\sim 12\,MPa$ in the first wall circuit and $\sim 3\,MPa$ in the blanket) and a modest pumping power requirement ($\sim 45\,MWe$) with a thermal power cycle efficiency of $\sim$ 44%.

A unique feature of the TITAN-I design is the use of the integrated-blanket-coil (IBC) concept. With the IBC concept the poloidal flow lithium circuit is also the electrical conductor of the toroidal-field and divertor coils. Use of the IBC concept eliminates the need for TF-coil shielding and simplifies the maintenance procedure. Three dimensional neutronics analysis yields a tritium breeding ratio of 1.18. A molten salt extraction technique is employed for the tritium extraction system. The high neutron wall loading of the TITAN reactor results in a c year lifetime for the first wall and blanket. The shield, however, will be replaced every five years. Almost every FPC component would qualify for Class C waste disposal.

The compactness of the design allows the use of single-piece maintenance of the FPC. The use of single-piece maintenance procedures is expected to provide the shortest period of downtime resulting from scheduled and unscheduled FPC repairs. Reduced downtime is achieved because the replacement FPC is fully pre-tested in an on-site, non-nuclear test facility. This maintenance procedure is expected to increase the plant availability. The general arrangement of the fusion power core provides for vertical lifts to remove the core components during maintenance.

The entire FPC operates inside a vacuum tank, which is surrounded by an atmosphere of inert argon gas to impede the flow of air in the system in case of an accident. The top-side coolant supply and return virtually eliminate the possibility of a complete LOCA occurring in the FPC. The peak temperature during a LOFA

is 991 °C.

ACKNOWLEDGEMENT

Work supported in part by the United States Department of Energy under Contract No. DE-FG03-86ER52126.

REFERENCES

1. F. Najmabadi, R. W. Conn, N. M. Ghoniem, S. P. Grotz, J. Blanchard, *et al.*, "The TITAN Reversed-Field Pinch Fusion Reactor Study; The Final Report," UCLA-PPG-1200, Joint Report of University of California - Los Angeles, GA Technologies, Inc., Los Alamos National Laboratory, and Rensselaer Polytechnic Institute, January 1988. Also see F. Najmabadi, N. M. Ghoniem, R. W. Conn, *et al.*, "The TITAN Reversed-Field Pinch Fusion Reactor Study; Scoping Phase Report," UCLA-PPG-1100, January 1987.

2. R. W. Conn, F. Najmabadi and the TITAN Research Group, "The TITAN Reversed-Field Pinch Fusion Reactor Study," proceedings of the *IEEE 12th Symposium on Fusion Engineering*, Monterey, California, October 1987.

3. C. P. C. Wong, R. L. Creedon, S. P. Grotz, E. T. Cheng, S. Sharafat *et al.*, "The TITAN-II Reversed-field Pinch Reference Aqueous Blanket Design," in *Proceedings of the International Symposium on Fusion Nuclear Technology*, Tokyo, Japan April 10–19, 1988.

4. H. A. Bodin, R. A. Krakowski, and O. Ortolani, "The Reversed-Field Pinch: from Experiment to Reactor," *Fusion Technology* vol. 10, p. 307, 1986.

5. J. B. Taylor, "Relaxation of Toroidal Plasma and Generation of Reversed Magnetic Fields," *Phys. Rev. Lett.* vol. 33, pp. 1139-1141, 1974.

6. J. B. Taylor, "Relaxation of Toroidal Discharges," *Proc. 3rd Topical Conf. on Pulsed High-Beta Plasmas*, Abingdon (Sept. 1975), Pergamon Press, London p. 59, 1976.

7. D. Steiner, R. C. Block and B. K. Malaviya, "The Integrated Blanket-Coil Concept applied to the Poloidal Field and Blanket Systems of a Tokamak Reactor," Fusion Tech. Vol. 7 (1985) pp. 66.

8. M. I. Baskes, "DIFFUSE 83," Sandia National Laboratory, SAND-83-8231 (1983).

9. E. Yachimiak, V. Gilberti, and M. S. Tillack, "LITFIRE User's Guide,"MIT report, PFC/RR-83-11, June, 1983.

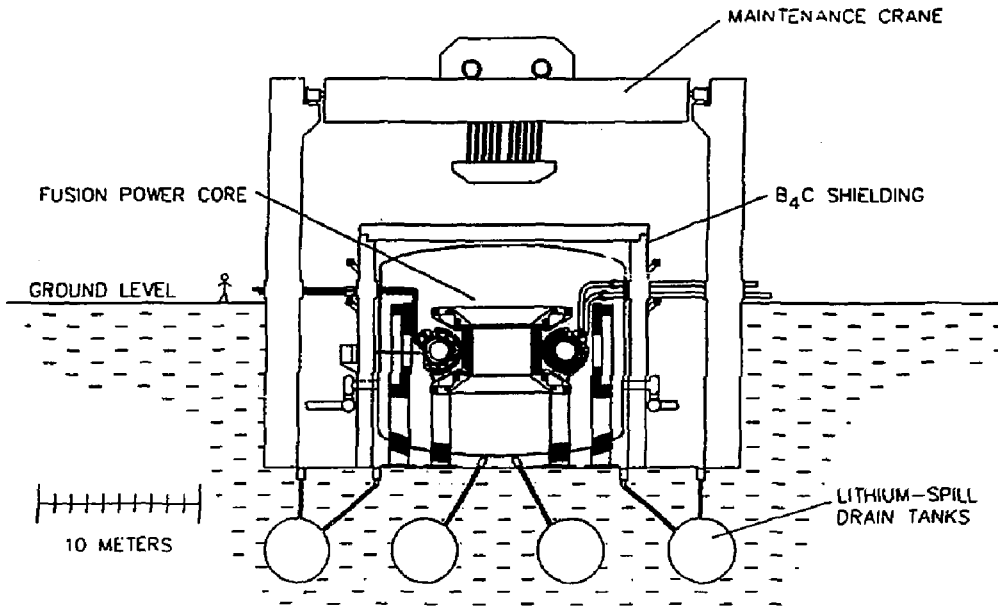

Figure 1. General arrangement of the TITAN-I fusion power core.

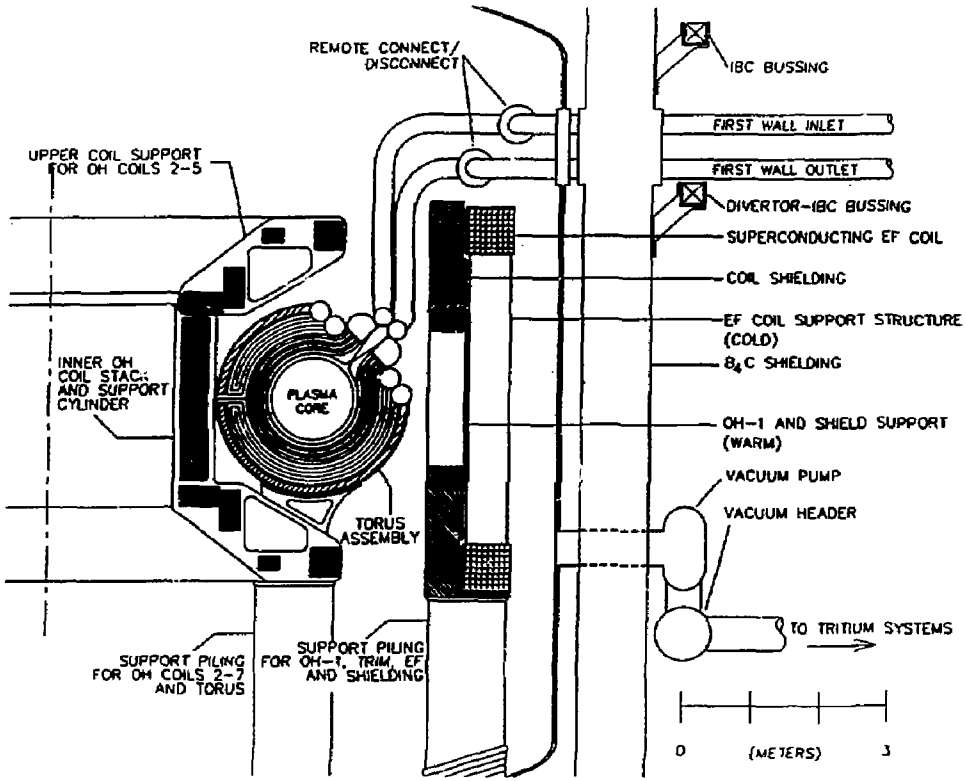

Figure 2. Poloidal cross section of the TITAN-I fusion power core.

Table 1

Major Operating Parameters of TITAN-I

DIMENSIONS	
Major plasma radius	3.9 m
Minor plasma radius	0.6 m
First wall minor radius	0.66 m
First wall surface area	160 m^2
Thickness of first wall, blanket and shield	0.77 m
First wall pipes diameter	10.5 mm
IBC pipes diameter	52.5 mm
PLASMA	
Neutron wall loading	18 MW/m^2
Plasma density	9.45×10^{20} m^{-3}
Poloidal beta	0.22
Poloidal field at first wall	5.44 T
Toroidal field at first wall	0.36 T
POWER	
Fusion power	2288 MW
Total thermal power	2918 MW
Gross electric power	1284 MW
Net electric power	998 MW
Mass power density	700 kW_e/tonne
Blanket energy multiplication	1.2
Thermal cycle efficiency	
Cycle 1	0.37
Cycle 2	0.465
Average	0.44
Net plant efficiency	0.34
Surface heating, peak	
First wall	4.5 MW/m^2
Divertor	7.5 MW/m^2
Volumetric heating, peak	95 MW/m^3
HYDRAULIC	
Li Coolant inlet temperature	320 °C
Li Coolant outlet temperature	
First wall and divertor	440 °C
IBC and hot-shield	700 °C
Li Coolant pressure, inlet	
Divertor	12. MPa
First wall	10. MPa
IBC and hot shield	2.9 MPa

OVERVIEW OF THE TITAN-II REVERSED-FIELD PINCH AQUEOUS FUSION POWER CORE DESIGN

C. P. C. Wong,[2] R. L. Creedon,[2] S. P. Grotz[1],
E. T. Cheng,[2] S. Sharafat,[1] P. I. H. Cooke,[1,‡] and
The TITAN Research Group
J. R. Bartlit,[3,*] C. G. Bathke,[3] J. P. Blanchard,[1] Y. Chu,[1] R. W. Conn,[1] E. Dabiri[6]
W. P. Duggan,[4] O. Fischer,[2,**] N. M. Ghoniem,[1] P. J. Gierszewski,[7] G. E. Gorker,[6]
M. Z. Hasan,[1] C. G. Hoot,[2] D. C. Keeton,[6] W. P. Kelleher,[4] C. E. Kessel,[1]
R. A. Krakowski,[3] O. Kveton,[7] D. C. Lousteau,[6] R. C. Martin,[1] R. L. Miller,[3]
F. Najmabadi,[1] R. A. Nebel,[3] G. E. Orient,[1] A. K. Prinja,[1,‡‡] K. R. Schultz,[2]
D. Steiner,[4] D. K. Sze,[5] S. L. Thomson,[6] S. G. Visser,[2] E. L. Vold,[1] K. A. Werley,[3]

General Atomics, San Diego, California 92138-5608, U. S. A.

ABSTRACT

TITAN-II is a compact, high power density Reversed-Field Pinch fusion power reactor design based on the aqueous lithium solution fusion power core concept. The selected breeding and structural materials are $LiNO_3$ and 9-C low activation ferritic steel, respectively. TITAN-II is a viable alternative to the TITAN-I lithium self-cooled design for the Reversed-Field Pinch reactor to operate at a neutron wall loading of 18 MW/m^2. Submerging the complete fusion power core and the primary loop in a large pool of cool water will minimize the probability of radioactivity release. Since the protection of the large pool integrity is the only requirement for the protection of the public, TITAN-II is a level 2 of passive safety assurance design.

[1] University of California, Los Angeles.
[2] GA Technologies Inc.
[3] Los Alamos National Laboratory.
[4] Rensselaer Polytechnic Institute.
[5] Argonne National Laboratory.
[6] Fusion Engineering Design Center.
[7] Canadian Fusion Fuels Technology Project.
[*] TSTA program.
[‡] Permanent address: UKAEA Culham Lab., Abingdon, Oxon OX14 3DB, U.K.
[**] Permanent address: Swiss Federal Inst. for Reactor Research (EIR), Wurenlingen, Switzerland.
[‡‡] Present address: University of New Mexico, Albuquerque, NM 87107.

1. INTRODUCTION

TITAN is a two-year study which began in December 1985 to investigate the potential of the Reversed-Field Pinch concept as a compact, high-power-density fusion energy system [1]. It is a multi-institutional project, having participants from universities, industry, and national laboratories, including international participation. During the scoping phase of this study, we evaluated different blanket concepts which have the potential of operating at a high neutron wall loading of 18 MW/m^2. A lithium self-cooled and the water-cooled design were selected for further investigation. Details of the lithium self-cooled design are reported in Ref. 2. This paper presents an overview of the TITAN-II design which uses the Near-term, Aqueous, Unit-Torus, Immersed-Loop, Ultimately-Safe **NAUTILUS** concept.

The basic safety design principle of the Swedish Secure-P fission reactor design [3] was reviewed and applied to the TITAN-II "loop-in-pool" configuration as shown in Fig. 1. By adopting the aqueous lithium solution concept [4], the selection of breeder and structural material becomes very important, and the related concerns of corrosion, hydrogen embrittlement and radiolysis effects were evaluated. The trade-offs between the lithium concentration in the coolant, neutronics performance, fluid heat transfer, and power conversion system selection were evaluated before the selection of the TITAN-II reference design. Since water was selected as the blanket coolant, its capability of removing high surface heat flux was also made use of in the divertor design [5]. Based on the extensive fission reactor tritium control experience from Canada [6], the key concerns of tritium extraction and control were addressed. The questions of waste disposal, reactor safety and maintenance implications of the reference design were studied and the results are also presented in this paper.

2. PROJECT OBJECTIVES AND SAFETY DESIGN GOAL

Two primary objectives of the TITAN program are to determine the technical feasibility and key developmental issues of a Reversed-Field Pinch (RFP) fusion

reactor, and to determine its potential economics, cost of electricity, safety and environmental features. In the evolution and selection of the aqueous concept, key elements of design simplicity, high availability, passive safety and minimum cost have been used as design objectives. By considering safety at the beginning of the conceptual design process, safety features can be built-in, while maintaining design simplicity which can have favorable impacts on availability and cost of electricity. Four levels of safety assurance were used to facilitate the preliminary evaluation of different designs [7]. These levels are not precisely defined licensing criteria nor rules for formal safety evaluation. They are relatively simple guides for designers to use to evaluate their designs and improve on their safety features. For the TITAN-II design we were aiming for level 2 of safety assurance, which means in order to keep the public safe we have only to maintain the integrity of the large-scale geometry, atmospheric pressure water pool.

3. MATERIAL SELECTION

Tritium breeding in the aqueous blanket design is accomplished by dissolving lithium in the blanket coolant [4]. Different lithium compounds were evaluated [1]. The key questions for the selection are solubility of the compound in water, corrosion effects of the solvent with the materials in contact, and radiolysis effects under the fusion environment. An obvious lithium compound is LiOH. In order to get adequate lithium concentration in an LiOH solution, it will have a pH value of above 14, which can cause significant corrosion problems to the structural material. $LiNO_3$ solution has a pH value close to the neutral value of 7, and can be much less corrosive. Preliminary radiolytic yield estimates indicated that the formation of explosive gas mixtures of hydrogen and oxygen could be avoided for $LiNO_3$ by the presence of the nitrate ions. Based on these results, the selected TITAN-II primary coolant is a solution of $LiNO_3$ containing 6.4 at.% of lithium. Estimated properties of this solution, which are quite different from water, were used in the thermal-hydraulics calculations. Details of this are presented in Refs. 8 and 12.

Evaluation of V, Cu, Zr and ferritic steel alloys was performed for the TITAN-II design. Due to potential problems in corrosion resistance for the V-3Ti-1Si alloy and helium embrittlement for the V-15Cr-5Ti alloy, they were not considered further [1]. For the Zr-alloy, the problem of hydrogen embrittlement prevents its use for this design. Potential magnetic field error problems for the high electrical conductivity copper alloys at the beginning of life and the much-reduced thermal conductivity due to transmutation at the end of life for other Cu-alloys generates uncertainties in the design. When compared to ferritic steel, Cu-alloys become back-up alloy candidates. Among the reduced activation ferritic steel alloys, two seem to be suitable for this design. The first one is the high-strength 12Cr-0.3V-1W-6.5Mn-0.08C alloy, called 9-C, developed by Gelles, Ghoniem and Powell [9]. It has room-temperature measured yield strength of 531 MPa, after an irradiation dose of 14.3 dpa at $531°C$. The second is the GA Reduced Activation Ferritic Steel (GA-RAFS) developed by Lechtenberg [10]. Because of its superior yield and ultimate strength, 9-C alloy was selected as the reference structural material. Since the GA-RAFS alloy has the minimum measured swelling and ductile-to-brittle transition temperature (DBTT) effects under irradiation, it is retained as the alternate ferritic steel structural material.

The potential concerns of corrosion, radiolysis, and hydrogen embrittlement of ferritic steel in an aqueous solution of $LiNO_3$ were evaluated. Based on limited experimental data, it was found that with water chemistry control, this nitrate salt and structural material combination should have an acceptable corrosion rate. At the same time, by operating the coolant and wall interface at $> 400°C$this combination of 9-C ferritic steel and nitrate salt should not be susceptible to hydrogen embrittlement. Preliminary evaluation indicates that by operating the coolant at the relatively high coolant temperature of $\sim 300°C$in conjunction with the relatively high hydrogen concentration, the reference TITAN-II coolant system may be quite tolerant to the effects of radiolysis [11].

4. CONFIGURATION DESIGN

For the TITAN-II design, we have immersed the high-pressure primary loop including the RFP torus and the heat exchangers into a pool of low-temperature water, as shown in Fig. 1. This concept uses near-term aqueous solution technology and has the potential for completely passive safety. The fusion power core is inserted and removed from the pool as a single unit. This is called the NAUTILUS concept for "Near-term, Aqueous Solution Unit Torus, Immersed Loop, Ultimately Safe" concept.

During the evaluation phase of the aqueous solution design, different first wall and blanket configurations were investigated. The basic requirements are a thin first wall to take the high-surface heat flux, and a strong enough structure to take the high coolant pressure. Additional requirements are design simplicity, vertical fluid flow to allow natural circulation, and a simple arrangement of the coolant plena. Details of the resulting design are shown in Fig. 2.

The selected blanket design configuration is the integrated first wall and blanket lobe design illustrated in Figs. 3 and 4. The pressurized coolant at 70 MPa is enclosed in the lobes. The lobe width is 3 cm, with wall thickness 1.5 mm which includes an erosion allowance of 0.25 mm facing the plasma. The coolant comes in from the bottom of the torus and exits from the top. In between, the coolant flows in the 3 cm-thick lobes through the first wall and blanket zone in a poloidal direction. The first wall and blanket zones are separated by a flow barrier, such that detailed tailoring of the first wall flow is possible by adjusting the flow resistance in the blanket. Beryllium rods clad in 9-C ferritic steel, 0.125 mm thick, will be packed closely in the blanket zone. The structural load from the pressurized lobes is supported by the outer support shell. Details of the individual lobes are illustrated in Fig. 4.

As illustrated in Fig. 3, the inboard and outboard segments are self-contained units. Four of the illustrated segments can then be used to form a sector of one-

third of the torus. Three sectors can then be joined between the divertor chambers to form the complete RFP torus. As illustrated, the vacuum boundary of the torus is located at the back of the shield.

5. THERMAL-HYDRAULICS AND POWER CONVERSION

In order to handle the high neutron wall loading of 18 MW/m^2 and the corresponding surface wall loading of 4.2 MW/m^2, subcooled flow boiling heat transfer will be needed for the first wall cooling [12]. Due to the coolant property changes of the aqueous solution pointed out earlier, all the heat transfer characteristics of the solution have to be adjusted. Considering the equations for incipient boiling, subcooled flow boiling (SFB) heat transfer and critical heat flux (CHF) correlations for pure water, and comparing the properties of the solution to those of water, we believe that it is conservative to use the pure water CHF as a guide for the TITAN-II design. We have also estimated the impact to SFB heat-transfer from different concentrations of $LiNO_3$ in water. In the concentration range of 2 to 6 at.% of lithium, we found that the reduction in SFB heat-transfer can be from 8 to 20%, which is acceptable, considering the temperature of the structural material. Compared to water, this solution has higher density, lower specific heat capacity, and a higher boiling point. Taking advantage of the last property, the reference design is selected to operate at a coolant pressure of 7 MPa, with inlet and outlet temperatures at 298°$C$and 330°C, respectively. By using subcooled-flow-boiling heat transfer, we found that it is feasible to handle the neutron wall loading of 18 MW/m^2 and a corresponding first wall surface heat flux of 4.6 MW/m^2. At the beginning-of-life, before the first wall erosion occurs, the 9-C ferritic steel first wall has a maximum midwall temperature of 503°Cwhich is quite acceptable. The secondary coolant was selected to operate at a higher coolant pressure of 7.2 MPa, thus reducing the probability of leakage of the tritium-containing primary coolant into the steam generator system. This power conversion system has a gross thermal efficiency of 35% [12].

6. NEUTRONICS ANALYSIS

Neutronics calculations were performed to evaluate different design options, and to select the reference design. With the use of high strength 9-C ferritic steel, the required structure volume fraction is about 11%, this leads to a total blanket and shield thickness of thickness of 41.5 cm. This radial thickness includes the first wall, 20 cm of beryllium multiplier zone, 10 cm of ferritic steel reflector and 10 cm of shield. At a ^{6}Li enrichment of 12% in the $LiNO_3$ solution, the tritium breeding ratio and blanket energy multiplication were calculated to be 1.2 and 1.4, respectively [12]. This indicates more than adequate neutronics performance for the TITAN-II design. If D_2O were used to replace H_2O, we found that beryllium would still be needed in order to obtain adequate tritium breeding.

7. TRITIUM ISSUES

Tritium control and extraction from a fusion reactor blanket has always been a serious concern in conceptual reactor designs. For the TITAN-II aqueous blanket, the basic technology of tritium control and extraction have already been developed by the Canadian CANDU fission reactor program. We performed a trade-off study between operating tritium loss, primary coolant tritium concentration and process equipment cost. We compared different methods of tritium recovery and the design options with and without an intermediate heat exchanger for the primary coolant loop. Since the TITAN-II reference design is to operate the primary loop at a lower pressure than the secondary loop, an intermediate heat exchanger will not be necessary. At a primary loop tritium concentration of 50 Ci/liter, the tritium extraction system total installed cost is \$170 M and the corresponding tritium release rate is 50 Ci/day [12], which are both relatively high yet acceptable values.

8. REACTOR MAINTENANCE

Due to the high-power-density of the RFP design, the fusion torus including the blanket, shield and the toroidal field coil systems can be designed to have a total

mass of less than 500 tonnes. This allows the use of the unit-torus design approach. That is, the blanket, shield and TF-coil systems can be removed in one piece by vertical lift. This approach can also facilitate pre-testing before the torus system is lowered into place in the reactor pool.

9. WASTE MANAGEMENT

The question of waste disposal was also addressed. Mainly due to the presence of the alloying element tungsten in the 9-C ferritic steel, after one year of operation at 75% availability, and a neutron fluence of 13.6 MW-yr/m^2, the average waste disposal rating for the blanket structure was found to be equal to 1.43. This means that the blanket will need to be disposed of as high level waste. Class C waste classification can still be attained by operating at lower fluence or by reducing the content of tungsten in the 9-C ferritic steel by a factor of three [12].

10. SAFETY ISSUES

Based on the NAUTILUS concept of the TITAN-II design, different scenarios for the handling of accident situations were evaluated [13]. The basic sources of thermal energy after reactor shutdown are from the plasma thermal and magnetic energy, the thermal energy of the hot loop, and the induced afterheat from the torus first wall and blanket structures. The first wall and blanket coolant channel configurations are designed to allow natural circulation to be developed in the case of a loss-of-flow accident (LOFA). During normal operation, the fusion power core is designed to thermally conduct away 34 MW of power through the heat exchanger and primary coolant piping walls into the low temperature pool. This will allow the passive removal of 34 MW of shutdown afterheat power, corresponding to the maximum blanket afterheat power, during a LOFA. The maximum first wall temperature under a LOFA was 348°C, 355 sec after shutdown. This design approach will thus eliminate the probability of a LOFA leading to a LOCA. Even under the catastrophic accident of loss of primary coolant pressure, the low pressure

and low temperature cold pool of water, coupled with the heat transmission of the blanket afterheat to the surrounding earth, will make it possible to control the pool temperature to less than 100°C for longer than 90 days. This should allow enough time for the recovery or installation of active afterheat removal system. This will minimize the probability of radioactivity release. Since the protection of the large pool integrity is the only requirement for the protection of the public, by definition TITAN-II is a level 2 of passive safety assurance design.

11. DESIGN PARAMETERS

Table 1 shows the design parameters of the TITAN-II design.

12. SUMMARY AND CONCLUSIONS

We have evaluated and selected the reference design of the TITAN-II RFP aqueous solution design. It is a loop-in-pool design that can operate at a neutron wall loading of 18 MW/m^2. The selected breeding and structural material are $LiNO_3$ and reduced activation, high-strength 9-C ferritic steel, respectively. The lithium concentration in the water is 6.4 at.%. A lobe configuration was selected for the integrated first wall and blanket design. Adequate neutronics performance was predicted at a total blanket shield thickness of 41.5 cm. Based on the low-pressure pool configuration, reactor safety implications were assessed. By using the pool to absorb the fusion power core thermal and afterheat energy, this design is passively safe and can achieve level 2 of safety assurance.

Design approaches to address different critical design areas have been identified. Some of these are based on engineering extrapolation of existing results. Others require experimental investigation and design improvements. These are: measurement of the nitrate solution physical properties; confirmation of the nitrate salt subcooled flow boiling heat transfer, critical heat flux and pressure drops; experimental measurements of the effects of corrosion, hydrogen embrittlement and radiolysis effects; reduction of tritium extraction cost; and the control of tritium

Table 1
TITAN-II Design Parameters
(Superconducting equilibrium field coils)

Major radius, m	3.9
Minor first wall radius	0.6
Neutron wall loading, MW/m^2	18.0
Surface loading, MW/m^2	4.2
Thermal power, MWe	~3000
Net electricity power, MWe	~900
Tritium breeder	$LiNO_3$
Neutron multiplier	Be
1-D Tritium breeding ratio	1.2
Blanket energy multiplication	1.4
Primary coolant	7.0 MPa
Secondary coolant	7.2 MPa
T_{in}, °C	298
T_{out}, °C	330
First wall material	9-C ferritic
Structural material	9-C ferritic
First wall thickness, mm	1.5
Allowable erosion thickness, mm	0.25
Maximum mid-first wall temperature, °C	503
Gross thermal efficiency, %	35

leakage to the public. In addition, further development of acceptable low activation alloys that can be classified as Class C waste material will be needed for design improvement.

We concluded that the TITAN-II aqueous loop-in-pool reactor is a passively safe design. Since most of the needed technologies require only minimum extrapolations from existing practice, TITAN-II can be considered a near-term design. It is also able to handle the high neutron wall loading of 18 MW/m^2 and has as high a

thermal performance as the best existing fission pressurized water reactors. Further studies will be needed to address some of the critical issues. Reduction in the cost of tritium extraction and in the routine release of tritium will definitely enhance its overall attractiveness as a design.

ACKNOWLEDGMENT

This work was supported in part by the U.S. Department of Energy, Office of Fusion Energy, under Contract DE-AC03-84ER53158, and the University of California, Los Angeles, under Contract 0205 B 02744.

REFERENCES

1. F. Najmabadi *et al.*, "The TITAN Reversed-Field Pinch Fusion Reactor Study, Scoping Phase Report," University of California, Los Angeles Report UCLA-PPG-1100, January 1987, and "The TITAN Reversed-Field Pinch Fusion Reactor Study, Final Report," University of California, Los Angeles Report UCLA-PPG-1200, March 1988, and R. Conn, F. Najmabadi, *et al.*, "The TITAN Reversed-Field Pinch Fusion Reactor Study," Proceedings of IEEE 12th Symp. on Fusion Engineering, Monterey, California, (1987) 503.
2. S. P. Grotz *et al.*, "Overview of the TITAN-I Fusion-Power Core," Int. Symp. on Fusion Nuclear Technology, Tokyo, Japan, April 10-19, 1988.
3. K. Hannerz, "Adapting the LWR to future needs: SECURE-P (PIUS)," Power Engineering, September 1985.
4. D. Steiner *et al.*, "A Heavy Water Breeder Blanket," 11th Symp. on Fusion Engineering, Austin, Texas, November, 1985.
5. P. I. H. Cooke *et al.*, "Engineering Design of the TITAN-II Divertor," Int. Symp. on Fusion Nuclear Technology, Tokyo, Japan, April 10-19, 1988.
6. K. Y. Wong *et al.*, "Canadian Tritium Experience," Ontario Hydro, 1984.
7. S. J. Piet, "Approaches to Achieving Inherently Safe Fusion Power Plants," Fusion Technology **10** (1986) 7.
8. P. I. H. Cooke *et al.*, "Properties of Concentrated Aqueous Lithium Nitrate Solutions and Applications to Fusion Reactor Design," Int. Symp. on Fusion Nuclear Technology, Tokyo, Japan, April 10-19, 1988.
9. D. S. Gelles, N. M. Ghoniem, and R. W. Powell, "Low Activation Ferritic Alloys, Patent Description," University of California, Los Angeles Report UCLA/ENG-87-9, UCLA-PPG-1049, March 1987.
10. C. Y. Hsu and T. Lechtenberg, "Microstructure and Mechanical Properties of Unirradiated Low Activation Ferritic Steel," J. Nucl. Mater. **141-143** (1986) 1107.
11. S. Sharafat *et al.*, "Material Selection for the TITAN Reversed-Field Pinch Reactor," Int. Symp. on Fusion Nuclear Technology, Tokyo, Japan, April 10-19, 1988.
12. F. Najmabadi *et al.*, "The TITAN Reversed-Field Pinch Fusion Reactor Study, Final Report," University of California, Los Angeles Report UCLA-PPG-1200, March 1988.
13. C. P. C Wong *et al.*, "The Safety Designs for the TITAN Reversed-Field Pinch Reactor Concepts," Int. Symp. on Fusion Nuclear Technology, Tokyo, Japan, April 10-19, 1988.

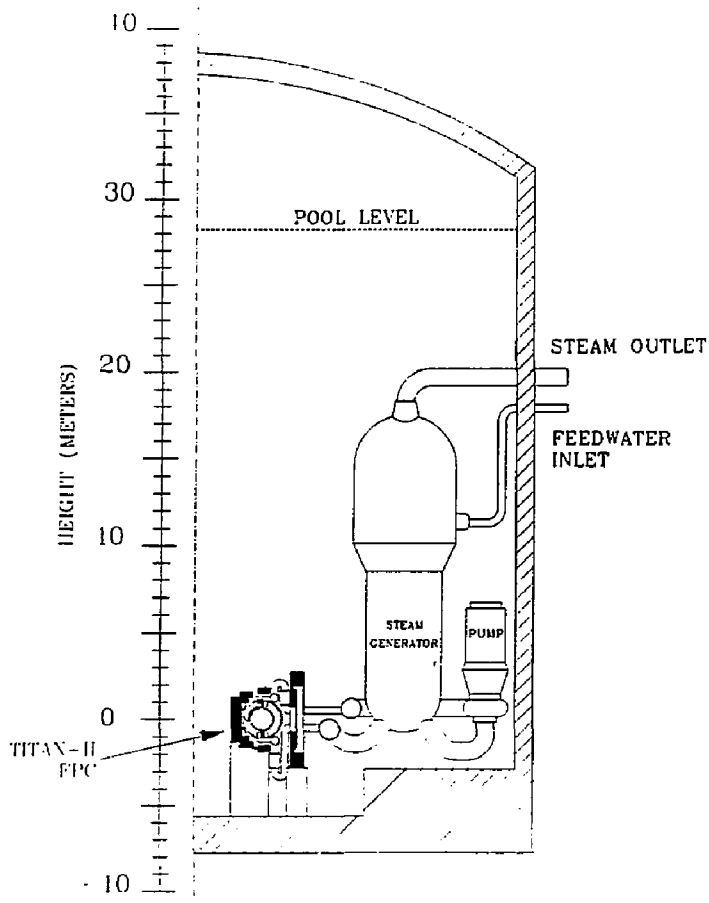

Figure 1. The TITAN-II loop-in-pool design.

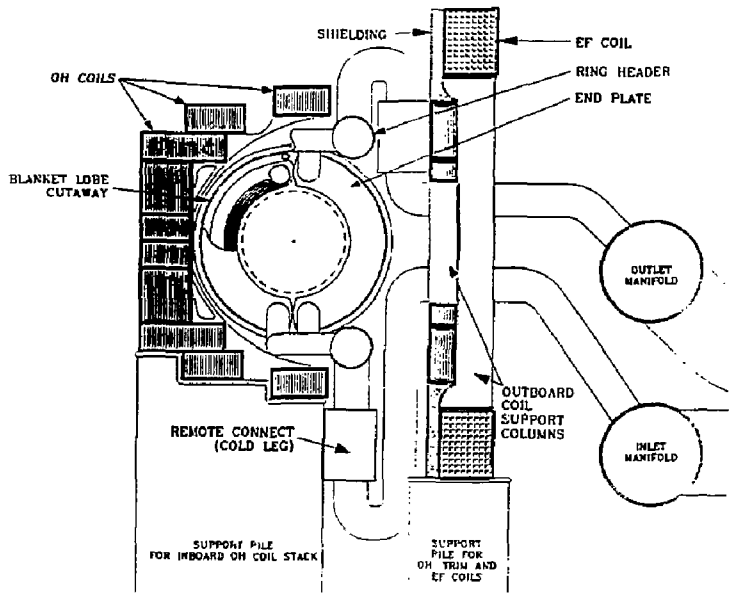

Figure 2. The TITAN-II fusion power core design.

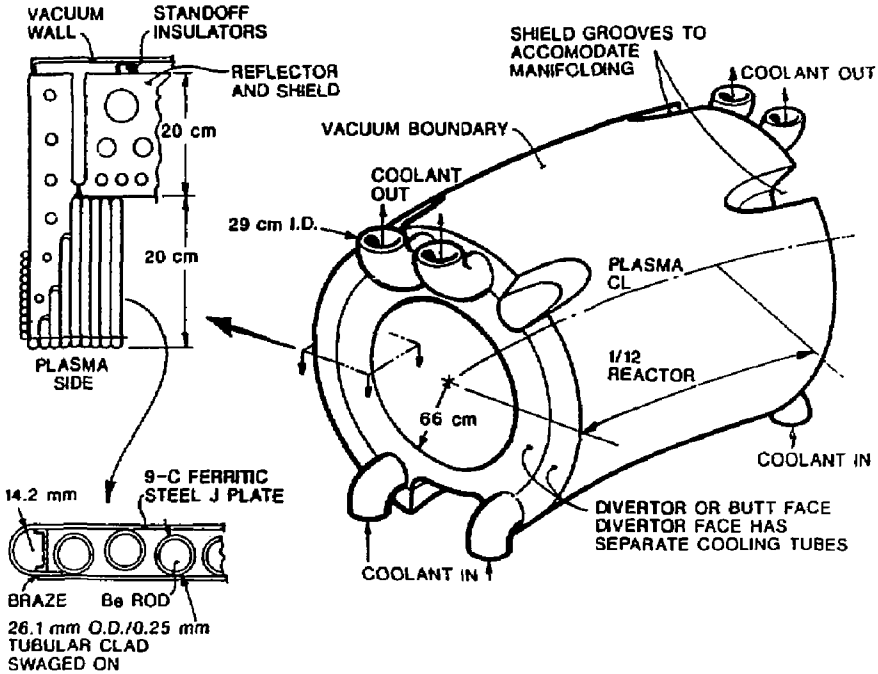

Figure 3. The TITAN-II blanket segment.

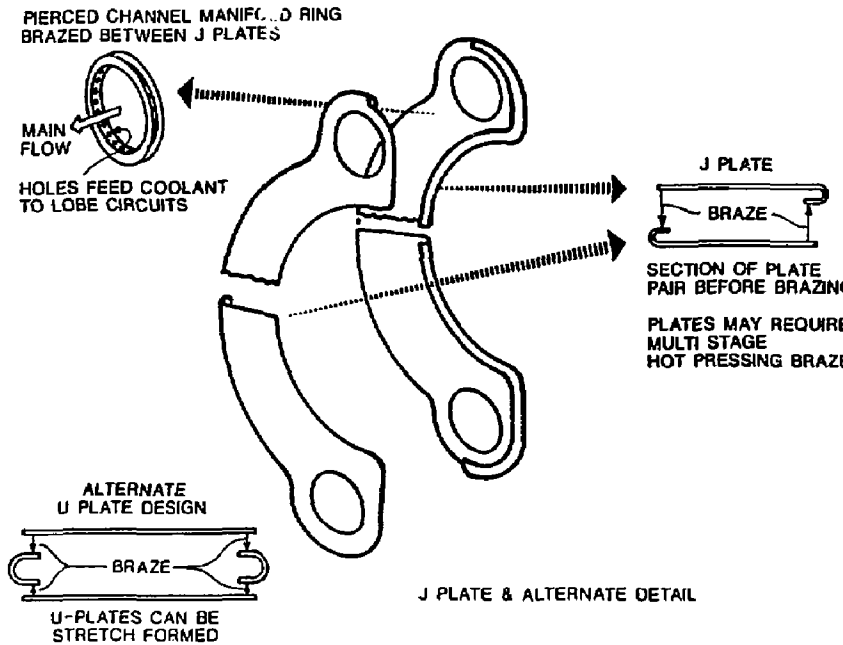

Figure 4. The TITAN-II blanket lobe J plate design.

THE SAFETY DESIGNS FOR THE TITAN REVERSED-FIELD PINCH REACTOR STUDY

C. P. C. Wong, S. P. Grotz[1], J. P. Blanchard,[1] E. T. Cheng, S. Sharafat,[1]
R. L. Creedon, C. G. Hoot, F. Najmabadi,[1] K. R. Schultz, and
The TITAN Research Group

General Atomics, San Diego, California 92138-5608, U. S. A.
[1] Department of Mechanical, Aerospace and Nuclear Engineering
and Institute for Plasma and Fusion Research
University of California, Los Angeles
Los Angeles, CA 90024-1597

ABSTRACT

TITAN [1] is a study to investigate the potential of the reversed-field pinch concept as a compact, high-power density energy system. Two reactor concepts were developed, a self-cooled lithium design with vanadium structure and an aqueous solution loop-in-pool design, both operating at 18 MW/m^2. The key safety features of the TITAN-I lithium-vanadium blanket design are in material selection, fusion power core configuration selection, lithium piping connections and passive lithium drain tank system. Based on these safety features and results from accident evaluation, TITAN-I can at least be rated as level 3 of safety assurance. For the TITAN-II aqueous loop-in-pool design, the key passive feature is the complete submersion of the fusion power core and the corresponding primary coolant loop system into a pool of low temperature water. Based on this key safety design feature, the TITAN-II design can be rated as level 2 of safety assurance.

1. INTRODUCTION

TITAN is a two-year study which began in December 1985 to investigate the potential of the Reversed-Field Pinch (RFP) concept as a compact, high-power density fusion reactor system [1]. Two fusion power core concepts were studied in detail: they are the TITAN-I lithium self-cooled design [2] and the TITAN-II aqueous loop-in-pool design [3]. Safety is an important activity in the TITAN study. This activity was incorporated at the beginning of the study into the process of design selection and integration. We did not take the approach of add-on safety, which is to analyze the safety implications of a design after it was finished and to add in safety features in order to satisfy regulatory requirements. Instead, we took the active approach of identifying safety design features and recommending them at the beginning to guide the development of the TITAN designs. This approach was projected to enhance the potential of attaining the goals of simplicity, passive safety, high availability and low cost of electricity. This paper presents the safety designs and evaluations of the TITAN-I lithium self-cooled reactor and the TITAN-II aqueous loop-in-pool reactor concepts.

2. SAFETY DESIGN GOALS

For the TITAN safety design, we have two objectives. The first one is to satisfy all the safety design criteria as specified by the U.S. Nuclear Regulatory Commission (USNRC) on accidental releases, occupational doses, and routine effluents. The second one is to aim for the best possible level of safety assurance.

In accordance to the first safety objective, we follow the existing USNRC safety design criteria observed by the fission reactor industry. Although the accident scenarios and classification systems developed by the U.S. fission industry may not apply directly to fusion reactors, the dose guidelines used by the fission industry will probably either be directly applicable or serve as useful references in defining the radiological safety requirements for fusion reactor designs. These regulations are

described in the Code of Federal Regulations 10CFR20, 10CFR50, and 10CFR100 [4].

For conceptual fusion reactor design studies, four levels of safety assurance were created to facilitate the preliminary evaluation of different designs [5]. These levels are not precisely defined licensing criteria nor rules for formal safety evaluation. They are relatively simple guides to designers who can then make use of these definitions of different levels of safety to evaluate their designs or to improve on their safety features when appropriate.

The following summarizes the interpretation of these four levels of safety assurance as suggested by S. Piet [5] of INEL (also see Ref. 6).

Level 1 — *"Inherent safety."* In a level 1 reactor, safety is assured by passive mechanisms of release limitation no matter what the accident sequence. The radioactive inventories and material properties in such a reactor preclude a violation of release limit regardless of the reactor's condition.

Level 2 — *"Large-scale passive safety assurance."* In a level 2 reactor, safety is assured by passive mechanisms of release limitation as long as severe reconfiguration of large-scale geometry is avoided, and escalation to fatality-producing reconfigurations from less severe initiating events can plausibly be precluded by passive design features. In such a reactor, natural heat-transfer mechanisms suffice to keep temperatures below those needed — given its radioactivity inventories and material properties — to produce a violation of release limits unless the large-scale geometry is badly distorted.

Level 3 — *"Small-scale passive safety assurance."* In a level 3 reactor, safety is assured by passive mechanisms of release limitation as long as severe violations of small-scale geometry — such as a large break in a major coolant pipe — are avoided, and escalation to fatality-capable violations from less severe initiating events can plausibly be precluded by passive design features. In such a reactor, sufficiency

of natural heat-transfer mechanisms to keep temperatures low enough — given its radioactivity inventories and materials properties — to avoid a violation of release limits can only be assured while the coolant boundary is substantially intact.

Level 4 — "Active safety assurance." In a level 4 reactor, there are credible initiating events that can only be prevented from escalating to site boundary release limit violations or reconfigurations by means of active safety systems.

The public is adequately protected by all four levels of safety assurance. To understand the meaning of adequate protection of the public, the concept of safety assurance can be further strengthened in the context of probabilistic risk assessment. The risk-based safety goal for TITAN is that fusion accidents would not increase the individual cancer risk of the public by more than 0.1% of the prevailing risk. As a consequence of this goal, we have followed the fission reactor 10CFR100 [4] site boundary accidental release whole body dose limit of 25 rem as our accidental release limit.

3 LITHIUM SELF-COOLED DESIGN SAFETY DESIGN AND ANALYSIS

For the TITAN-I lithium self-cooled design, we have taken four basic safety design approaches. The first approach is the physical separation of potentially reactive materials, such as lithium, water, concrete and air. The second approach is to minimize the amount of induced radioactivities. The third approach is to reduce the maximum material temperature due to afterheat generation, and the fourth approach is to minimize the amount of vulnerable lithium coolant. The first approach can be achieved by the use of multiple physical barriers and steel liners. The second approach can be achieved by the use of reduced activation materials. The third approach can be achieved by the selection of low afterheat materials and by providing conducting paths from the front to the back of the blanket. These safety design approaches helped us to generate a list of design recommendations

from which specific safety design options were generated, evaluated and selected for the TITAN-I design.

3.1. Design Features

The selected key safety features of the lithium self-cooled design are:

- The selection of a low afterheat structural material, V-3Ti-1Si.
- The selection of a relatively high ^6Li enrichment at 12%, to aid in the further reduction of afterheat and radioactive wastes.
- The use of three enclosures separating the lithium and air. These enclosures are the blanket tubes, the vacuum vessel, and the argon inert gas-filled confinement building as shown in Fig. 1.
- All piping connections are located at the top of the torus to prevent a complete loss of the first wall and blanket coolant.
- Lithium drain tanks are provided to reduce the vulnerable blanket lithium inventory.
- A steel liner is used to cover the confinement building floor to minimize the probability of lithium and concrete reactions.

Most of these features are illustrated in Fig. 1.

3.2. LOFA and LOCA Analysis

With the above design features we found that during a loss-of-flow accident (LOFA), the first wall temperature rises to a maximum of $990°C$, well below its melting point. We also found that the hydrostatic pressure of the lithium is not sufficient to over-stress the first wall and blanket and lead to thermal creep-induced rupture. Coupled with the design feature of locating all the piping connections above the fusion power core, a LOFA will not lead to a loss-of-coolant accident (LOCA), and a complete LOCA due to coolant drainage will not be possible.

3.3. Lithium Fire Analysis

In the event of major primary pipe breaks and failure of the confinement building and vacuum vessel, air could enter the vacuum chamber and start a lithium fire. Based on the design configuration of the drain tank system, as shown in Fig. 1, which is designed to drain the maximum amount of lithium in less than 30 sec, we found that during the perceived worst accidental condition of a lithium fire, the maximum combustion zone temperature is less than $1000°C$. The tritium release in this case would be about 60 Ci which is quite acceptable under this worst accident scenario. Critical concerns under the lithium fire scenario are the formation and release of vanadium oxide. Further measurement of vanadium oxide formation and its vapor pressure with temperature, and the calculation of potential releases to the public based on the TITAN-I configuration and accidental scenarios will need to be performed.

3.4. Tritium Inventory and Leakage

The total tritium inventories in the lithium primary loop and the secondary loop are 344 and 300 g, respectively. These are acceptable inventories when passive drain tanks are used to control the amount of possible tritium releases. The tritium inventory in the blanket structure is less than 10 g, which is also acceptable. The tritium leakage rate from the primary loop was estimated to be 7 Ci/day which is within the 10 Ci/day design goal.

Based on the analyses summarized above, TITAN-I does not need to rely on any active safety systems to protect the public. A LOFA will result in no radioactive release and will not lead to a more serious LOCA. A complete LOCA from credible events is not possible. Only the assurance of piping and vacuum vessel integrity will be needed to protect the public. TITAN-I therefore meets the definition of level 3 of safety assurance, "small-scale passive safety assurance." Pending information on vanadium oxide formation and releases from the TITAN-I vacuum chamber under

the lithium fire accident scenario, the qualification of TITAN-I as a level 2 of safety assurance design, "large-scale passive safety assurance," may be possible.

4. AQUEOUS LOOP-IN-POOL SAFETY DESIGN AND ANALYSIS

For the TITAN-II aqueous loop-in-pool safety design, we are dealing with a pressurized water system. To handle different accident scenarios, we have to devise a passive system to control the potential release of high pressure primary coolant containing tritium at a concentration of 50 Ci/liter, and to prevent the release of induced radioactivities in the reactor structural materials under the conditions of a LOCA. The general approach we took to handle the scenario of a LOCA is to minimize its probability of occurrence and to reduce its impact. We designed the configuration of the reactor to make sure that a LOFA will not lead to a LOCA. Based on this approach, we were led to the use of the low-pressure pool design, wherein the high-pressure primary loop is submerged in a low-pressure water pool as show in Fig. 2.

The basic sources of thermal energy at reactor shutdown are from the plasma thermal and magnetic energy, the thermal energy of the hot loop, and the induced afterheat power from the torus first wall and blanket structures. In the case of a LOFA, the fusion power core and the primary loop piping routing is designed such that natural circulation can be developed to remove the blanket afterheat to the secondary loop.

4.1. LOFA and LOCA Analysis

Two of the postulated accidents for fusion reactors are LOFA and LOCA. A finite element heat conduction code was used in the evaluation of the TITAN-II design. Three accident scenarios were studied. The first case is a LOCA without a pool. This case was studied to verify the necessity of the low-temperature atmospheric-pressure pool. The second case is the LOFA (with pool as the heat sink). The final case studied is the LOCA with pool. In this case the primary coolant

piping is assumed to have ruptured into the low-pressure pool. The primary coolant will flash to steam, leaving the fusion power core uncooled until the pool refloods the core through the broken piping.

For the case of LOCA without a pool, the calculated peak temperature in the first wall is 1780°$C$and in the beryllium, 1755°C. These are 360°$C$and 471°Cabove the melting points for the ferritic steel and beryllium, respectively. These temperatures are clearly unacceptable, and a safety design approach is the use of the low-temperature pool. For the case of LOFA with a pool, the peak temperature of 348°$C$was calculated to occur at the first wall 355 sec after shutdown. Assuming a reflood time of 300 sec for the case of LOCA with a pool, the peak temperatures at the first wall and the beryllium zones are 732°$C$and 481°C, respectively. The temperatures for the last two cases are quite acceptable. When reflood was not assumed, the maximum temperature of 856°C, beyond which the structure cannot be reused, will be reached in 9 min. The melting temperature of the structure will be reached in 47 min. These effects will need to be considered in the detailed design for the purpose of investment protection, but due to the presence of the low-temperature pool, these accidents are not of concern for public safety.

4.2. Safety Scenarios

Based on the loop-in-pool concept of the TITAN-II design, different scenarios for the handling of normal and off-normal situations were evaluated. They are discussed in the following:

4.2.1. Normal operation

Under normal operation, the fusion power core will be actively cooled by the primary coolant loop system, and the thermal power will be removed by the heat exchangers for power conversion. At the same time, 34 MW of thermal power is conducted through the heat exchanger vessel and piping walls to the atmospheric pressure cold pool. This power is then removed by separate heat exchangers in the

pool.

4.2.2. Loss of primary coolant flow

In the accidental condition of the loss of primary coolant flow, the plasma reaction will need to be terminated. The primary heat exchangers are located above the fusion power core, at a distance of much higher than 1 m which is the minimum static head required to establish natural circulation in the loop. Thus, natural circulation will be established in the primary loop to remove the afterheat generated in the fusion power core. This afterheat power can then be removed from the primary loop by the active secondary loop heat removal system.

4.2.3. Loss of secondary coolant flow

In the situation of the loss of secondary coolant flow, the plasma reaction will need to be terminated. The afterheat power from the fusion power core can then be removed by natural circulation in the secondary loop or by conduction to the cold pool through the primary heat exchanger vessel walls and coolant piping, and then removed by the heat removal system in the cold pool.

4.2.4. Loss of secondary coolant

In the case of the loss of secondary coolant, the plasma reaction will have to be terminated and the afterheat power will be conducted to the cold pool and removed by the afterheat removal system in the pool.

4.2.5. Loss of primary coolant pressure

In the case of the loss of primary loop coolant pressure, which can potentially be caused by any sizable leakage in the primary coolant loop, the plasma reaction will need to be terminated. The thermal energy in the coolant of the primary loop will be mixed with the coolant of the cold pool. This pool coolant will also absorb the afterheat power from the first wall and blanket system. The discharged thermal energy in the pool can then be removed by the afterheat removal system in the

pool. If the pool afterheat removal system also fails, it becomes crucial to find out how fast the pool temperature would rise. A finite element transient heat transfer calculation was used for the evaluation. By including the earth surrounding the pool to help absorb the afterheat energy, results show that with an initial pool temperature of $70°C$, it would take more than 90 days for the water in the pool to reach $100°C$. This shows that the TITAN-II pool is fully adequate to handle the fusion power core shutdown afterheat, while allowing enough time for the recovery or replacement of the active afterheat power removal system.

4.2.6. Catastrophic failure of primary loop and pool containment

Only the catastrophic situation of the failure of the primary loop and the pool containment, would we face the worst case accident of release of the tritium inventory of the primary loop and the activation products from the first wall (LOCA without pool). Considering tritium alone, at a primary coolant loop tritium concentration of 50 Ci/liter, the complete release of the primary loop water would amount to 1.37 kg of tritium. This would be higher than the maximum allowable release of ~200 gm [7] which would give a site boundary dose of 25 Rem, the maximum allowed during severe hypothetical accidents (10CFR100) [4]. Due to the presence of the large pool of water, this is a very unlikely event.

4.3. Routine releases

For the TITAN-II design, routine tritium releases and handling of ^{14}C waste are more of a concern than the releases under severe accidents. The potential tritium leakage rate becomes a trade-off between tritium release and the costs of leakage control and the tritium extraction system. At a primary loop tritium concentration of 50 Ci/liter, the tritium extraction system total installed cost is \$170 M and would have a routine release rate of 50 Ci/day. These are relatively high yet acceptable values. Due to the generation of ^{14}C from the nitrate salt, frequent replacement of the water purification system ion exchange resin beds may been needed. Care in

the handling of the resin beds will be needed to control the routine release of ^{14}C to within allowable levels. The ^{14}C may require the resins to be treated as high level waste.

5. PLASMA CURRENT TERMINATION

A significant amount of energy is stored in the poloidal magnetic field in RFPs. For TITAN, I_p = 18 MA and the poloidal field energy of $1/2\, L_p\, I_p \approx 2$ GJ. Any rapid release of this stored energy caused by uncontrolled current termination, or loss of the equilibrium control system, can lead to severe consequences for both TITAN-I and TITAN-II fusion power core designs.

In order to guard against plasma accidents, a passive shutdown system is envisioned for the TITAN reactor which rapidly removes the poloidal field energy and reduces the plasma current while maintaining the plasma equilibrium and toroidal-field reversal. Such an emergency shutdown procedure starts with discharge of the superconducting equilibrium field (EF) coil through a resistor. As a result of the strong magnetic coupling between the plasma and the EF and ohmic heating (OH) coils in TITAN, the plasma current is reduced rapidly. The parameters of the EF and OH circuits can be chosen such that the plasma equilibrium is maintained during this discharge. The large time constant for field penetration of the Integrated Blanket Coil (IBC) toroidal field (TF) [2] coils is also utilized to ensure maintenance of field-reversal during the shutdown, similar to the current ramp-down technique. Preliminary simulations of such a shutdown procedure indicate that most of the poloidal field field energy is removed from the system and only about 200 MJ of energy is transferred to the first wall in a time scale of 50 to 100 ms, resulting in an average temperature rise in the first wall of about 300°C; failure of the first wall is not expected.

6. CONCLUSIONS

Based on the safety designs for the TITAN-I lithium self-cooled design, the following conclusions and recommendations can be made:

Judicious choices of safety design can limit the damage potential of the TITAN-I lithium self-cooled design. These choices are in the areas of material selection, neutronics design, cover gas, drain tanks, and configuration selection. Based on the analysis summarized above, TITAN-I does not need to rely on any active safety systems to protect the public. A LOFA results in no radioactive release and will not lead to a more serious LOCA. A complete LOCA from credible events is not possible. TITAN-I therefore meets the definition of level 3 of safety assurance, small-scale passive safety assurance. In the event of major primary pipe breaks and failure of the confinement building, air could enter the vacuum chamber. Because of the low lithium fire temperatures predicted during such an event, radioactive release due to reaction between air and the hot vanadium alloy may be quite modest.

The above results also indicate that the TITAN-II aqueous loop-in-pool design is a passively safe design by using the large pool of low temperature, atmospheric pressure water to dilute the contained thermal and afterheat energy to low enough temperature levels such that the tritium or other radioactive materials in the blanket coolant system will not be released. That means we can keep the public safe by maintaining the integrity of the water pool. Since the water pool structure can be considered a large-scale geometry, the TITAN-II design can be rated as a level 2 of safety assurance design.

To further quantify or to improve the safety features of the TITAN-I and TITAN-II designs, we will need some experimental data and to address some key issues. For the TITAN-I lithium self-cooled design, in order to further quantify the impacts from lithium fire, material data will be needed on oxidation of V-alloy at high temperature. For the TITAN-II aqueous loop-in-pool design, better control of the routine tritium releases and the handling of routine ^{14}C waste disposal will

enhance its safety features. For both TITAN-I and TITAN-II fusion power core designs, the safety impact of plasma accidents should be further investigated and various passive means for a safe plasma shutdown should be further explored.

ACKNOWLEDGEMENT

This is a report of work supported by the U.S. Department of Energy, Office of Fusion Energy, under Contract DE-AC03-84ER53158, and the University of California, Los Angeles, under Contract 0202 B 02744.

REFERENCES

1. F. Najmabadi *et al.*, "The Titan Reversed-Field Pinch Fusion Reactor Study, Scoping Phase Report," Joint Report of University of California, Los Angeles, GA Technologies Inc., Los Alamos National Laboratory and Rensselaer Polytechnic Institute, UCLA-PPG-1100, January 1987.

2. S. P. Grotz, N. M. Ghoniem, *et al.*, "Overview of the TITAN-I Fusion-Power Core," *International Symposium on Fusion Nuclear Technology, Tokyo, Japan*, April 10-19, 1988.

3. C. P. C. Wong *et al.*, "Overview of the TITAN-II Reversed-Field Pinch Aqueous Fusion Power Core Design," General Atomics Report GA-A19239, presented at the International Symposium on Fusion Nuclear Technology, Tokyo, Japan, April 10-19, 1988.

4. "Standards for Protection Against Radiation," U. S. N. R. C., Code of Federal Regulations, Title 10, Part 0 to 199, January 1986.

5. S. J. Piet, "Approaches to Achieving Inherently Safe Fusion Power Plants," Fusion Technology, **10** 1986, and "Inherent/Passive Safety For Fusion," 7th Topical Meeting on the Technology of Fusion Energy, Reno, Nevada, June 1986.

6. J. P. Holdren *et al.*, "Summary of the Report of the Senior Committee on Environmental, Safety and Economic Aspects of Magnetic Fusion Energy," Lawrence Livermore National Laboratory Report, UCRL-53766-Summary, September 10, 1987; and "Exploring the Competitive Potential of Magnetic Fusion Energy: The Interaction of Economics with Safety and Environmental Characteristics," Fusion Technology, **13** (1988).

7. I. Maya, K. R. Schultz, *et al.*, "Final Report, Inertial Confinement Fusion Reaction Chamber and Power Conversion System Study," General Atomics Report GA-A17842, October 1985.

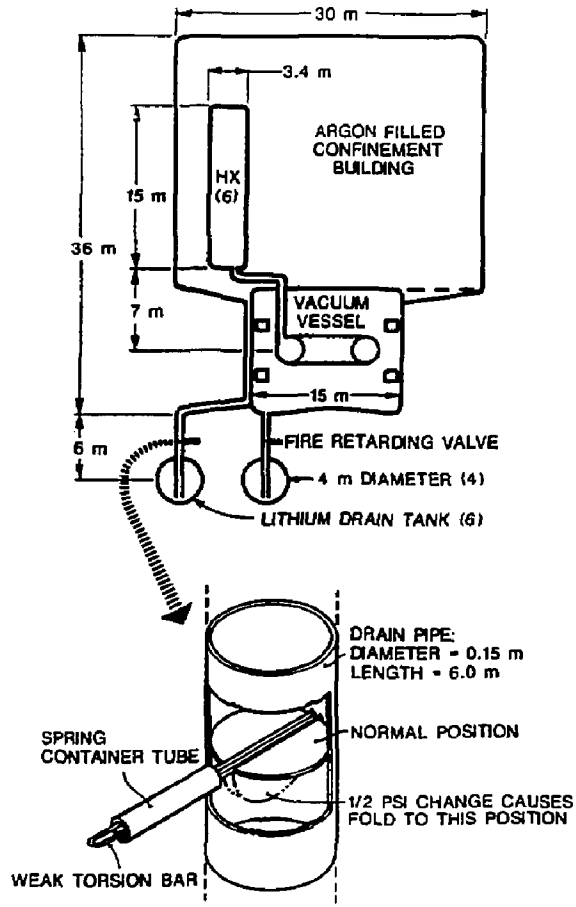

Figure 1. TITAN-I Safety Design Schematic with Fire Retarding Valves.

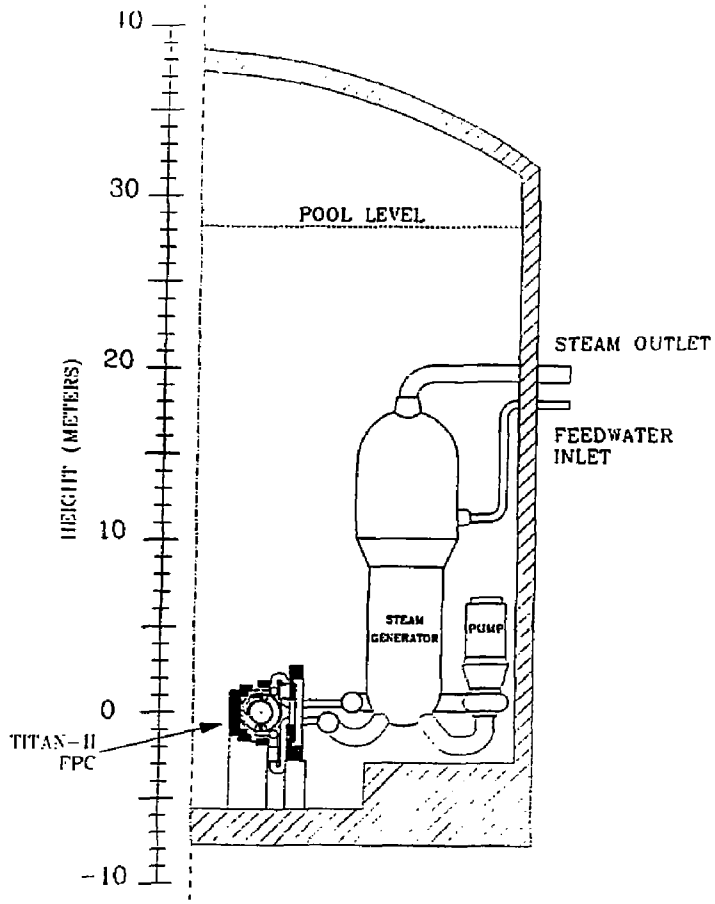

Figure 2. TITAN-II RFP Reactor Design.

ACTIVATION AND WASTE DISPOSAL OF THE TITAN RFP REACTORS

E T. Cheng, R. W. Conn,[1] and
The TITAN Research Group

General Atomics, San Diego, California 92138-5608, U. S. A.
[1] University of California, Los Angeles, California 90024-1600, U. S. A.

ABSTRACT

The TITAN-I lithium self-cooled and TITAN-II aqueous lithium nitrate solution-cooled fusion reactors are based on the reversed-field-pinch (RFP) toroidal confinement concept and operate at high power density with an 18.1 MW/m^2 neutron wall loading. These designs were analyzed to study the activation and waste disposal aspects of such high-power density reactors. It was found that because of the use of V-3Ti-1Si (TITAN-I) and reduced activation ferritic steel (TITAN-II) as structural alloys for the first wall, blanket, reflector, and shield components, all the TITAN components except the divertor collector plates can be classified as shallow-land burial (10CFR61 Class C or better) nuclear waste for disposal, provided that the impurity elements, niobium and molybdenum, can be controlled below about 1 and 0.3 appm levels, respectively. The average annual disposal masses were estimated to be 150 and 96 tonnes, respectively, for the 1000 MW TITAN-I and TITAN-II reactors. This corresponds to about 11% of the total mass in the fusion power core of both reactors. The divertor collector plates are fabricated with tungsten because of its low particle sputtering properties. These divertor collector plates in the TITAN-I reactor will be qualified as Class C waste after 18.1 MW-y/m^2 operation. The waste disposal rating of the divertor collector plates in the TITAN-II reactor, however, is estimated to be a factor of 4 higher than allowed for Class C disposal, because of the soft neutron spectrum in the beryllium environment. The annual disposal mass of this non-Class C waste is 0.35 tons, about 0.04% of the average annual discharge mass for the TITAN-II reactor. An additional 74 m^3 annual discharge of Class C waste containing ^{14}C may be needed for the TITAN-II reactor because of the use of nitrate salt in the aqueous coolant as the tritium breeder. The conclusions derived from the TITAN reactor study are general, and provide strong indications that Class C waste disposal can be achieved for other high-power density approaches to fusion, for example, the tokamak.

1. INTRODUCTION

Shallow land burial waste disposal (10CFR61 Class C or better) is an attractive goal for handling nuclear waste [1]. The fusion reaction (D + T → He + n) itself does not produce radioactive waste, and hence fusion energy has the potential of achieving the Class C waste disposal if the reactor materials are carefully selected and processed.

The conceptual design of the TITAN RFP fusion reactor, a high-power density reactor based on the reversed-field-pinch (RFP) toroidal confinement concept, was conducted recently [2]. A lithium self-cooled, vanadium alloy structured blanket and an aqueous solution-cooled, beryllium multiplier, ferritic steel structured blanket were selected as the promising concepts for the high neutron wall loading (18.1 MW/m^2) reactor design study. The activation of reactor materials and corresponding waste disposal issue were very important parameters considered during the neutronics design of the reactor. In this paper we present issues and results of analysis relevant to the waste disposal aspects of the reference TITAN RFP reactors, TITAN-I and TITAN-II.

2. RADIOACTIVE WASTE DISPOSAL ISSUES

The classification of nuclear waste disposal is given under the Code of Federal Regulations 10CFR61 [3]. Four waste classes have been defined: Class A (segregated waste), Class B (stable waste), Class C (intruder waste), and geologic waste. The first three classes of waste disposal involve shallow-land or better (near-surface) burial of nuclear waste, while the last class needs deep geologic burial. Most radionuclides with half-lives less than five years will decay by at least six orders of magnitude in 100 years after disposal. These radionuclides can be reasonably managed to meet either Class A or Class B disposal requirements. The long-lived radionuclides with half-lives greater than 100 years, however, will be difficult to meet both Class A and Class B disposal requirements solely by radioactive decay

to reduce the activity level. To qualify as Class C or better nuclear waste, the nuclear components in a fusion reactor should minimize the quantity of their alloying and/or impurity elements that would produce long-lived radionuclides.

The limiting specific activities for near-surface (Class A, B and C) disposal of nuclear waste are specified in 10CFR61 regulations for the following radionuclides: ^{59}Ni, ^{94}Nb, ^{99}Tc, ^{129}I, ^{90}Sr, ^{137}Cs, and alpha-emitting transuranic nuclide with half-lives greater than five years. Note that these limiting specific activities are given primarily for radionuclides relevant to present-day applications such as fission reactors. Many radionuclides with half-lives greater than five years, such as ^{42}Ar (half-life 33 y), ^{108m}Ag (127 y), and ^{186m}Re (2×10^5 y), may be produced in fusion reactors in the elements constituting the structural materials such as vanadium alloy, the particle collecting plates such as tungsten, and in impurities in the structural alloys. However, the limiting specific activities for near-surface disposal of nuclear waste containing these nuclide are not available in 10CFR61. There are also several important radionuclides whose specific activity limits are not given by 10CFR61 evaluations or other estimates: ^{39}Ar, ^{152}Eu, ^{192m}Ir, ^{137}La, ^{186m}Re, ^{121m}Sn, and ^{158}Tb. A complete evaluation was recently performed by Fetter [4], providing limiting specific activities for near-surface disposal of all radionuclides with proton numbers less than 84. These evaluations, consistent in methodology with the 10CFR61 regulations, will be employed in the waste disposal analysis of the TITAN study. Note that there may exist discrepancies between Fetter's evaluations and 10CFR61 or other estimates. The major discrepancy occurs with the nuclide Ni-63 for which Fetter's evaluation is greater than 10CFR61 evaluation by more than two orders of magnitude. Comparison of these evaluations and resolution over the discrepancies should be carried out frequently as the development of fusion energy technologies goes along.

3. REFERENCE DESIGN AND NEUTRON FLUXES

Neutronics designs of the vanadium-alloy (V-3Ti-1Si) structured, lithium self-

cooled TITAN-I and nitrate salt aqueous solution-cooled TITAN-II reactors were performed considering several parameters including tritium breeding radio, replacement mass of the blanket/shield, afterheat, and radiation damage to the ohmic heating (OH) magnets. The details of the blanket/shield design for both reactors are given in Refs. 5 and 6. The reference designs derived from the neutronics design study are given in Table 1 and summarized below. The TITAN-I reference design consists of a 10 mm first wall, a 0.28 m integrated blanket coil (IBC) zone, a 0.3 m reflector, and a 0.15 m shield, as shown in Table 1. The first wall is based on the tube concept and is composed of 40% vanadium alloy, 37.5% lithium, and 22.5% void, all by volume. The IBC zone consists of 18% vanadium alloy, 72% lithium and 10% void. The reflector is made of 30% vanadium and 70% lithium. Finally, the shield is composed of 90% vanadium and 10% lithium. The ^{6}Li enrichment in lithium is chosen at 30% for the reference design as a compromise between neutronics performance and cost of enrichment.

The TITAN-II design, also shown in Table 1, consists of a 15 mm first wall, a 0.2 m beryllium multiplying zone, a 0.17 m reflector zone, a 30 mm shield, and a 50 mm TF coil zone. The first wall is made of 16.7% ferritic steel, 61.8% coolant, and 21.5% void. The compositions in the beryllium zone are 12.2% ferritic steel, 29.1% coolant, and 58.7% beryllium (90% dense). The reflector is composed of 9% ferritic steel structure and 91% coolant. The shield consists of 91% ferritic steel and 9% coolant. A copper TF coil is needed for the TITAN-II design. It is located immediately behind the shield and cooled by cold water. The first wall, blanket, reflector and shield are cooled by an aqueous solution of lithium nitrate dissolved in water. The lithium content in the aqueous coolant is 6.4 at.%. The ^{6}Li enrichment in lithium is adjusted to optimize the tritium breeding ratio which is 1.2 in the one-dimensional model. The corresponding ^{6}Li enrichment in the TITAN-II reference design is 12%.

The neutron fluxes calculated for the reference TITAN reactors were employed

as the input to the activation calculation code, REAC [7]. The neutron spectra at the first wall, reflector, shield, and OH magnet components are discussed below. The neutron fluxes integrated from thermal to 14.5 MeV for TITAN-I and TITAN-II are 4.4×10^{15} and 5.5×10^{15} n/cm^2/sec, respectively, at the first wall, when the neutron wall loading is 18.1 MW/m^2. The maximum integrated neutron fluxes at the reflector, shield, and OH magnet components are about 1.5×10^{15}, 4.6×10^{14}, and 1.7×10^{14} n/cm^2/sec, respectively, for the TITAN-I design and 8.0×10^{14}, 3.8×10^{14}, and 7.2×10^{13} n/cm^2/sec, respectively, for the TITAN-II design. The neutron flux reduction factors in the blanket, reflector, and shield components are, therefore, 2.9, 3.3, and 2.7, respectively for the TITAN-I design. They are, however, 6.6, 3.5 and 1.3, respectively, for the TITAN-II design. It is obvious from the above comparison that beryllium is a much better neutron moderator/attenuator than lithium.

For the TITAN-I lithium blanket design, the contribution of neutron flux by neutrons at energies above 0.1 MeV is about 82% at the first wall. It then drops to 70%, 52% and 43%, respectively, at the reflector, shield and OH magnet components. For the TITAN-II aqueous solution-cooled blanket design, however, the contribution of neutron flux above 0.1 MeV at the first wall is about 60% and it remains so throughout these components. This indicates a relatively high fraction of low-energy neutrons in respective components due to either enhanced neutron moderation (TITAN-II) or reduced lithium content (TITAN-I reflector and shield). The increase of low-energy neutron population in the reactor components will result in a higher production rate of long-lived radionuclides, such as Nb-94 which depends on (n,γ) reactions in niobium.

4. ANALYSIS OF RADIOACTIVITY AND DECAY-HEAT

Activation calculations were performed for the TITAN-I and II components following one full-power-year operation at 18.1 MW/m^2 wall loading. Table 2 shows the elemental compositions used in the analyses. Note that the lists of elements

shown in Table 2 include all major constituent elements in both V-3Ti-1Si alloy and reduced activation ferritic steel. But they do not cover all possible impurity elements in these alloys. The implications of the lack of information on complete lists of impurities will be addressed whenever appropriate. The results of activation calculations for structural alloys at the first wall are given in Tables 3 and 4. The results in components other than the first wall are primarily very similar except that the levels of activation will be reduced according to the attenuation of neutron fluxes when the location is moved away from the first wall.

Tables 3 and 4 give the induced radioactivity and decay-heat values, respectively, in the first wall component for V-3Ti-1Si alloy and reduced activation ferritic steel in the TITAN-I and -II neutron radiation environment. They are presented at one minute, one day, one year, and 100 years after shutdown. The corresponding major contributing radionuclides are also identified in these two tables. As shown in Table 3, the activity induced in V-3Ti-1Si alloy is about 200 Ci/cm^3 at one minute after shutdown. It drops to 60 and 6.3 Ci/cm^3, respectively, at one day and one year after shutdown. Within one year after shutdown, the activities induced in V-3Ti-1Si alloy are primarily dominated by ^{48}Sc (half-life 43.7 h), ^{49}V (330 d), ^{47}Sc (3.35 d), ^{97}Ru (2.9 d), ^{99m}Tc (6.02 h), and a few very short-lived radionuclides such as ^{51}Ti (5.76 min) and ^{52}V (3.75 min), as seen in Table 3. The dominating radionuclides, except ^{97}Ru and ^{99m}Tc, are all induced from the constituent elements, namely vanadium, titanium, and silicon. The radionuclides ^{97}Ru and ^{99m}Tc are due to the impurity element, molybdenum (351 appm), included in the activation calculations, as shown in Table 2. A minor contribution (less than 10%) is also observed at one year after shutdown due to iron impurity (568 appm), while the main contributor is ^{49}V resulting from ^{50}V $(n, 2n)$ reactions. At 100 years after shutdown, the activity is reduced to about 1×10^{-3} Ci/cm^3, and is primarily dominated by radionuclides induced from impurities included in the calculation. As shown in Table 3, these dominating radionuclides are ^{99}Tc (2.6×10^6 y), ^{91}Nb (700 y), and

^{93}Mo (3.5×10^3 y), all from molybdenum impurity; ^{14}C (5730 y) from nitrogen (0.22%), and ^{63}Ni (100 y) from copper impurity (59 appm). This implies that the induced activity in V-3Ti-1Si alloy due to major constituent elements drops significantly at times beyond about 10 years after shutdown, and the long term activity is primarily due to either minor constituents such as nitrogen or impurities such as Mo and Cu.

The activity profile for reduced activation ferritic steel is very similar to that for V-3Ti-1Si alloy, except that the long-term activity is also contributed to significantly by the constituent elements, Fe (80.3%), and W (0.89%). The activity at one minute after shutdown is about 1.4×10^3 Ci/cm^3, as shown in Table 3. It then drops to about 5.5×10^2, 2.3×10^2, and 9.9×10^{-4} Ci/cm^3, at one day, one year, and 100 years after shutdown. The dominating radionuclides up to one year after shutdown are ^{55}Fe (2.68 y), ^{54}Mn (313 d), and ^{51}Cr (27.7 d), mainly resulting from neutron reactions with Fe, Mn (6.47%), and Cr (11.8%) isotopes. The dominating radionuclides at 100 years after shutdown are ^{178}Hf (31 y) and ^{186m}Re (2×10^5 y) from W; and ^{53}Mn (3.7×10^6 y) from Fe. The contribution to long-term radioactivity due to impurities not shown in Table 2 should be comparable to the level induced from the main constituent elements, as will be described in detail in the next section.

Table 4 shows the decay-heat heating values, the integrated decay energy, and the corresponding dominating radionuclides for V-3Ti-1Si and reduced activation ferritic steel at several times after shutdown. As seen in Table 4, the decay-heat heating values from V-3Ti-1Si are about 2.5, 0.77, 2.94×10^{-3}, and 2.2×10^{-8} W/cm^3, respectively, at one minute, one day, one year, and 100 years after shutdown. The dominating radionuclides contributing to the afterheat within one year after shutdown are primarily ^{48}Sc [induced from ^{51}V (n, α) reactions], and two other short-lived radionuclides, ^{51}Ti and ^{52}V, from Ti and V. Manganese-54 is induced from Fe impurity but its activity is not significant until about one year after shutdown as shown in Table 4. At 100 years after shutdown, again the

major contributors are those induced from minor constituents, namely nitrogen and impurities. The integrated decay energies for V-3Ti-1Si in the TITAN-I first wall are, as indicated in Table 4, about 1.4×10^{2}, 7.3×10^{4}, 1.7×10^{5}, and 2.0×10^{5} J/cm^3, respectively, at one minute, one day, one year and 100 years after shutdown.

The decay-heat heating values for the reduced activation ferritic steel in the TITAN-II first wall are, as also shown in Table 4, about 12.4, 0.72, 0.26, and 3.3×10^{-9} W/cm^3, respectively, at one minute, one day, one year, and 100 years after shutdown. The corresponding integrated decay energies at these times are 7.5×10^{2}, 2.5×10^{5}, 2.4×10^{6}, and 1.1×10^{7} J/cm^3, respectively. The dominating radionuclides at times up to about one year are primarily ^{54}Mn and ^{56}Mn from Fe and Mn. The decay-heat heating values at 100 years after shutdown are, however, dominated by ^{178m}Hf and ^{186m}Re, all from the minor constituent element, W, although these values are relatively insignificant.

5. ANALYSIS OF RADIOACTIVE WASTE DISPOSAL

The activation calculations performed for the TITAN reactor components at 18.1 MW/m^2 neutron wall loading were analyzed to obtain the allowable concentrations of alloying and impurity elements, in terms of atom % or appm in the vanadium alloy that possesses a number density of 7.22×10^{22} atoms/cm^3, and in the reduced activation ferritic steel that has a number density of 8.37×10^{22} atoms/cm^3, in the materials constituting the first wall/blanket, reflector, shield, and magnet components of the TITAN-I and TITAN-II reactors. Note that the two main alloying elements in the V-3Ti-1Si alloy, namely vanadium and titanium, have no limits on their concentrations as far as Class C nuclear waste is concerned at any locations in the TITAN-I reactor. The other alloying element, silicon, also poses no problem for the Class C disposal of the vanadium alloy since its allowable concentration (23%) is much higher than needed in this alloy (1 wt%). By the same token, for the TITAN-II reactor, the main alloying elements of reduced activation ferritic steel, namely iron, chromium, and manganese, and all

minor constituent elements also have no limits on their concentrations for Class C near-surface disposal. It appears, hence, that impurities and their levels are the most important subjects for investigation in the nuclear reactor materials for both TITAN-I and TITAN-II.

The impurity elements and their levels in the V-3Ti-1Si alloy and the reduced activation ferritic steel are not specifically given in literature. The information compiled in Ref. 8 for V-15Cr-5Ti and modified ferritic steel was employed for comparison in this study. Table 5 gives the allowable concentration levels of alloying and impurity elements for Class C disposal of TITAN I and TITAN-II components. The impurity elements shown in this table are those considered to be the most important ones, as identified in a recent study [4]. By comparing Table 5 and Ref. 8 we found that Nb (4 appm in Ref. 8) and Mo (3 ppm in Ref. 8) are probably the only impurity elements that have to be controlled for the TITAN-I and TITAN II blanket/shield component, respectively. As shown in Table 5, the allowable impurity level for Nb in the TITAN-I blanket/reflector/shield is about 1.4 appm, while the allowable concentration level for Mo is about 0.27 appm for the TITAN-II reactor materials. Although the list of impurity elements is given in Ref. 8, caution should be made with some elements that are not shown in the list require strict concentration limits (1 appm or less) for Class C disposal. These elements are Ag, Ir, and Tb and their concentration limits for TITAN-I materials are 1.3, 0.1, and 0.4 appm, respectively, as shown in Table 5. The allowable concentration levels of Ag and Ir for TITAN II materials are, still, more restrictive due to a softer neutron spectrum. These levels are, as shown in Table 5, 0.05 and 0.001 appm, respectively. The allowable concentration level of Tb for TITAN-II materials, 1.1 appm, is slightly higher than for TITAN-I material. The crustal abundance of Ag, Ir, and Tb are, however, 0.07, 0.001, and 0.9 appm, respectively. This implies that with the natural crustal abundance, the Tb impurity concentration in the TITAN-I reactor, and Ag impurity concentration in the TITAN-II reactor, may exceed the limit for Class C

disposal. Special attention has to be made to control the concentration of these impurity elements, Tb and Ag.

Table 5 also gives the allowable concentrations of tungsten in the TITAN first wall, blanket, reflector and shield components. Tungsten collector plates are needed in the divertor component because of their low particle sputtering and high temperature properties. Tungsten is also a minor alloying element in the reduced activation ferritic steel structure (replacing the more restrictive molybdenum in the regular ferritic steel) for the TITAN-II blanket and shield. The allowable concentration of tungsten in the divertor collector plates, located mostly close to the plasma, is more than 100% for the TITAN-I reactor, and is about 13% for the TITAN-II reactor, if the branching ratio to produce the isometric ^{186m}Re nuclide is only 1%. Mixing with the adjacent vanadium alloy and ferritic steel in the TITAN-I and -II reactors, respectively, the tungsten concentration in the collector plates/tubes is about 50%. This gives the divertor component a Class C waste rating for the TITAN-I, unless the branching ratio is much higher than 1% or other more restrictive alloying elements are employed. The waste disposal rating of the divertor collector plates in the TITAN-II reactor will be, however, a factor of 4 higher than the limit for Class C disposal. Nevertheless, the quantity involved in the divertor collector plate component to be disposed of annually is very small, only about 0.35 tons (0.03 m^3 by volume). A non-Class C disposal of the divertor component should result in little impact on the waste disposal characteristics of these TITAN reactors. We may conclude from the above discussions that all TITAN components, except the divertor collector plates in the TITAN-II reactor, may be classified as Class C or better nuclear waste if the impurity elements (mainly niobium and molybdenum) are controlled below the allowable limits.

Table 6 summarizes the TITAN-I and TITAN-II materials and related quantities for Class C disposal. Note that the total weight in the fusion power core of the TITAN-I reactor is about 1363 tons, of which about 73% is due to the mag-

netic systems (OH and EF coils, and EF shield) that have a 30 full-power-year lifetime. The total weight in the fusion power core of the TITAN-II reactor is about 846 tonnes, of which about 60% is due to the TF coils and other magnetic systems that also have a 30 full-power-year lifetime. The disposal of these magnetic system materials is needed only at decommissioning of the power plant. The average annual replacement mass of the fusion power core is about 150 tonnes (23.8 m^3), as shown in Table 6 for the TITAN-I reactor. It is about 96.4 tonnes (12.3 m^3) per year, for the TITAN-II reactor, as also shown in Table 6. For the TITAN-II reactor, because of use of nitrate salt in the aqueous coolant, ^{14}C is produced due to ^{14}N (n,p) reactions. The annual production rate of ^{14}C is about 52,000 Ci. An additional 74 m^3 by volume quantity of Class C waste in the form of ion exchange resins contaminated with ^{14}C needs to be disposed of annually.

6. CONCLUSIONS

As a result of the waste disposal analysis, we found that a compact, high-power density fusion reactor, particularly the TITAN reactor, can be designed to meet the criteria for Class C waste disposal. The key features for achieving Class C waste in the TITAN reactors are attributed to (1) materials selection and (2) control of impurity elements. The materials selected for the TITAN reactors are V-3Ti-1Si and lithium, and reduced activation ferritic steel and aqueous coolant, for the first wall, blanket, reflector and shield. The main alloying elements of these materials do not produce long-lived radionuclides with activity levels exceeding the limits for Class C disposal. The impurity elements, however, mainly niobium, molybdenum, and possibly silver, terbium, and iridium, need to be controlled in the vanadium alloy and ferritic steel to part per million levels or less.

The average annual disposal mass for the TITAN-I reactor was estimated to be 150 tonnes (23.8 m^3), about 11% of the total mass in the fusion power core, for producing 1000 MW electric power. It is 96.4 tonnes (12.3 m^3) for the TITAN-II reactor, representing also about 11% of the total mass in the fusion power core.

The divertor collector plates are fabricated with tungsten because of its low particle sputtering properties. The waste disposal rating of the divertor collector plates for the TITAN-II reactor was estimated to be a factor of 4 higher than allowable for Class C disposal. The annual disposal mass of these non-Class C divertor collector plates, however, is only 0.35 tonnes, about 0.4% of the average annual discharge rate for TITAN-II. Nitrate salt is chosen in the TITAN-II design as the lithium compound to be dissolved in the aqueous solution for tritium breeding purpose. The production of significant quantity of ^{14}C due to ^{14}N (n,p) reactions results in the disposal of additional Class C waste, about 74 m^3 annually.

The conclusions derived from the TITAN reactor study are general, and provide strong indications that Class C waste disposal can be achieved for other high-power density approaches to fusion, for example, the tokamak. These conclusions also depend on the acceptance of recent evaluations of specific activity limits carried out under 10CFR61 methodologies.

ACKNOWLEDGEMENTS

This work was supported by the U.S. Department of Energy, Office of Fusion Energy, under contract DE-AC03-84ER53158. It was performed as part of the TITAN RFP reactor study project.

REFERENCES

1. R. W. Conn *et al.*, "Report of the DOE Panel on Low Activation Materials for Fusion Applications," University of California, Los Angeles Report UCLA/PPG-728, June 1983; also see R. W. Conn *et al.*, Nucl. Technology/Fusion **5**, (1984) 291.

2. R. W. Conn *et al.*, "The TITAN Reversed-Field Pinch Fusion Reactor Study," Proc. 12th Symp. Fusion Engineering, Monterey, California, October 12–16, 1987.

3. Code of Federal Regulations, "Licensing Requirements for Land Disposal of Radioactive Waste," Title 10, part 61 (Washington, DC: Nuclear Regulatory Commission, December 30, 1982).

4. S. Fetter, E. T. Cheng, and F.M. Mann, "Long-term Radioactivity in Fusion Reactors," accepted for publication in Nucl. Eng. Design/Fusion; also see references cited in this paper.

5. E. T. Cheng *et al.*, "Neutronics Designs of Blanket and Shield for the TITAN High Wall Loading RFP Reactor," Proc. 12th Symp. Fusion Engineering, Monterey, California, October 12–16, 1987.

6. F. Najmabadi, R. W. Conn, N. M. Ghoniem, S. P. Grotz, J. Blanchard, *et al.*, "The TITAN Reversed-Field Pinch Fusion Reactor Study; The Final Report," UCLA-PPG-1200, Joint Report of University of California - Los Angeles, GA Technologies, Inc., Los Alamos National Laboratory, and Rensselaer Polytechnic Institute, March 1988.

7. F. M. Mann, "Transmutation of Alloys in MFE Facilities as Calculated by REAC (A Computer Code for Activation and Transmutation Calculations)," Hanford Engineering and Development Laboratory Report HEDL-TME 81-37 (1982).

8. D. L. Smith *et al.*, "Blanket Comparison and Selection Study, Final Report," Argonne National Laboratory Report ANL/FPP-84-1 (September 1984), Chap. 6, Table 6.12-1A.

Table 1

Dimensions and Material Compositions

of the TITAN-I and -II Reactors for Neutronics Analysis

	TITAN-I		*TITAN-II*	
Region	Thickness (m) (lifetime)	Material Composition	Thickness (m) (lifetime)	Material Composition
First wall	0.01 (1 FYP)	40% structure[a] 35% lithium[b] 22.5% void	0.015 (1 FPY)	16.7% structure[c] 61.8% coolant[d] 21.5% void
Breeding blanket	0.28 (1 FPY)	18% structure 72% lithium 22.5% void	0.20 (1 FPY)	12.2% structure 29.1% coolant 58.7% beryllium[e]
Reflector	0.28 (5 FPY)	30% structure 70% lithium	0.17 (1 FPY)	9% structure 91% coolant
Hot shield	0.15 (5 FPY)	90% structure 10% lithium	0.03 (1 FPY)	91% structure 9% coolant
TF coils	0.0 —	Integrated-blanket-coil concept employed	0.05 (30 FPY)	10% structure 10% spinel 10% H_2O 70% copper

Cold shield	0.0 —	none	0.05 (30 FPY)	H_2O
OH coils	0.42 (30 FPY)	10% structure 10% spinel 10% helium 70% copper	0.42 (30 FPY)	10% structure 10% spinel 10% H_2O 70% copper

[a]Vanadium alloy, V-3Ti-1Si.

[b]*30% ^6Li in lithium.*

[c]Reduced activation ferritic steel.

[d]Aqueous solution with lithium nitrate dissolved in water. The lithium content in the solution is 6.4 at.n%. The ^{6}Li enrichment in lithium is 12% to optimize the tritium breeding ratio (1.2).

[e]90% dense.

Table 2

Elemental Compositions (atomic percent) of V-3Ti-1Si Alloy and Reduced Activation Ferritic Steel Employed for TITAN-I and -II Analyses

Element	V-3Ti-1Si	Reduced Activation Ferritic Steel
V	93.65	0.280
Ti	3.72	—
Si	2.13	0.110
Fe	0.0586	80.33
Cr	0.0172	11.81
Cu	0.00585	—
Mo	0.0351	—
N	0.2216	0.0030
C	0.0846	0.0970
O	0.0856	—
Nb	0.00053	—
Mn	—	6.47
S	—	0.0050
P	—	0.0050
W	—	0.890

Table 3
Radioactivity and Corresponding Major Contributing Radionuclides Induced in Main Alloying Elementsfor V-3Ti-1Si (TITAN-I) and Reduced Activation Ferritic Steel (TITAN-II) at the First Wall After One Full-Power-Year Operation at (18.1 MW/m² Neutron Wall Loading)

		Time After Shutdown			
		1 minute	1 day	1 year	100 years
V-3Ti-1Si (TITAN-I)	Activity (Ci/cm³)	1.99×10^{2}	5.96×10^{1}	6.26	1.02×10^{-3}
	Dominating radionuclides (half-life)	^{51}Ti (5.75 min)[a]; ^{52}V (3.75 min)[a]; ^{48}Sc (43.7 h)[a]; ^{99m}Te (6.02 h)[a]; ^{49}V (330 d)[a]; ^{28}Al (2.24 min)[b]; ^{47}Sc (3.35 d)[b]; ^{97}Ru (2.9 d)[b]	^{48}Sc[a]; ^{49}V[a]; ^{47}Ca[a]; ^{97}Ru[a]; ^{46}Sc (83.8 d)[b]; ^{97m}Tc (90.5 d)[b]; ^{45}Ca (164 d)[b]	^{49}V[a]; ^{55}Fe (2.68 y)[a]	^{99}Tc (2.6×10^{5} y)[a]; ^{93}Nb (700 y)[a]; ^{14}C (5730 y)[a]; ^{63}Ni (100 y)[a]; ^{93}Mo (3.5×10^{3} y)[b]
Reduced activation ferritic steel (TITAN-II)	Activity (Ci/cm³)	1.37×10^{3}	5.47×10^{2}	2.32×10^{2}	9.9×10^{-4}
	Dominating radionuclides (half-life)	^{56}Mn (2.6 h)[a]; ^{55}Fe (2.68 y)[a]; ^{54}Mn (313 d)[a]; ^{51}Cr (27.7 d)[b] ^{52}V (3.75 min)[b]; ^{185m}W (1.67 min)[b]; ^{185}W (75.1 d)[b]; ^{187}W (23.9 h)[b]; ^{186}Re (90.6 h)[b]	^{55}Fe[a]; ^{54}Mn[a]; ^{51}Cr[a]; ^{185}W[b]; ^{187}W[b]; ^{186}Re[b]	^{55}Fe[a]; ^{54}Mn[a]	^{178}Hf (31 y)[a]; ^{186m}Re (2×10^{5} y)[a]; ^{53}Mn (3.7×10^{6} y)[a]

[a]More than 10% contribution.
[b]Contribution more than 1% but less than 10%.

Table 4
Decayheat, Integrated Decay Energy, and
Corresponding Major Contributing Radionuclides
Induced in Main Alloying Elements for V-3Ti-1Si (TITAN-I)
and Reduced Activation Ferritic Steel (TITAN-II) at the First Wall
(After One Full-Power-Year Operation
at 18.1 MW/m^2 Neutron Wall Loading

		Time After Shutdown			
		1 minute	1 day	1 year	100 years
V-3Ti-1Si (TITAN-I)	Decayheat (W/cm^3)	2.54	7.70×10^{-1}	2.94×10^{-3}	2.21×10^{-6}
	Integrated decay energy J/cm^3	1.41×10^2	7.31×10^4	1.71×10^5	2.01×10^5
	Dominating radionuclides (half-life)	^{51}Ti (5.76 min)^a; ^{48}Sc (43.7 h)^a; ^{52}V (3.75 min)^a; ^{28}Al (2.24 min)^b	^{48}Sc^a; ^{47}Sc (3.35 d)^b; ^{46}Sc (83.8 d)^b; ^{97}Ru (2.9 d)^b	^{49}V (330 d)^a; ^{54}Mn (313 d)^a; ^{60}Co (5.27 y)^b	^{99}Tc (2.6×10^6 y)^a; ^{14}C (5130 y)^a; ^{94}Nb (2×10^4 y)^a; ^{98}Tc (4.2×10^6 y)^a; ^{91}Nb (700 y)^b; ^{63}Ni (100 y)^b; ^{93}Mo (3.5×10^3y)^b
Reduced activation ferritic steel (TITAN-II)	Decayheat (W/cm^3)	1.24×10^1	7.21×10^{-1}	2.57×10^{-1}	3.34×10^{-6}
	Integrated decay energy (J/cm^3)	7.54×10^2	2.50×10^5	2.42×10^6	1.13×10^7
	Dominating radionuclides	^{56}Mn (2.6 h)^a; ^{54}Mn (313 d)^b; ^{52}V (3.75 min)^b	^{54}Mn^a; ^{187}W (23.9 h)^b	^{54}Mn^a; ^{55}Fe (2.68 y)^b	^{178m}Hf (31 y)^a; ^{186m}Re (2×10^5 y)^a

^{a}More than 10% contribution.
^{b}Contribution more than 1% but less than 10%.

Table 5
Allowable Concentration Levels of Impurity Elements
in TITAN First Wall, Blanket, Reflector and Shield Materials
to Qualify as Class C Near-Surface Disposal After Full Scale Exposure

Element	Major Nuclide (activity limit)[a]	TITAN-I Self-Cooled Lithium No Multiplier	TITAN-II Lithium Nitrate Aqueous Solution Beryllium Multiplier	Crustal Abundance (ppm)
Ag	^{108m}Ag (3 Ci/m^3)	1.3 ppm	0.05 ppm	0.07
Ir	^{192m}Ir (2 Ci/m^3)	0.1 ppm	0.001 ppm	0.001
Mo	^{99}Tc (0.2 Ci/m^3 ^{94}Nb (0.2 Ci/m^3)	65 ppm	0.27 ppm	6
Nb	^{94}Nb (0.2 Ci/m^3)	1.4 ppm	8.3 ppm	20
Tb	^{158}Tb (4 Ci/m^3)	0.4 ppm	1.1 ppm	0.9
W	^{186m}Re (9 Ci/m^3)	500%	75%[b]	2

[a]See Ref. 4.
[b]The allowable level in the first wall component is 13% only.

Table 6
Summary of TITAN-I and TITAN-II Reactor
Materials and Related Waste Quantities
for Class C Near-Surface Disposal

Component	TITAN-I			TITAN-II		
	Material (Lifetime)	Volume[a] (m^3/y)	Mass[b] (tonnes/y)	Material (Lifetime)	Volume (m^3/y)	Mass (tonnes/y)
FW/blanket	V-3Ti-1Si (1 FPY)	6.8	41.7	RAFS[c] (1 FPY)	2.8	21.7
Reflector and shield	V-3Ti-1Si (5 FPY)	8.7	53.5	RAFS (1 FPY)	5.9	45.8
OH, EF coils and shield	Copper + steel + B_4C + insulator (30 FPY)	4.7	33.3	Copper + steel + insulator (30 FPY)	3.1[d]	25.1[d]
Divertor shield	V-3Ti-1Si	3.6	22.4	RAFS	0.5	3.8
	Total Class C Waste	23.8	151	Total Class C Waste	12.3	96.4

[a]Annual average disposal value.
[b]Annual average disposal mass.
[c]Reduced activation ferritic steel.
[d]Including TF coils.

MAINTENANCE PROCEDURES FOR THE TITAN-I AND TITAN-II REVERSED FIELD PINCH REACTORS

S. P. Grotz, R. L. Creedon[1], P. I. H. Cooke[2], W. Duggan[3], R. Krakowski[4], F. Najmabadi and C. P. C. Wong[1], and *The TITAN Research Group*

Department of Mechanical, Aerospace and Nuclear Engineering
and Institute for Plasma and Fusion Research
University of California, Los Angeles
Los Angeles, CA 90024-1597

ABSTRACT

The TITAN reactor is a compact, high-power-density (neutron wall loading 18 MW/m^2) machine, based on the reversed-field-pinch (RFP) confinement concept. Two designs for the fusion power core have been examined; TITAN-I uses a self-cooled lithium loop with a vanadium-alloy structure for the first wall, blanket and shield, and TITAN-II is based on an aqueous loop-in-pool design with a $LiNO_3$ solution as the coolant and breeder. The compact design of the TITAN fusion power cores (FPCs) reduces the system to a few small and relatively low mass components, making toroidal segmentation of the FPC unnecessary. A single-piece maintenance procedure is possible. The potential advantages of single-piece maintenance procedures are: 1) shortest period of down time resulting from scheduled and unscheduled FPC repairs, 2) improved reliability resulting from integrated FPC pretesting in an on-site, non-nuclear test facility where coolant leaks, coil alignment, thermal expansion effects, etc., would be corrected prior to committing to nuclear service using rapid, and inexpensive, hands-on repair procedures, 3) no adverse effects resulting from the interaction of new materials operating in parallel to radiation damaged materials, and 4) ability to continually modify the FPC design as may be indicated by reactor performance and technological developments. Increased availability can be expected from a fully pre-tested, single-piece FPC. Pre-testing of the FPC throughout the assembly process and prior to installation into the reactor vault is discussed.

---

[1] *General Atomic Technologies, Inc., San Diego, California 92138, USA*
[2] *Permanent address: UKAEA Culham Lab., Abingdon, Oxon OX14 3DB, U. K.*
[3] *Rensselaer Polytechnic Institute, Troy, New York 12180 USA*
[4] *Los Alamos National Laboratory, Los Alamos, New Mexico 87545, USA.*

1. INTRODUCTION

The TITAN Reversed-Field Pinch (RFP) fusion reactor research effort [1,2] has been undertaken to determine the technical feasibility and key developmental issues of an RFP fusion reactor, especially at high power density, and to determine the potential economics (cost of electricity), operations, safety, and environmental features of high-mass-power-density fusion systems. Two different detailed designs, TITAN-I and TITAN-II, have emerged and parametric systems studies have been utilized both to optimize the point designs and to determine the parametric design window associated with each approach. This combination of parametric and point design work is referred to as a "parapoint" study. Complete details of the TITAN-I and TITAN-II fusion power core designs can be found in the TITAN Final Report [1]. This paper summarizes the maintenance procedures for both designs. Also discussed are the potential advantages of single-piece maintenance and pre-testing of the FPC.

TITAN is a compact, high neutron wall load reversed-field pinch reactor. The small size of the fusion power core, (FPC) permits the design of the reactor to be a single piece rather than a modular system. The potential advantages of single-piece maintenance procedures are: 1) shortest period of down time resulting from scheduled and unscheduled FPC repairs, 2) improved reliability resulting from integrated FPC pretesting in an on-site, non-nuclear test facility where coolant leaks, coil alignment, thermal expansion effects, etc. would be corrected prior to committing to nuclear service using rapid, and inexpensive, hands-on repair procedures, 3) no adverse effects resulting from the interaction of new materials operating in parallel to radiation damaged materials, and 4) ability to continually modify the FPC as may be indicated by reactor performance and technological developments.

A key assumption for the TITAN maintenance program is that a high degree of automation is available. Specifically, powered-joints are used extensively for

hydraulic and electrical connect/disconnects. The use of powered-joints allows many tasks to be done quickly and in parallel, thus reducing the time required for maintenance. Typical powered-joints can be found in Reference 3. Automation and remote connections are highly specialized components, designed to perform only a single function. This ensures that they can be designed robustly, have good reliability and operate quickly. An analogy can be drawn to the automotive industry. Replacement of a flat tire on a passenger car is a task that requires many minutes, at best. However, replacement of the tire on a racing car, using highly specialized tooling and automation is routinely done in under 15 seconds. With a high level of automation, we have assumed that the TITAN scheduled fusion-power core maintenance can be performed during the same period as the scheduled balance-of-plant (BOP) maintenance, about 30 days. If future advances in automation and remote technologies are substantial, then scheduled fusion power core maintenance may be faster than BOP maintenance. Such a situation would then place demands on BOP designers to decrease down time and increase availability.

2. TITAN-I MAINTENANCE PROCEDURES

The elevation view of TITAN-I is shown in Fig. 1. All of the maintenance procedures are with vertical lifts which are done with a moveable gantry crane. The heaviest component is the moveable set of OH coils and its support structure, ~300 tonnes. The first wall and blanket of TITAN-I consist of extruded vanadium tubes cooled by liquid lithium. The shield is also made of vanadium, however large square channels are provided to reduce the void fraction. The lifetime of the first wall and blanket is 14 MW yr/m^2, thus a neutron wall load of 18 MW/m^2 and plant availability of 75 percent require replacement of the first wall and blanket annually. The hot shield has a lifetime of 5 years, therefore, to reduce rad-waste, the shield is reused following replacement of the first wall and blanket.

The entire TITAN-I confinement building has an argon atmosphere to prevent lithium fires in the event of a lithium spill. New, pre-tested first wall, blanket and

divertor assemblies (FW/B/D) are also stored in the inert argon. This reduces outgasing when the assembly is installed into the vacuum tank. A plan-view of the confinement building, Fig. 2, illustrates the lay-down areas for the components moved during maintenance and the storage area for the new FW/B/D assemblies. Major operating parameters for the TITAN reactors are listed in Table 1.

Seventeen principal tasks must be accomplished for the annual, scheduled maintenance of TITAN-I. These steps are summarized in Table 2. Although many of the tasks are the same for single-piece and modular designs, four are not. These four tasks are marked as such in Table 2. Any unscheduled maintenance of the FW/B/D assembly will follow the same removal procedure as for the scheduled maintenance.

3. *TITAN-II MAINTENANCE PROCEDURES*

An elevation view of TITAN-II is shown in Figure 3. The entire primary loop is submerged in a low-pressure pool of pure water. The pool acts as a heat sink during off-normal operation and as a barrier to prevent off-site release of activation products. The structural material used is a low-activation, high-strength ferritic steel, 9-C [4]. The coolant is a solution of water and $LiNO_3$. Tritium breeding takes place in the primary coolant. The lifetime of the first wall is one year at 75% availability, therefore, annual replacement of the torus is required.

Maintenance procedures for TITAN-II are outlined in Table 3. Vertical lifts are used, as in TITAN-I. Extensive use of automated remote connects and disconnects are also used. The significant difference between the two reactor configurations is the low-pressure pool used in TITAN-II. Several maintenance options are available. One is to drain the pool and another, retain the water in the pool and perform the torus removal procedures under water. The latter option requires isolation valves at all of the remote connects to prevent infiltration of the pool water into the system. This isolation is required at all of the hydraulic, electrical and vacuum

systems. Draining the pool requires a storage tank for the water and time to transfer the water. A third option is to divide the pool into an inner cylinder and an outer annulus by installing a vertical cylindrical wall just outside the FPC. During maintenance, only the inner cylinder, which contains the FPC, needs to be drained.

Accessing the old torus requires the removal of the upper OH coil set. Following the removal of the coils, the used torus assembly is removed as a single unit and transported to a hot cell for disposal preparation. The torus assembly consists of the first wall, blanket and shield modules connect by three divertor sectors, encircled by the TF coils all of which is contained within the vacuum shell. The new, pre-tested torus assembly is installed and the OH coil set replaced. The remote connects are oriented in a vertical position so that the tori can be removed with a single vertical lift. This eliminates the need for complex twisting and tilting of the large torus.

4. FUSION-POWER CORE PRE-TESTING

An important feature of the TITAN design is the inclusion of a pre-test facility. This facility allows the plant personnel to fully test new FW/B/D assemblies in a non-nuclear environment prior to committing it to power operations in the reactor vault. Any faults discovered during pre-testing can be quickly repaired using inexpensive hands-on maintenance. Furthermore, additional testing can be used as a shake-down period to reduce the infant-mortality rate of the new assemblies. Although difficult to quantify, a well detailed pre-test program could greatly increase the reliability of the fusion-power core, hence increasing plant availability.

A list of pre-tests for the TITAN-I design is included in Table 4. The tests are categorized by level of assembly and by type of test. Level of assembly includes sub-modules, modules and full torus. Sub-modules are such items as formed first wall pipes, blanket pipes and ring headers. Modules are the assembled blanket units as shipped from the factory to the site (12 per reactor). The full torus is the unit

that is installed into the reactor vault (12 blanket modules and 3 divertor modules mechanically attached together). Full-torus pre-testing is subdivided into with- and without plasma tests.

The benefits of pre-testing (higher reliability, higher availability) must be balanced with the additional cost associated with the pre-test facility. The more representative that the tests are of actual operation, then more duplication of primary loop components is required. For example, vacuum field mapping and divertor plate alignment will require a vacuum system, simulated OH, EF, TF and divertor field coils and the diagnostics for the tests. Furthermore, since the TF and divertor coils are IBC-type coils [5] (i.e., the poloidal-flow lithium coolant circuit is used as as the electrical conductor of the coil) then a lithium circuit will be required for pretest. The optimum level of pre-testing can be determined with a detailed trade-off study to compare the benefits of higher reliability and availability versus the cost penalties associated with the pre-test equipment. The new technologies and configurations proposed for fusion systems, and thus a lack of operating experience and data, would lead to a great degree of uncertainty in that type of trade-off study. Simple models of availability have been developed [6] and could be used to show relative benefits of increased reliability. In situations where several reactors are clustered together, the cost of a single pre-test facility could be shared.

5. BENEFITS OF SINGLE-PIECE MAINTENANCE PROCEDURES

A simplistic comparison can be made between the single-piece and modular maintenance schemes.[1] Examination of the maintenance steps listed in Table 2 indicates that only 4 of the 17 tasks would be more time consuming for a modular reactor. Specifically, the differences are associated with steps that involve interfaces

[1] For purposes of discussion, a modular design is assumed. The same dimensions and wall loading are used but toroidal segmentation separates the unit into three or more units.

between modules and lifting of individual modules. Since only a few steps are different, it is possible that the total time required to change-out the entire FW/B/D assembly is comparable for TITAN and the assumed-modular design. If, however, these few steps are *much more* time consuming than the others, then a modular design will have a proportionally longer period of downtime. The mean-time-to-repair will be longer for scheduled maintenance of the modular design, and longer for the unscheduled maintenance of the single-piece design. The difference results because only single module replacement is required for unscheduled maintenance, but in single-piece designs, that module is the entire core. The sector-to-sector interfaces in the modular design adds to the number of possible fault areas, hence, possibly reducing the reliability. An absolute comparison between our single-piece and modular designs would not be possible for two reasons; 1) There is no operating experience with large-scale, remote maintenance fusion machines and 2) our assumption for a modular design is not for an optimized, fully-engineered reactor.

Vertical lifts have been chosen for the component movements during maintenance. The absolute choice between vertical and horizontal transport is not self evident. In the TITAN configuration, fewer components need to be moved to access the FW/B/D assembly via vertical lifts, hence the choice for this design. Vertical lifts also provide for a more compact reactor building, consistent with the FPC design goal. Lift limits for conventional cranes is around 500 tonnes, with special order crane capacities in excess of 1000 tonnes. The most massive component lifted during TITAN-I maintenance is the upper OH coil set. This coil set weighs about 300 tonnes, within conventional limits. The four major component lifts are illustrated in Fig. 4a-d. Temporary storage for the vacuum lid, upper OH coil set and upper hot-shield is provided, as shown in Fig. 2. These three components are re-installed following the installation of the new FW/B/D assembly. Once the new torus is lowered into position, horizontally oriented remote connects attach the torus to the

stationary primary lithium supplies. Access to the TITAN-II torus requires only the lifting of the upper OH coil set.

6. CONCLUSIONS

The major tasks required for annual maintenance of the TITAN-I and TITAN-II fusion power cores have been identified. Single-piece maintenance of the first wall, blanket and divertor assembly appears feasible and must be performed yearly. Vertical lift of three components is required to access the torus assembly of TITAN-I, and none of the component's masses is beyond the limits of present-day crane technology. The maintenance of TITAN-II requires lifting only the upper OH coil set to access the torus, but partial draining of the pool may be necessary. Following the removal of the old torus, a new, fully pre-tested assembly is installed. A high level of pre-testing ensures that the new tori will behave as designed and will have higher reliability than individual modules that have not been tested together as a single, operating unit under reactor-like conditions. The compactness of the reactor allows for single-piece torus design and maintenance. Single-piece, as opposed to modular compact designs, should lead to higher availability due to a shorter duration for torus replacement.

ACKNOWLEDGEMENT

Work supported in part by the United States Department of Energy under Contract No. DE-FG03-86ER52126.

REFERENCES

1. F. Najmabadi, R. W. Conn, N. M. Ghoniem, S. P. Grotz, J. Blanchard, *et al.*, "The TITAN Reversed-Field Pinch Fusion Reactor Study; The Final Report," UCLA-PPG-1200, Joint Report of University of California - Los Angeles, GA Technologies, Inc., Los Alamos National Laboratory, and Rensselaer Polytechnic Institute, March 1988. Also see F. Najmabadi, N. M. Ghoniem, R. W. Conn, *et al.*, "The TITAN Reversed-Field Pinch Fusion Reactor Study; Scoping Phase Report," UCLA-PPG-1100, January 1987.

2. R. W. Conn, F. Najmabadi and the TITAN Research Group, "The TITAN Reversed-Field Pinch Fusion Reactor Study," proceedings of the *IEEE 12th Symposium on Fusion Engineering*, Monterey, California, October 1987.

3. C. Copenhaver, R. A. Krakowski, N. M. Schnurr, R. L. Miller, C. G. Bathke, et al., "Compact Reversed-Field Pinch Reactors (CRFPR)," Los Alamos National Laboratory report, LA-10500-MS, August 1985, page 94.

1. D. S. Gelles, N. M. Ghoniem and R. W. Powell, "Low Activation Ferritic Alloys Patent Description," University of California, Los Angeles report, UCLA/ENG-87-9 and PPG-1049, March 1987.

5. D. Steiner, R. C. Block and B. K. Malaviya, "The Integrated Blanket-Coil Concept applied to the Poloidal Field and Blanket Systems of a Tokamak Reactor," Fusion Tech. Vol. 7 (1985) pp. 66.

6. J. Sheffield, R. A. Dory, S. M. Cohn, J. G. Delene, L. F. Parsley, et al., "Cost Assessment of a Generic Magnetic Fusion Reactor," Oak Ridge National Laboratory report, ORNL/TM-9311, March 1986, page 103.

Table 1

MAJOR OPERATING PARAMETERS

OF THE TITAN REACTORS

Major plasma radius	3.9 m
Minor plasma radius	0.6 m
Neutron wall loading	18. MW/m^2
Poloidal beta	0.2
Toroidal field (at first wall)	– 0.36 T
Poloidal field (at first wall)	5.44 T
Primary structural material	
TITAN-I	V-3Ti-1Si
TITAN-II	9-C ferritic
Coolant	
TITAN-I	lithium
TITAN-II	aqueous solution
Total thermal power	
TITAN-I	2918 MW
TITAN-II	3012 MW
Net electric power	
TITAN-I	998 MW
TITAN-II	910 mw

Table 2

TITAN-I MAINTENANCE PROCEDURES.

1. Orderly termination of plasma including TF, OH, EF and DIV coil discharge
2. Continue reduced first wall, blanket and shield cooling until decay heat is sufficiently low to allow for natural convection in the argon atmosphere (about 12 to 24 hours)
3. During cool down:
   a Vacuum pumping is continued until sufficient tritium is removed from the FPC
   b Break vacuum (valve-off vacuum pumps and cut weld at vacuum tank lid)
   c Remove vacuum lid to storage
   d Disconnect electrical and coolant supplies from the OH coils (numbers 2-5, upper)
4. Drain lithium from first wall, blanket and shield
5. Lift OH coil set and store
6. Disconnect lithium supplies*
7. Lift upper shield and store
8. Lift torus and move to hot cell*
9. Inspect fusion power core area
10. Install new torus assembly*
11. Connect lithium supplies*
12. Replace upper shield and connect coolant
13. Replace OH coils and connect electrical and coolant supplies
14. Hot test first wall, blanket, shield and OH coils
15. Replace vacuum tank lid
16. Pump down system
17. Initiate plasma operations

* The time required to complete these tasks is likely to be longer for a modular system than for a single-piece system, assuming similar configurations.

Table 3

TITAN-II MAINTENANCE PROCEDURES.

1. Orderly termination of plasma including TF, OH, EF and DIV coil discharge
2. Continue reduced first wall, blanket and shield cooling at reduced rate until decay heat is sufficiently low to allow natural convection.
3. During cool down:
   a. Vacuum pumping is continued until sufficient tritium is removed from the FPC
   b. Begin to drain pool above FPC[1]
4. Drain first wall, blanket and shield
5. Lift OH coil set and store
6. Disconnect coolant supplies and vacuum ducts
7. Lift torus and move to hot cell
8. Inspect fusion power core area
9. Install new torus assembly
10. Reconnect coolant supplies and vacuum ducts
11. Replace OH coils and connect electrical and coolant supplies
12. Hot test first wall, blanket, shield, TF and OH coils
13. Pump down system
14. Initiate plasma operations

[1] Pool draining is only required if submerged isolation valves are not provided.

Table 4

MAIN PRE-OPERATIONAL TESTING

ACTIONS OF SINGLE-PIECE FUSION POWER CORE.

TEST	Submodule[a]	Module[a]	Full Torus[b] w/o Plasma	Full Torus[b] w/ Plasma[c]
Mechanical				
·tube-bank vibration (first wall, blanket)	X	X	X	
·tube-bank expansion (first wall, blanket)	X	X	X	
·inter-module and full-torus deflection			X	
·plasma chamber (shell)/coil displacement			X	
Thermal hydraulic				
·flow rates, pressure drops, vibrations, leaks, etc.			X	
-first wall, divertor, blanket, shield	X			
-coils			X	
-manifolds, headers			X	
·remote couplings, disconnects	X	X	X	
·"at-temperature" FPC tests (*i.e.*, pressure drops, vibrations)			X	
-electrically-heated coolant			X	
-plasma-derived heat fluxes				X
Electrical				
·Magnet tests (*i.e.*, forces, deflections, voltages, etc.)			X	X
·vacuum-field mapping (TF ripple, vertical field, etc.)			X	
·plasma transients				
-RFP formation			X	X
-fast-ramp phase			X	X
-slow-ramp phase				X
·current-drive (steady-state) phase				X
·active feedback control			X	X
·eddy currents (transient startup, current drive)				
-first-wall shell			X	X
-blanket/shield			X	X
-coil casings, structure, pumps, etc.			X	X
·termination control/response				X
Vacuum/Fueling/Impurity Control				
·base vacuum			X	
·full gas load test			X	
·pellet injection				X
Neutronic				
·breeding efficiency				X
·energy recovery efficiency				X
·shielding effectiveness, streaming				X

a) Performed at factory site.
b) Performed at plant site during operational year.
c) Performed in the reactor, during the 28-day scheduled maintenance.

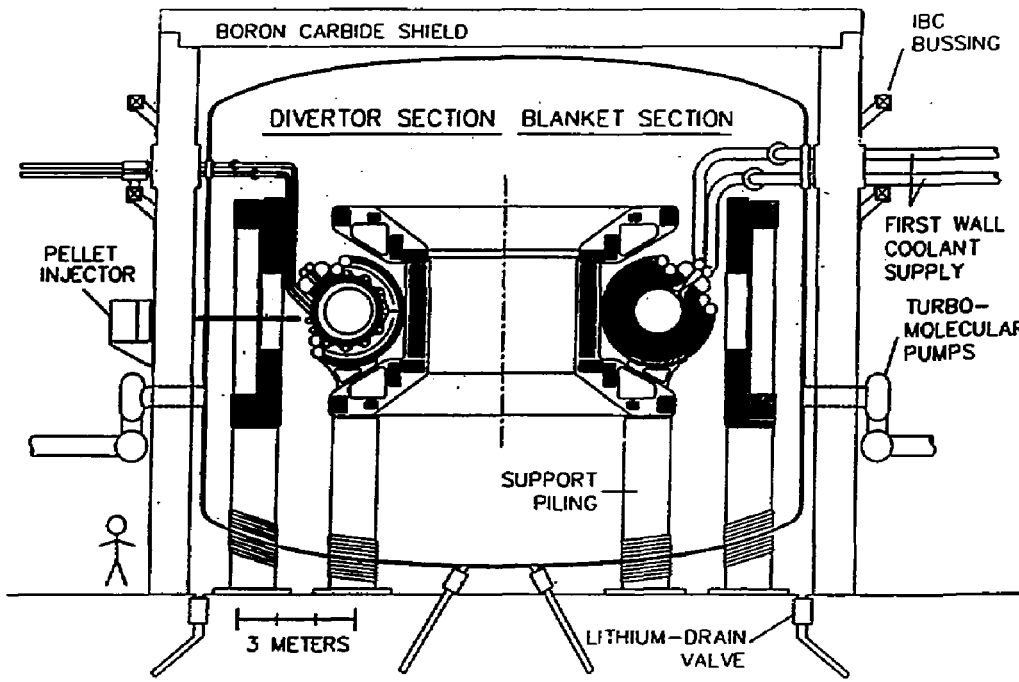

Figure 1. Elevation view of the TITAN-I reactor.

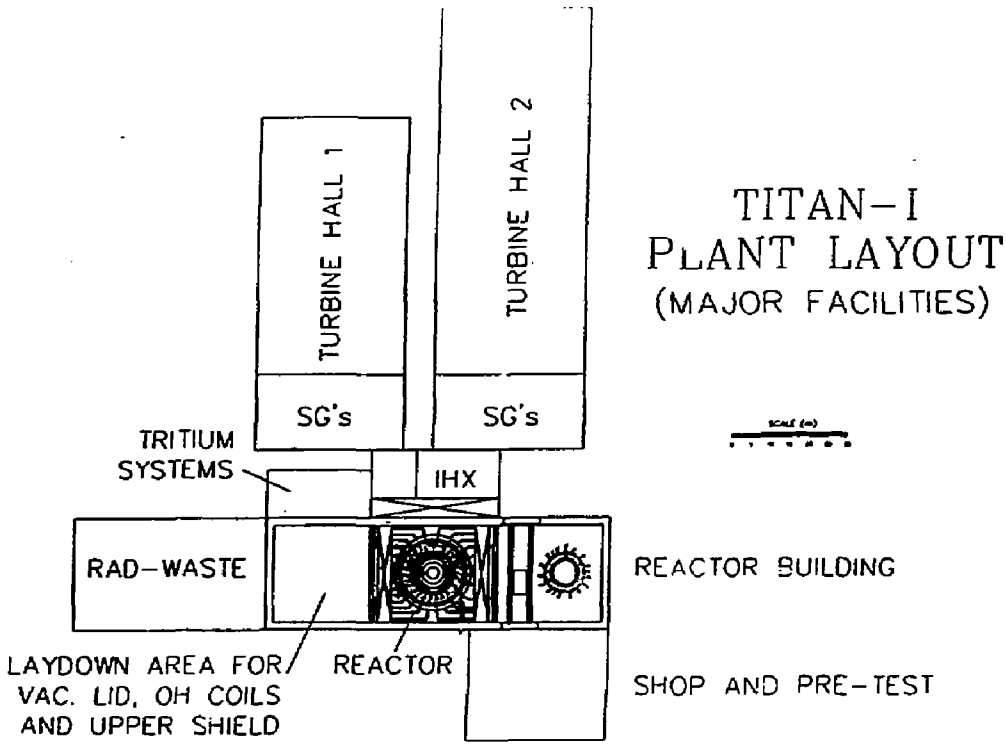

Figure 2. Plan-view of the TITAN-I reactor power plant.

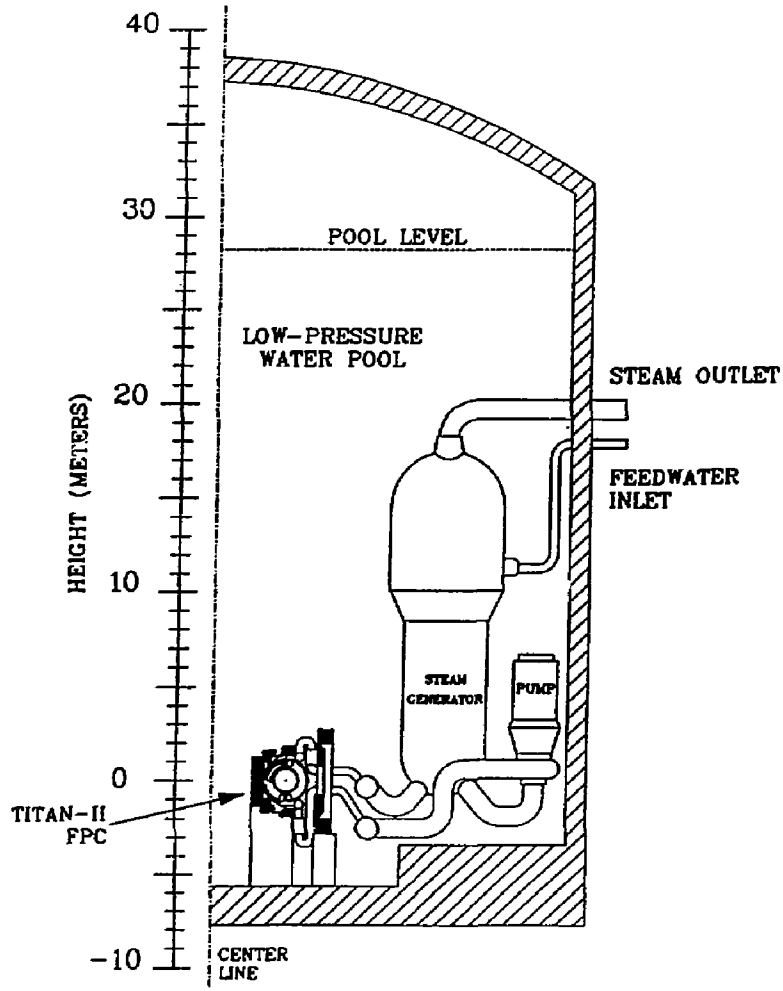

Figure 3. Elevation view of the TITAN-II reactor.

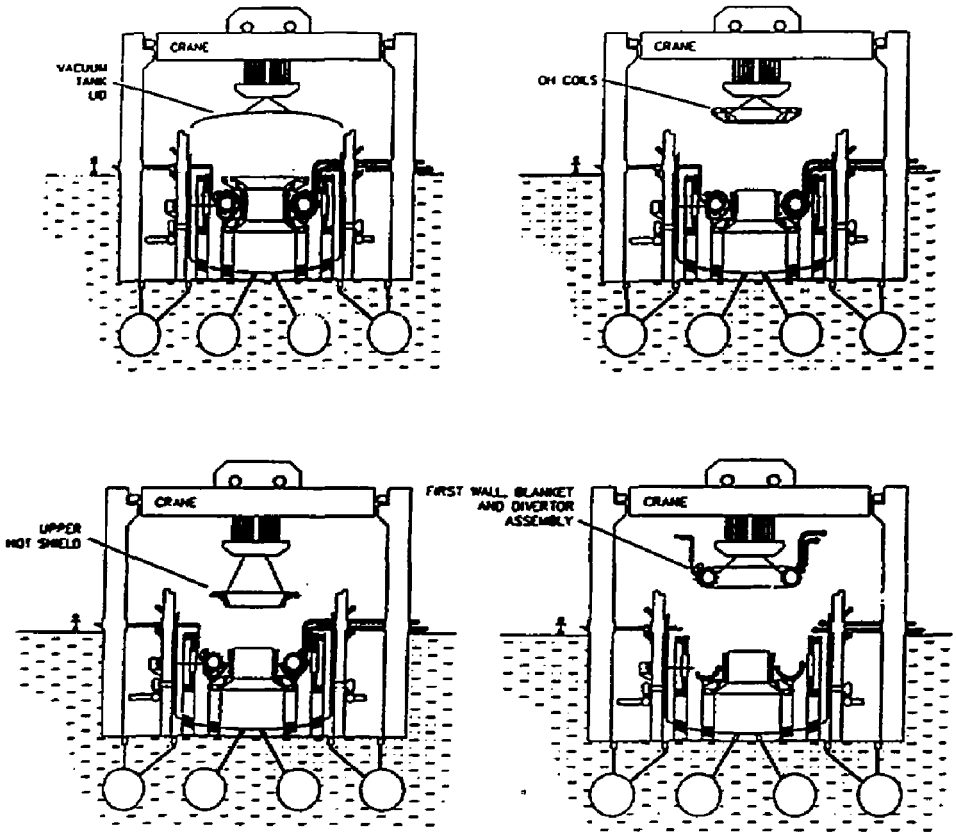

Figure 4. Major component lifts during TITAN-I scheduled maintenance. Lifted are: a; vacuum vessel lid, b; upper OH coils, c; upper hot-shield and d; first wall, IBC and divertor assembly.

MATERIAL SELECTION FOR THE TITAN REVERSED-FIELD PINCH REACTOR

S. Sharafat, N. M. Ghoniem, P. I. H. Cooke and
The TITAN Research Group

Department of Mechanical, Aerospace and Nuclear Engineering
and Institute for Plasma and Fusion Research
University of California, Los Angeles
Los Angeles, CA 90024-1597

ABSTRACT

The operating conditions of a compact, high neutron wall loading fusion reactor severely limit the choices for structural, shield, insulator and breeder materials. In particular the response of plasma-facing materials to radiation, thermal and pressure stresses, and their compatibility with coolants are of primary concern. Material selection issues were investigated for the compact, high mass power density TITAN reactor design study. In this paper the major findings regarding material performance are summarized. The retention of mechanical strength at relatively high temperatures, low thermal stresses, and compatibility with liquid lithium make vanadium-base alloys a promising material for structural components. The thermal creep behaviour of V-3Ti-1Si and V-15Cr-5Ti alloys has been approximated. In addition, irradiation behaviour including the effects of helium generation and coolant compatibility issues were investigated which led to the choice of V-3Ti-1Si as the primary structural material candidate for the liquid lithium cooled TITAN-I. For the water-cooled TITAN-II reactor, ferritic alloys are favoured among structural material candidates. Depending on the choice of lithium salt dissolved in water, the radiolytic effects and corrosion characteristics of the aqueous breeding solution may be severe. $LiOH$ and $LiNO_3$ have been identified as the most viable salts, however, radiolytic and corrosion behaviour of these salts in aqueous solutions differ substantially. The radiolytic behaviour of the aqueous salt solutions have been examined and various molecular decomposition product yields were estimated for the TITAN-II irradiation conditions. Insulator material issues of concern include irradiation induced swelling and radiation induced conductivity. Both issues have been investigated and operating temperatures for minimum swelling and dielectric breakdown strength have been identified for spinel ($MgO - Al_2O_3$). The high heat flux and sputtering/erosion issues limit the choice of the materials for the divertor target plate. Mechanical properties of various tungsten-rhenium alloys have been investigated. A highly ductile $W - Re$ alloy containing 26 atomic percents rhenium was identified as a viable plasma-facing material.

1. INTRODUCTION

Two different safety issues play a role in the economic feasibility of fusion power. One is the level of demonstrable public safety and the other is the capital investment safety. From a public point of view minimizing radioactive inventory and designing an inherently and passively safe reactor are desired. Both of these issues are directly a function of the material choices made. Capital investment risks can be minimized if structural materials are selected to withstand accidents of highest severity without inflicting major damage to the fusion power core (FPC).

The TITAN reactor study was undertaken to study the aspects of economic and engineering feasibility and safety of a compact fusion reactor. TITAN [1] is a compact, high-power-density reactor (major radius 3.9 m, plasma minor radius 0.6 m, neutron wall loading 18 MW/m^2), based on the reversed-field-pinch (RFP) confinement concept. Two options for the TITAN fusion power core were considered: TITAN-I, a liquid-lithium cooled design with a vanadium-base alloy structure and TITAN-II, an aqueous lithium salt solution cooled with a low activation, high strength ferritic alloy as structure.

Many of the engineering feasibility and safety related issues of a such a fusion reactor hinge on material performances under normal and off-normal operating conditions. The material selection effort concentrated on fulfilling these performance and safety requirements. The TITAN-I and TITAN-II material selection issues are summarized in this paper. A more detail discussion of the material selection efforts can be found in Reference [2].

2. TITAN-I STRUCTURAL MATERIALS

TITAN-I is a self cooled liquid lithium design. The retention of mechanical strength at relatively high temperatures, low thermal stresses, and compatibility with liquid lithium make vanadium-base alloys a promising material for structural components. Compared with HT-9, vanadium-base alloys have better physical

properties such as higher melting temperature, lower thermal expansion coefficient and lower density. The high melting temperature (T_m = 1890°C) can have significant bearings on safety related issues. The higher ultimate tensile strength ($\sigma_u \sim 600$ MPa at 600°C), lower expansion coefficient and slightly higher thermal conductivity of vanadium-base alloys results in higher heat load capabilities. When compared with ferritic alloys at a nominal neutron wall loading of 1 MW/m^2, vanadium-base alloys have about half the nuclear heating rate (~ 25 W/cm^3), about a third of the helium generation rate (~ 57 He-appm), about half the hydrogen production rate (~ 240 H-appm/MW-yr/m^2) and lower long-term afterheat [3].

Among the various vanadium-base alloys the most promising candidates for fusion reactor applications are V-15Cr-5Ti, VANSTAR-7(V-9Cr-3Fe-1Zr), and V-3Ti-1Si. In the past the V-15Cr-5Ti alloy had been adopted as the class model alloy in the U.S. In particular V-15Cr-5Ti has a higher thermal creep resistance than the other two alloys. Investigation of the effects of neutron irradiation with pre-implanted helium atoms, however, suggest that V-15Cr-5Ti may be subject to unacceptable losses in ductility [4]. Braski [4] irradiated specimens of V-15Cr-5Ti,V-3Ti-1Si and VANSTAR-7 at 420,520 and 600°C to a damage level of 40 *dpa* (displacements per atom) with helium atoms implanted up to a concentration of 30 appm. Tensile tests showed that V-3Ti-1Si suffers the least amount of swelling, irradiation hardening and He-embrittlement. However, V 3Ti-1Si has the lowest thermal creep resistance among the three vanadium alloys.

Creep-rupture data at 650, 750 and 850°C was used to develop a phenomenological stress rupture equation for the V-3Ti-1Si alloy. Among various creep-rupture data extrapolation techniques, the Modified Minimum-Commitment-Method ($MMCM$) [5] has the advantage of not being sensitive to creep data behavior. Results of the $MMCM$ [6] analysis are depicted in Figure 1. Also shown are the TITAN-I first wall operating stresses during normal and off-normal operations. Allowable design stresses have to include the effects of irradiation hardening and

helium embrittlement. Limited helium embrittlement data [7] was used to estimate the allowable stresses after 1 full power year (FPY) of TITAN. This corresponds to an estimated damage dose of about 160 dpa. Our analysis indicates that the maximum allowable primary stress for V-3Ti-1Si is 108 MPa at 650°C, 44 MPa at 750°C, and 20MPa at 850°C.

2.1 Coolant Compatibility

One of the most significant advantages of vanadium alloys over ferritic alloys is their corrosion resistance to liquid lithium. At 600°C the dissolution rate for vanadium is $\sim 5 \times 10^{-2}$ mg/m^2/h and for HT-9 about 50 mg/m^2/h [8]. Recently a bimetallic loop experiment investigated the corrosion of V-3Ti-1Si in flowing liquid lithium [9]. The experiment consisted of high purity liquid lithium flowing at 7 cm/s in a titanium stabilized stainless steel (*X10CrNiMoTi1810*) loop at 823 K for a duration of up to 2056 hr. The measured corrosion rate of V-3Ti-1Si was in the range of 10^{-2} to 10^{-3} g/m^2/h. The more significant finding, however, was the formation of a very dense and adhesive vanadium-nitride layer ($(V,Ti)_xN$; x$\sim$ 1.56-1.66). The thickness of the nitride layer (2-5 μm) was found to be exposure time independent. Another issue regarding coolant compatibility is the high lithium flow velocity (21 m/s at the TITAN-I first-wall). Investigations showed that 21 m/s is far from the erosion threshold velocity of $\sim$120 m/s, measured for most metals and ceramics [10]. Experiments [11] have been performed with high velocity liquid lithium flowing at 50 m/s in Nb-1Zr tubes at 1073-1143°C. Measured corrosion rates after 500 hours of lithium flow were about 0.1 mm/yr.

3. TITAN-II STRUCTURAL MATERIALS

TITAN-II is an aqueous loop-in-pool reactor design. For the water-cooled TITAN reactor, ferritic alloys are favored among structural material candidates. To reduce waste disposal management problems low activation ferritic alloys are being developed. Preliminary evaluations indicate that a reduced activation alloy can be

developed without compromizing mechanical properties, primarily by replacing Mo by W. Several low activation ferritic alloys have been investigated. For the TITAN-II reactor the HEDL/UCLA 12Cr-0.3V-1W-6.5Mn alloy (Alloy 9-C) was chosen as structural material for TITAN-II primarily due to its good strength and elongation behavior after irradiation [12]. The high Cr content ensures excellent corrosion resistance and the low carbon content ensures better weldability characteristics, higher sensitization resistance, and reduced hydrogen embrittlement. The high concentration of Mn in Alloy 9-C prevents the formation of delta-ferrite phases. The delta-ferrite phase formation is responsible for high DBTT and low hardness.

Alloy 9-C has a very high yield strength of 810 MPa and a high tensile strength of 1002 MPa at room temperature with a total elongation of 10.1 %. Similar to other ferritic alloys, 9-C shows little or no irradiation hardening (change in yield stress) at low temperatures. At irradiation temperatures above 300°C alloy 9-C softens, having a total elongation of about 19 % at 600°C after 14 dpa of damage dose. Table 2 shows selected irradiated and unirradiated properties of this alloy.

3.1 Aqueous Solution Compatibility

The tritium breeder in the TITAN-II reactor is a lithium salt dissolved in the water coolant. The salt of choice based on the radiolytic behaviour is $LiNO_3$ (see next section). From a corrosion point of view the data base of corrosion of ferritics in $LiNO_3$ salt solutions is very limited. Indications are, however, that a high concentration lithium nitrate aqueous salt solution does not exhibit unacceptable corrosion problems. Recent high temperature corrosion scoping experiments support this statement [13].

Stress-corrosion cracking (SCC) is a major concern in the nuclear industry. Most recent experiences with SCC in nuclear environments clearly show that SCC can be suppressed by reducing the oxygen content through the addition of hydrogen to the coolant [14]. The production of tritium in an aqueous lithium salt solution

is seen as an inherent SCC controlling mechanism. The proper choice of structural material can further reduce the probability of SCC. In particular a high Cr content coupled with a low C content are shown to reduce SCC. Both of these requirements are fulfilled by Alloy 9-C.

3.2 Radiolysis

Gamma-ray radiolysis yields of $LiNO_3$ salt solutions are known as a function of salt concentration [15]. At high concentrations the H_2 yields are very small and the H_2O_2 yield decreases by a factor of about 3 relative to pure water. Oxygen yields due to light particle radiation are fairly salt concentration independent.

Alpha-ray radiolysis due to nuclear reactions with lithium in the aqueous $LiNO_3$ salt solution were estimated as a function of salt concentration based on the power law measurements of 3.4 MeV α's [16]. The oxygen production due to heavy particle radiation increases while the yields of H_2, H_2O_2, H, OH, HO_2 all decrease with increasing salt concentration.

The limited data suggests that neither the light nor the heavy particle radiation of a highly concentrated $LiNO_3$ salt solution leads to high levels of radiolytic decomposition products, except for the formation of oxygen. In fact, an increase of salt concentration leads to a decrease in the production of H_2O_2, H_2, H, OH, and HO_2 and a slight increase in NO_2^- yields relative to highly diluted salt solutions [15].

The effect of elevated temperature on radiolysis was investigated. From experience gained in the fission industry with pure water [14], it can be ascertained that the stability of non-boiling water to radiolysis increases as temperature increases. The apparent stability is actually due to an increase in radical recombination reaction rates at elevated temperatures.

Although many uncertainties remain and much research is required in the area of radiolysis, the use of a highly concentrated aqueous $LiNO_3$ salt solution should

not lead to the formation of volatile or explosive gas mixtures. The effects of radiolytic decomposition products on corrosion, however, remains a subject of great uncertainty until an experimental data base of radiolytic decomposition products in a fusion environment becomes available.

4. INSULATOR MATERIAL

Application of electrical insulators include current breaks in various *FPC* components. Depending on their location, these breaks can be exposed to high radiation levels. Technical requirements for insulating materials include: adequate electrical resistivity, radiation stability, minimum radiation induced conductivity, mechanical integrity and fabricability.

Organic insulating materials, generally do not meet high temperature requirements and also suffer from rapid resistivity degradation when exposed to ionizing radiation. Ceramic insulating materials, on the other hand, posses high melting or decomposition temperatures ($> 2000°C$) Electrical conductivity (σ) values for various oxide and nitride and appear to be more radiation damage resistant. insulators range between 10^{-8} and 10^{-14} (ohm-cm)$^{-1}$ at 500°C with BN having the lowest value. Exposed to a fusion reactor radiation field, ceramic insulators experience a change in their thermal conductivity, mechanical strength, electrical resistivity and in the dielectric breakdown strength (*dbs*).

A thermal conductivity independent of exposure-time is favored because of higher confidence in the thermal behavior design of magnets and insulator carrying components. The following insulators experience a 50 to 90% reduction in thermal conductivity after exposure to neutron irradiation: BeO, MgO, Al_2O_3, Y_2O_3, $Y_3Al_5O_{12}$, Si_3N_4, Si_2ON_2 and $Si_4Al_4O_2N_6$. Spinel ($MgAl_2O_4$) is one of the very few that does not show a reduction in thermal conductivity after neutron irradiation [17]. As far as tensile strength is concerned $MgAl_2O_4$, shows an increase in strength upon irradiation [17]. Among the insulating materials $MgAl_2O_4$ has

shown good swelling resistance. In Table 1 experimental swelling data are given [17]. A phenomenological swelling equation based on the swelling data of Table 1 was developed [6]. Sample swelling calculations for Spinel located at the TF-coils of the TITAN-I reactor are demonstrated in Figure 2.

Examining the Spinel swelling curves in Figure 2, a low or high operating temperature is favored. However, high temperatures degrade the dielectric breakdown strength (*dbs*) of ceramic insulators. The *dbs* is defined as the maximum potential gradient in the dielectric without the occurrence of electric breakdown. Below 200°C the *dbs* for alumina is ~12 kV/mm, it drops to ~8 kV/mm at 350°C and ~2.5 kV/mm at 700°C. Thus, Spinel offers good electrical resistivity even at high operating temperatures. Only components that need high resistivity values (>12 kV/mm) have to operate at temperatures below 200°C.

Another process that leads to an increase in electrical conductivity is ionizing radiation (γ-rays). The γ-ray photons interact with electrons resulting in an increase of conduction charge carrier concentrations. This phenomenon is a flux dependent effect (instantaneous) and is commonly known as radiation induced conductivity (*RIC*). *RIC* has been measured for alumina at temperatures below 300°C and was found to be directly related to the ionizing dose rate ($\dot{\gamma}$). Our analysis has shown that *RIC* for an 18 MW/m^2 neutron wall loading will increase the conductivity of Spinel to about 3.5×10^{-5} $(\Omega m)^{-1}$. Al_2O_3 doping experiments using 0.03 wt.% Cr_2O_3 shows a reduction of conductivity by more than one order of magnitude. Similar doping techniques can be used to reduce *RIC* of Spinel.

5. DIVERTOR-TARGET MATERIAL

The high particle fluxes encountered on impurity control components such as the divertor plates or the limiter, requires a high Z material to reduce the amount of sputtering. Simultaneously, high heat loads need to be dealt with and thus materials with high thermal conductivity and low thermal stresses are required. Among the

refractory metals a tungsten-rhenium alloy has been selected. Workability and mechanical properties of W-Re alloys, with Re contents in the range of 3 to 30 at.% have been found to be excellent. Furthermore, the thermal expansion coefficient of W-Re alloys can be tailored to a degree by varying the Re content. Suitable brazing materials with different application temperatures have also been developed to join W-Re alloys with other alloys.

Of importance is the high ductile-to-brittle transition temperature (DBTT) below which it cannot be worked due to its extreme brittleness. Pure tungsten has a DBTT of about 200 to 400°C depending on the impurity content, thermomechanical history, and thickness [18]. The addition of rhenium reduces the DBTT appreciably. Tungsten-26% rhenium has a DBTT of about 90°C [18] which is a great improvement from the pure tungsten DBTT. The 90°C DBTT requires that forming, cutting, milling, and drilling of this alloy must be done at temperatures well above this DBTT.

6. SUMMARY

The following is a summary of findings of material selection issues for the liquid lithium cooled TITAN-I and the aqueous loop-in-pool TITAN-RFP compact fusion reactors:

For the liquid lithium cooled TITAN-I reactor:

- V-3Ti-1Si was chosen over V-15Cr-5Ti due to its good radiation damage resistance: lowest helium embrittlement and lowest swelling rates.
- From the limited available creep data it seems that V-3Ti-1Si is able to operate satisfactorily at elevated temperatures ($\leq$700°C).
- Limited liquid lithium corrosion data indicates the possibility of a self-limiting corrosion rate on V-3Ti-1Si, due to the formation of a (V,Ti)-nitride surface layer
- Such an in-situ layer formation can have "self-healing" properties.

- Low swelling operating temperatures for Spinel ($MgAl_2O_4$) have been identified. If operated outside 150 to 300°C Spinel shows excellent swelling resistance.
- The principal feasibility of using tungsten-rhenium alloys for the high heat flux components is no longer a major issue.

For the TITAN-II aqueous loop-in-pool design:

- A low activation ferritic alloy (Alloy 9-C; HEDL/UCLA), has been identified as a viable structural material for fusion applications. It shows good strength and ductility behavior.
- Irradiation behavior data are sparse but scoping experiments show good retention of mechanical properties.
- The high chromium and low carbon content of this alloy ensure good aqueous corrosion resistance and reduce the degree of hydrogen embrittlement, respectively.
- The choice of $LiNO_3$ over LiOH as a breeding salt dissolved in the coolant was based on the radiolytic behavior of the salt solutions.
- Radiolysis of $LiNO_3$ salt solutions was investigated in detail. Recent experiments with γ-rays clearly show a reduction of radiolytic decomposition of the water, except for oxygen. However, the produced tritium will readily combine with the oxygen.
- The use of $LiNO_3$ salt coupled with the production of tritium results in:
  - elevation of water boiling point
  - decrease of SCC of some ferrous alloys
  - reduction of hydrogen attack.
- Although the aqueous lithium-salt solution blanket concept shows promising features, detailed but relatively simple experimental investigations are needed

before more decisive statements regarding the feasibility of a lithium salt aqueous solution blanket can be made.

ACKNOWLEDGEMENT

Work supported in part by the United States Department of Energy under Contract No. DE-FG03-86ER52126.

REFERENCES

1. F. Najmabadi, N. M. Ghoniem, R. W. Conn *et al.,* "The TITAN Reversed Field-Pinch Fusion Reactor Study : Scoping Phase Report", Joint Report of UCLA, GA Technologies Inc., Los Alamos National Laboratory and Rensselaer Polytechnic Institute, UCLA-PPG-1100 (January 1987).

2. F. Najmabadi, R. W. Conn, S. P. Grotz, N. M. Ghoniem, *et al.,* "The TITAN Reversed Field-Pinch Fusion Reactor Study : Final Report", Joint Report of UCLA, GA Technologies Inc., Los Alamos National Laboratory and Rensselaer Polytechnic Institute, UCLA-PPG-1200 (March 1988).

3. D. L. Smith, B. A. Loomis and D. R. Diercks "Vanadium-Base Alloys For Fusion Reactor Applications - A Review", *J. Nucl. Mat.*, vol. 135, pp. 125-139, 1985.

4. D. N. Braski, "The Effect of Neutron Irradiation on the Tensile Properties and Microstructure of Several Vanadium Alloys", presented at the ASTM Conference on Fusion Reactor Materials, Seattle, Washington, June 1986.

5. R. J. Amodeo and N. M. Ghoniem, "Development of Design Equations For Ferritic Alloys in Fusion Reactors", *Nuclear Engineering and Design/Fusion*, 2 (1985) 97-110.

6. S. Sharafat, N. M. Ghoniem *et al.,* "Structure and Insulator Material Choices for the TITAN Reversed-Field Pinch Reactor Study", Proc. 12th Symposium on Fusion Engineering, Monterey, CA, October 1987, to appear.

7. D. N. Braski "The Effects of Helium on the Tensile Properties of Several Vanadium Alloys",*ADIP* Report DOE/ER-0045/13, September 1984.

8. D. L. Smith, G. D. Morgan, M. A. Abdou, C. C. Baker, J. D. Gordon *et al.,* "Blanket Comparison and Selection Study", Final Report, ANL/FPP-84-1 vol. 2, p. 6.2-15 , 1984.

9. C. H. Adelhelm, H. U. Borgstedt, J. Konys "Corrosion of V-3Ti-1Si in Flowing Lithium", *Fusion Technology* vol. 8, pp. 541-545, 1985.

10. J. E. Field, S. van der Zwaag, D. Townsend "Liquid Impact Damage Assessment for a Range of Infra-Red Materials", *Proceedings of the Sixth International Conference on Erosion by Liquid and Solid Impact*, Newnham College, UK, Sept. 3-6, 1983, pp. 21.1-21.13.

11. E. E. Hoffman, R. W. Harrison "The Compatibility of Refractory Metals with Liquid Metals", *Proceedings of a Symposium on Metallurgy and Technology of Refractory Metals*, Washington, D. C., April 25-26, 1968, pp. 251-287.

12. D. S. Gelles, N. M. Ghoniem, and R. W. Powell,"Low Activation Ferritic Alloys Patent Description", University of California, Los Angeles, Report, UCLA/ENG-87-9 PPG-1049, 1987.

13. R. Waeben, W. Bogaert, and M. Embrechts,"Initial Corrosion Evaluation of Candidate Materials for an ASCB Driver Blanket For NET", Proc. 12th Symposium on Fusion Engineering, Monterey, CA, October 1987, to appear.

14. P. Cohen,"Water Coolant Technology of Power Reactors," American Nuclear Society, 1980.

15. M. Daniels,"Radiolysis and Photolysis of the Aqueous Nitrate System",in *Radiation Chemistry*, Vol. 1, Ed. R. F. Gould, Am. Chem. Soc., Washington D. C., 1968.

16. M. Burton and K. C. Kurien, *J. Phys. Chem.* 63 (1959) 899.

17. F. W. Clinard, Jr., G. F. Hurley, L. W. Hobbs, D. L. Rohr, R. A. Youngman "Structural Performance of Ceramics in a High-Fluence Fusion Environment",*J. Nucl. Mat.*, vol. 122 & 123, pp. 1386-1392, 1984.

18. Metallwerk Plansee GmbH, "Tungsten-Rhenium Alloys", in *Refractory Metals and Special Metals*, PLANSEE, 1987.

Table 1

SWELLING OF NEUTRON IRRADIATED SPINEL*.

Temp.(°K)	$\Delta V/V$(%)	Fluence(n/cm^2)*
323	0.03±0.01	3.2×10^{22}
407	0.08±0.01	2.1×10^{26}
680	-0.19±0.01	2.2×10^{26}
815	-0.35±0.01	2.2×10^{26}
925	±0.01	2.3×10^{24}

* $E_n > 0.1$ MeV

Table 2

PHYSICAL AND MECHANICAL PROPERTIES OF

ALLOY 9-C (HEDL/UCLA) LOW-ACTIVATION FERRITIC STEEL [12].

Property	Unit	Temperature (°C)				
		RT	300	400	500	600
Young' Modulus	GPa	225	200	193	180	150
Poisson's Ratio	-	0.4	0.4	0.4	0.4	0.4
Shear Modulus[a]	GPa	83	75	72	68	-
Tensile Strength	MPa	1002	-	810[a]	942[b]	749[c]
Yield Strength (irrad.)[c]	MPa	810	810	820	650	531
Total Elongation (irrad)[c]	%	10.1	13.8	15.0	17	19.4
Thermal Expansion Coeff.	10^{-6}/C	9.5	10.5	11	11.5	12
Specific Heat	J/kg-°C	450	570	600	680	780
Electric Resistivity	$\mu\Omega$-m	0.6	0/82	0.9	0.98	1.05
Thermal Conductivity	W/m-K	25	26.5	26.7	27.2	27.6
DBTT at 15/30 dpa[a]	°C	-	-	100/140	25/50	0/55

[a]Unavailable values replaced by HT-9.

[b]After 6 dpa of damage dose.

[c]Values given at irradiation temperatures after 14 dpa.

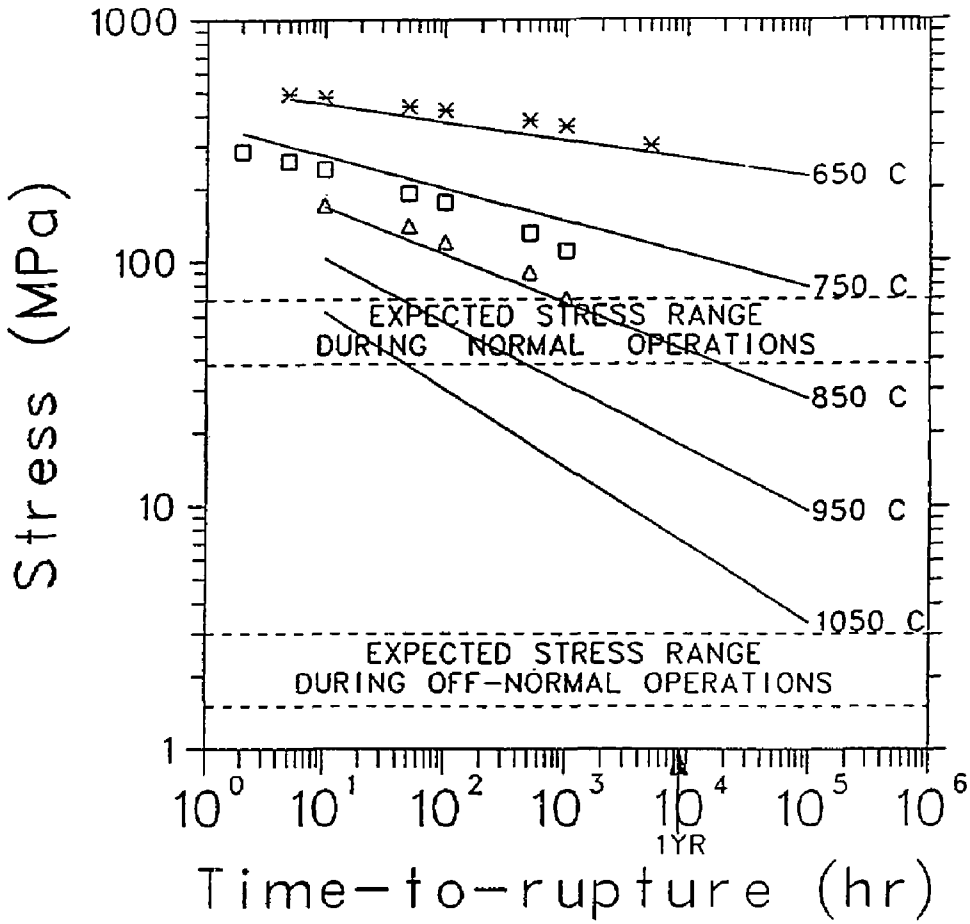

Figure 1. Creep-rupture stress of V-3Ti-1Si at various temperatures (symbols are creep-rupture data points; solid lines represent *MMCM* calculations).

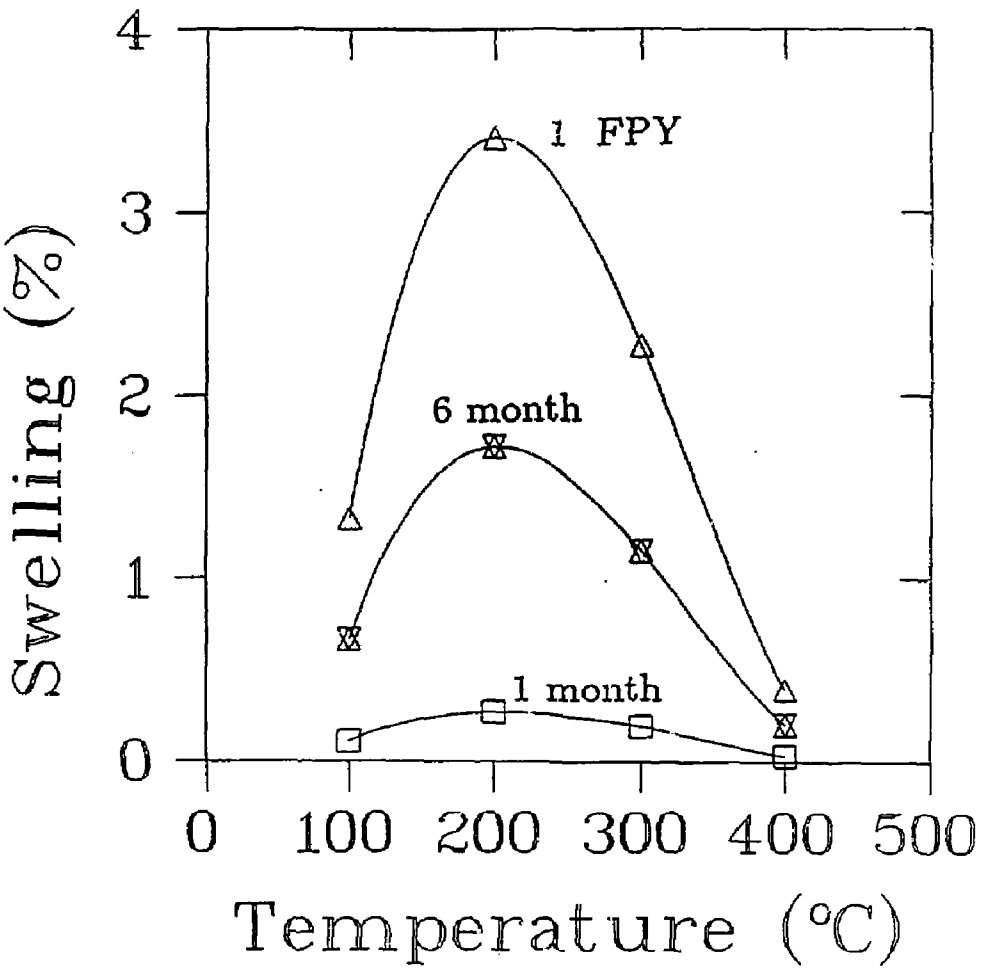

Figure 2. *Swelling of Spinel as a function of exposure time and temperature located at the TF-coils.*

THERMAL-HYDRAULIC AND STRUCTURAL DESIGN FOR THE LITHIUM-COOLED TITAN-I REVERSED-FIELD-PINCH REACTOR

M. Z. Hasan, J. P. Blanchard, and N. M. Ghoniem for
The TITAN Research Group

Department of Mechanical, Aerospace and Nuclear Engineering
and Institute for Plasma and Fusion Research
University of California, Los Angeles
Los Angeles, CA 90024-1597, USA

ABSTRACT

A thermal-hydraulic and structural design of the first wall and blanket for the 18 MW/m^2 neutron wall-loading TITAN reversed-field-pinch fusion reactor is presented. The primary coolant is liquid lithium and the structural material is the vanadium alloy, V-3Ti-1Si. Various design limits, which take the operational environment into consideration, for this vanadium alloy for the first wall and blanket are discussed. The first wall is made of small-diameter tubes. The blanket coolant channels are a combination of tubular, square, and rectangular channels. The first-wall and blanket coolant circuits are separate, allowing different coolant exit temperatures. The coolant channels are aligned with the larger poloidal magnetic field to reduce magnetohydrodynamic (MHD) pressure drops. At the design heat flux of 4.6 MW/m^2 on the first wall, MHD turbulent-flow heat transfer is used. Both the separation of the coolant circuits and the use of MHD turbulent-flow heat transfer substantially increase the heat flux limit on the first wall. These are favorable for high-power-density fusion reactors. The inlet temperature of lithium is 320°C and the exit temperatures are 440°C and 700°C for the first wall and blanket, respectively. The pressure drop in the first wall circuit is 10 MPa and is less than 3 MPa for the blanket circuit. The pumping power is less than 5% of electric output. The maximum structure temperature is less than 750°C and the material stresses are shown to be within the allowable limits. One-dimensional thermal and stress analyses are adequate for the thermal-hydraulic and structural design for TITAN-I. This is verified by two-dimensional, finite element analysis. The use of liquid lithium as the coolant and vanadium alloy as the structural material has enabled to remove the reactor thermal energy at high temperature which has resulted in a gross thermal efficiency of 44%.

1. INTRODUCTION AND DESIGN PHILOSOPHY

The TITAN study is a multi-institutional effort to investigate the potential of Reversed-Field-Pinch (RFP) confinement concept as a high-power-density fusion reactor [1,2]. Two engineering designs of the fusion power core have emerged. TITAN-I is a self-cooled lithium design with vanadium alloy as the structural material [3]. This paper deals with TITAN-I. The other, TITAN-II, is an aqueous salt-solution, loop-in-pool design with ferritic steel as the structural material [4].

One of the important reasons for selecting liquid lithium as the coolant and vanadium alloy as the structural material is to remove the thermal energy from the reactor at high temperature. This is possible because lithium has high boiling point and vanadium alloys have high operating temperature in fusion environment [5]. Of all the liquid metals, liquid lithium has the best overall thermo-physical properties such as heat capacity, thermal conductivity, electrical conductivity, etc. In addition, lithium can serve as breeder for tritium which is essential for a D-T fusion reactor. Lithium is also compatible with vanadium. Several earlier studies proposed liquid lithium as coolant for fusion applications [6-8].

TITAN-I fusion reactor operates at 18 MW/m^2 of neutron wall loading and 4.6 MW/m^2 of peak heat flux on the first wall at the design point. The design point corresponds to the radiation fraction of 0.95 which means that 95% of the alpha and ohmic dissipative power in the plasma is radiated directly on the first wall. For this high-power-density reactor, careful consideration must be given to the nature and spatial distribution of deposited thermal energy. A large amount of volumetric neutron thermal energy is deposited in the first few centimeters of the first-wall and blanket materials. Another component of thermal energy is in the form of a high surface heat flux incident only on the first wall. In RFPs, the poloidal magnetic field is dominant compared to the toroidal field. This characteristic feature of the RFP allows innovation and design solutions which are compatible with the nature and distribution of thermal energy deposition.

The first-wall and blanket coolant circuits have been separated which gives the needed degree of flexibility to the design by allowing lower coolant-exit temperature and efficient, high-velocity turbulent-flow heat transfer in the first-wall coolant channels. A circular tube has optimum geometry for both efficient heat transfer and stress considerations and is suitable for the first-wall coolant channel where radiation heat flux is high and MHD pressure drop is considerable due to the high-velocity turbulent flow.

In this paper, the thermal-hydraulic and structural design of the first wall and blanket of TITAN-I is presented. The relevant properties of the vanadium alloy is briefly discussed in the next section. In section 3, a description of the configurations of the first wall and blanket and the thermal-hydraulic design are provided. Two-dimensional finite element structural design is provided in section 4. Section 5 contains conclusions and performance evaluation.

2. FIRST-WALL/BLANKET STRUCTURAL MATERIAL

Vanadium alloys have a number of attractive features [5], particularly for the first-wall and blanket/shield design of the TITAN high-power-density fusion reactor. In addition to the low activation feature allowing near-surface radioactive waste disposal, the high melting temperature has a large impact on safety during accidents. The high ultimate tensile strength ($\sim$ 600 MPa at 600°C), lower expansion coefficient, and high thermal conductivity of the vanadium alloys result in superior thermal stress resistance. Vanadium is compatible with lithium, thus making it possible to use lithium for cooling and tritium breeding.

Nuclear transmutation production of hydrogen and helium in the vanadium structure of the first wall and blanket is a design concern for several reasons. It has been experimentally observed that a hydrogen content above 5000 $appm$ will cause a shift in the ductile-to-brittle transition temperature to above room temperature (as reported in Ref. [5]). Helium, on the other hand, forms bubbles in the grain interior

and on grain boundaries resulting in high-temperature helium embrittlement. The hydrogen problem may be avoided by operating the structure at high temperature (above $400°C$). Helium embrittlement can be mitigated by the appropriate choice of alloying elements and by limiting the maximum operational temperature. Among the various V-base alloys, the most promising candidates for fusion applications are V-15Cr-5Ti, VANSTAR-7 (V-9Cr-3Fe-1Zr), and V-3Ti-1Si. Based upon swelling and creep ductility, the V-3Ti-1Si alloy seems to be the most promising for our applications [9]. At the end of life, the maximum permissible primary stress is found to be 108 MPa at $650°C$ and 44 MPa at $750°C$. The temperatures are taken to be average wall temperatures. The maximum allowable secondary stress is determined by not allowing the total equivalent stress to exceed the ultimate tensile stress at the operating temperature. For details of the method, see Ref. [9].

3. THERMAL-HYDRAULIC DESIGN

Detailed thermal-hydraulic design is provided in this section. The thermal and stress analyses are performed using one-dimensional approximations except for the film temperature drop in the first-wall coolant tube because of the strong circumferential variation of the radiation heat flux incident on the first wall.

3.1. First-wall and blanket configurations

The first wall is made of small-diameter coolant tubes for several reasons (e.g., high heat transfer, high strength, and ease of manufacturing). The blanket consists of a combination of tubular, square, and rectangular channels. Figure 1 shows the configuration of the first wall and blanket for TITAN-I. The coolant channels are set along the poloidal direction to reduce MHD pressure drops. The inner diameter of the first-wall tube is 8 mm and the wall thickness is 1.25 mm which includes 0.25 mm for erosion allowance. The diameter of the coolant tube is decided by a compromise between the heat transfer performance which increases with the decrease in diameter and total number of tubes which increases with the decrease

in diameter, thus increasing the probability of a tube failure during operation. The blanket is 75 *cm* thick and consists of two zones, a 30 *cm* thick integrated blanket coil (IBC) [1] followed by a 45 *cm* thick hot shield. The IBC zone consists of 6 rows of tubular channels. The lithium in the tubular coolant channels of the IBC zone carry the electric current for producing the toroidal magnetic field. The first 30 *cm* of the hot shield consists of square channels and the remaining 15 *cm* has thick-walled rectangular channels.

3.2. Design procedure

The thermal-hydraulic design is based on concepts reported by Hasan and Ghoniem [10]. The design calculations are performed by a thermal-hydraulic design code for the design of the first wall and blanket of a RFP reactor [11]. The objective of the design calculations is to obtain a design window for a given coolant inlet temperature and coolant channel geometry. A design window shows possible limiting coolant-exit temperature as function of heat flux on the first wall. Limiting coolant-exit temperature is obtained by satisfying the design limits on maximum allowable structure temperature, pumping power for coolant circulation, and material stress. For a given heat flux on the first wall, the maximum allowable structure temperature determines the highest coolant-exit temperature possible. The limits on pumping power and pressure stress each sets one minimum possible coolant-exit temperature. Pumping power and pressure limits are reached by gradually decreasing the coolant-exit temperature which increases the coolant velocity. Hence, the pressure drop, pumping power, and pressure stress also increase. As the heat flux on the first wall increases, permissible maximum and minimum coolant-exit temperatures approach one another and close the design window. Thermal-hydraulic design with any higher heat flux on the first wall is not possible without exceeding one or more of the three design limits. Separation of the coolant circuits allows lower exit temperature for the first wall and thus extends the design window.

The maximum structure temperature is obtained by adding the temperature drops across the tube wall (ΔT_w) and across the coolant boundary layer (ΔT_f) to the coolant-exit temperature. ΔT_w is calculated from a one-dimensional heat conduction in the channel wall. ΔT_f is determined for laminar flow from a two-dimensional analytical solution with arbitrary circumferential heat flux on the first-wall tube [10]. For turbulent flow, ΔT_f is obtained from an empirical correlation for Nusselt number given by Kovner et al. [11]. The turbulent-flow velocity is determined from the relations, Ret = 60 $H_{\|}$ to Ret = 500 $H_{\perp}$ suggested in Ref. [13]. Here Re_t is the transition Reynolds number and $H_{\|}$ and $H_{\perp}$ are the parallel and transverse Hartmann numbers, respectively. The MHD pressure drops are calculated by using the available theoretical/empirical equations reported in Refs. [6,10]. The pressure and thermal stresses are obtained from one-dimensional equations for a thick-walled cylinder [14,15]. For the determination of the design window, the blanket is treated as a lumped parameter. This is a reasonable approximation for the design-window calculation because the heat load on the blanket coolant channels is entirely due to nuclear heating and hence is much smaller than that on the first-wall coolant channels. After a design point is selected from the design window, detailed blanket design is carried out by treating each row of coolant channel individually.

3.3. Design results

A summary of TITAN-I parameters which are relevant to the thermal-hydraulic design are furnished in Table 1. Figure 2 shows the design window. It is seen that design is possible up to about 5 MW/m^2 heat flux on the first wall. The heat flux on the first wall at the design point is 4.6 MW/m^2 for TITAN-I, which corresponds to a plasma radiation fraction of 0.95. The design window shows that 5% pumping power limit is more restricting than the imposed pressure stress limit of 80 MPa. At the design point, the coolant velocity in the first wall tube is 21 m/s and about 0.5 m/s in the blanket channels. The corresponding exit temperatures

are 440°C and 700°C, respectively. The pressure drops in the first wall and blanket channels are shown in Fig. 3. The delivery pressure of the first wall/divertor pump is 12 MPa as the maximum divertor pressure drop is 12 MPa. The pressure drop in the first and sixth rows of the IBC coolant channels are 3 MPa and 0.5 MPa, respectively. Pressure drops in the hot-shield channels are negligible since they are situated beyond the IBC zone which carries the current for toroidal magnetic field. Orifices are used to reduce the delivery pressure of the pump to those required at the inlet of the coolant channels. The pressure and thermal stresses in the first-wall tubes are below the design limits.

As a verification and final tune-up of the one-dimensional structural design presented in this section, two-dimensional, axisymmetric finite element structural design is presented in the next section.

4. STRUCTURAL DESIGN

In this section, results of two-dimensional thermal and stress analyses performed using the finite element code ANSYS [16] are presented for the final design. A detailed comparison [1] of these plane stress, plane strain, and axisymmetric stress analyses indicates that axisymmetric models are the most accurate for computing thermal stresses in toroidal tubes such as those in TITAN-I. Hence, the following results are based on an axisymmetric finite element model of the first-wall tubes.

The pressure stresses are quite small, with a peak of 39 MPa. The thermal analysis, which was also performed with ANSYS, indicates a peak temperature of 741°C occurring at the surface nearest the plasma. The temperature at the rear of the tube remains near the coolant bulk temperature. The thermal gradient caused by the incident heat flux causes relatively large thermal stresses, as seen in Fig. 4 which shows the equivalent thermal stress contours for the first wall. The peak thermal stress is 279 MPa. Given the allowable primary stress of 108 MPa at an average first-wall temperature of 650°C, which indicates an allowable pressure plus

thermal stress of 324 MPa, the analysis indicates that the present first-wall design conforms to the ASME Boiler and Pressure Code and the design is viable.

Tubular blanket channels are chosen to avoid stress concentrations introduced by the existence of corners in a square cross section and to avoid weld near the first wall. The blanket tubes are subjected to volumetric heating and internal coolant pressure. Because the coolant pressure in the blanket is fairly low (1 to 3 MPa) compared to the strength of the vanadium, the tube thickness is much less than its radius, so a simple one-dimensional analysis is sufficient. The tubes are designed to have a fixed coolant-exit temperature of $700°C$ for high thermal conversion efficiency and a fixed structure fraction for high energy multiplication. The structure fraction is controlled by adjusting the radius-to-thickness ratio of the tubes and by adjusting the spacing between adjoining tubes. The one-dimensional analysis of the tubes indicates that a thickness of 2.5 mm and a radius of 2.5 cm satisfies these design requirements and the ASME Code.

The structure volume fractions are 30% and 90% in the first and last zones of the shield, respectively. The size of the square channel is 6 cm side length and 0.5 cm wall thickness. The outer size of the rectangular channels is 11.25 cm by 3.75 cm. The wall thickness is 1.625 cm. The dimensions of these coolant channels are determined mainly on the basis of the limit on wall temperature and required structure volume fractions. Thermal and pressure stresses are very small because the temperature gradient across the wall is small and the pressure drop in these channels is negligible.

5. CONCLUSIONS AND PERFORMANCE EVALUATION

The thermal-hydraulic and structural design of the fusion power core of the 18 MW/m^2 neutron wall-loading TITAN-RFP reactor using liquid lithium as the primary coolant and V-3Ti-1Si as structural material results in an attractive and economic design. The high coolant-exit temperatures give a gross thermal efficiency

of 44% which is substantially higher than that obtainable with water as the primary coolant [17]. The MHD pressure drops and pumping power are moderate. The maximum structure temperature and material stresses are below the design limits. The one-dimensional calculations for temperature and material stresses are adequate for scoping design purpose as substantiated by the two-dimensional finite element calculations.

The distinguishing features of the present design are summarized as follows:

1. Liquid lithium is the primary coolant and V-3Ti-1Si is the structural material.
2. Small round tubes are used as first-wall coolant channels.
3. In order to efficiently remove the heat flux incident on the first wall, MHD turbulent-flow heat transfer is used.
4. Alignment of the coolant channels with the stronger poloidal magnetic field reduces the MHD pressure drops.
5. Separation of the first wall and blanket coolant circuits, each with its own coolant circulation pump and coolant exit temperature, achieves maximum thermal cycle efficiency.

For high-temperature applications, the vanadium structure and lithium coolant combination has several advantages, especially for compact RFP reactors where the magnetic field topology is favorable.

ACKNOWLEDGEMENT

This work was supported by the United States Department of Energy, Office of Fusion Energy, Grant No. DE-FG03-86ER52126.

REFERENCES

1. F. Najmabadi, R. W. Conn, *et al.*, "The TITAN Reversed-Field-Pinch Fusion Reactor Study, Final Report," Joint report of UCLA, GAT, LANL, and RPI, UCLA Report UCLA-PPG-1200 (1988).
2. F. Najmabadi, R. W. Conn, *et al.*, "The TITAN Reversed-Field-Pinch Fusion Reactor Study: Scoping-Phase Report," Joint report of UCLA, GAT, LANL and RPI, UCLA-PPG-1100, 1987.
3. S. P. Grotz, N. M. Ghoniem, *et al.*, "Overview of the TITAN-I Fusion Power Core," in these proceedings.
4. C. P. C. Wong, R. L. Creedon, *et al.*, "The TITAN-II Reversed-Field Pinch Reference Aqueous Blanket Design," in these proceedings.
5. D. L. Smith, B. A. Loomis, and D. R. Diercks, "Vanadium-base Alloys for Fusion Reactor Applications— A Review," J. Nucl. Mater. **135** (1985) 125.
6. J. H. Holroyd and J. T. D. Mitchell, "Liquid lithium as a Coolant for Tokamak Fusion Reactors," Culham Laboratory Report CLM-R231 (1982).
7. R. W. Moir, J. D. Lee, W. S. Neef, D. L. Jassby, D. H. Berwald, *et al.*, "Feasibility Study of a Fission Suppressed Tokamak Fusion Breeder," Lawrenec Livermore National Laboratory Report UCID-20514 (1984).
8. J. C. R. Hunt and R. Hancox, "The Use of Liquid Lithium as Coolant in a Toroidal Fusion Reactor–Part I: Calculation of Pumping Power," Culham Laboratory Report (Oct. 1971).
9. S. Sharafat, N. M. Ghoniem, and P. I. H. Cooke, "Material Selection for the TITAN Reversed-Field Pinch Reactor," in these proceedings.
10. M. Z. Hasan and N. M. Ghoniem, "The Use of Liquid-Metal Coolants in the Thermal-Hydraulic Design of the First Wall and Blanket of High-Power- Density Fusion Reactors," *UCLA Report UCLA-ENG-8742/PPG-1086 (1987)*(submitted to Fusion Eng. and Des.).
11. M. Z. Hasan, "A Computer Program for Optimum Thermal-Hydraulic Design of the First Wall and Blanket of a Reversed-Field Pinch Fusion Reactor," UCLA Report UCLA-ENG-8740/PPG-1045 (1987).
12. D. S. Kovner, E. Yu. Krasilnikov and I. C. Panevin, Magnitnaya Gidrodinamika **7** (1966) 101.
13. M. A. Hoffman and G. A. Carlson, "Calculation Techniques for Estimating the Pressure Losses for Conducting Fluid Flows in Magnetic Fields," UCRL Report UCRL-51010 (1971).
14. E. E. Sechler, "Elasticity in Engineering" (Wiley and Sons, New York, 1952).

15. R. A. Bolay and J. H. Weimer, "Theory of Thermal Stress" (Wiley and Sons, New York, 1960).

16. G. J. DeSalvo and J. A. Swanson, "ANSYS User's Manual," Swanson Analysis Systems, Inc. (1979).

17. M. Z. Hasan and D. K. Sze, "Optimum Rankine Cycle for a High-Power-Density Fusion Reactor Using Liquid Metal as Primary Coolant," UCLA Report UCLA-ENG-8801/PPG-1109 (1988).

Table 1

MAJOR PARAMETERS OF TITAN-I.

Major radius, R	3.9 m
First wall radius, a	0.66 m
Neutron wall load	18 MW/m^2
Poloidal field at first wall	5.44 T
Toroidal field at first wall	-0.36 T
Total thermal power, Pth	2918 MW_t
Power to first wall circuit	736 MW_t
Power to divertor circuit	29 MW_t
Power to blanket circuit	2153 MW_t
Lithium inlet temperature	320 ^oC

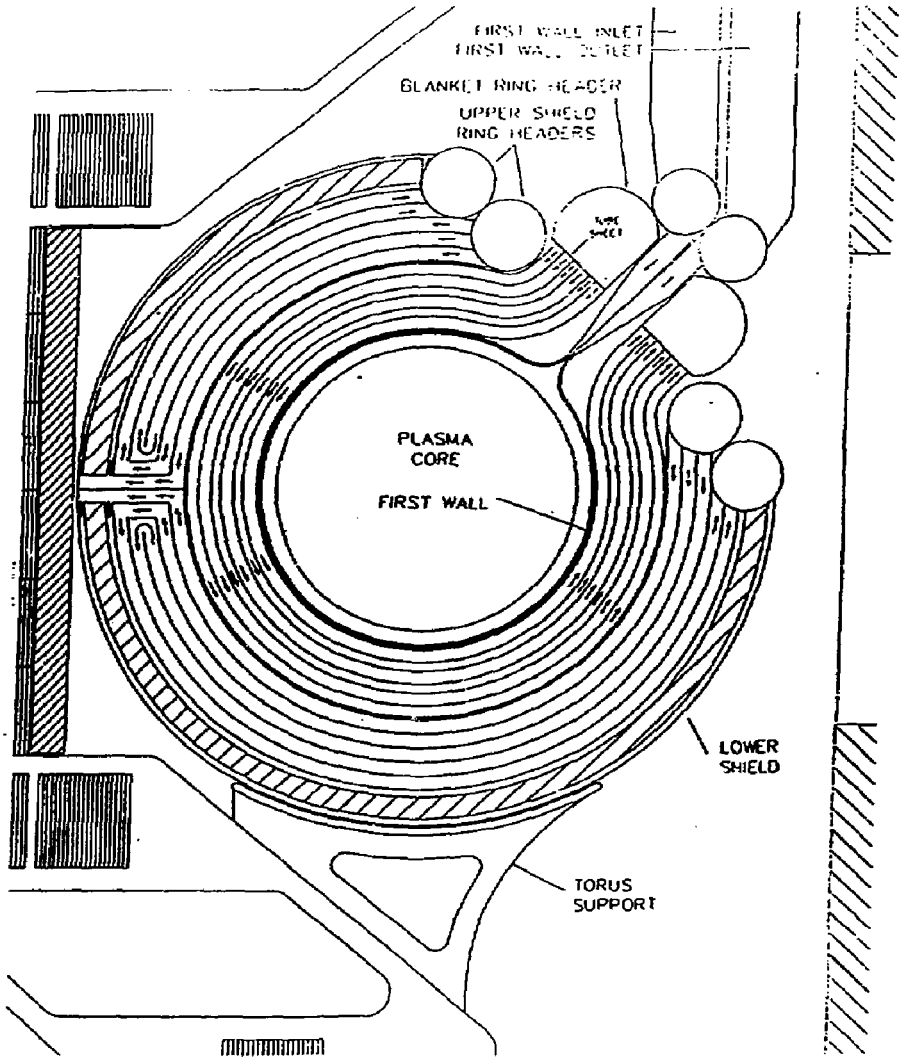

Figure 1. Configuration of FW/B for TITAN-I.

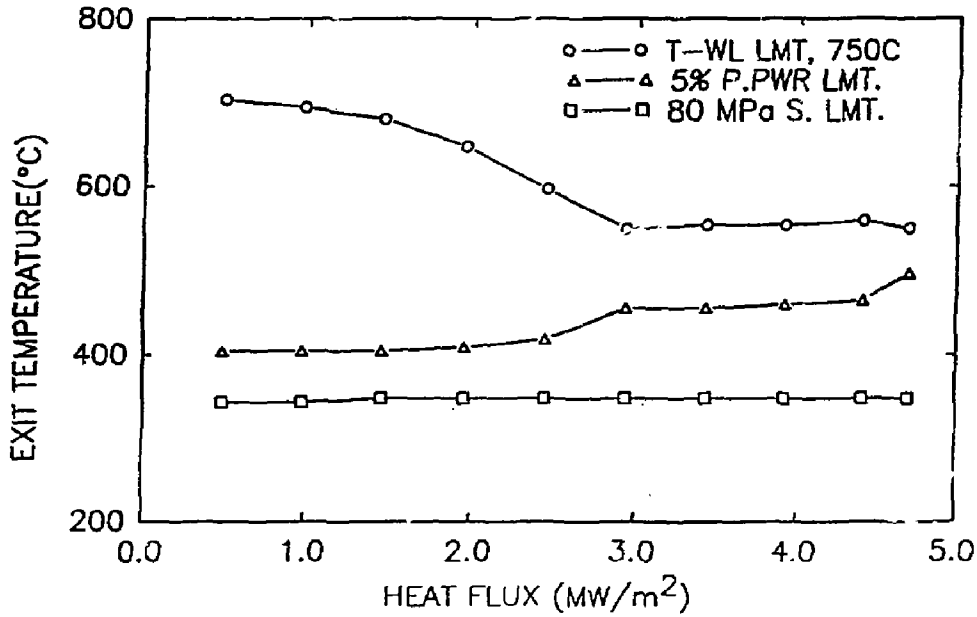

Figure 2. Design window.

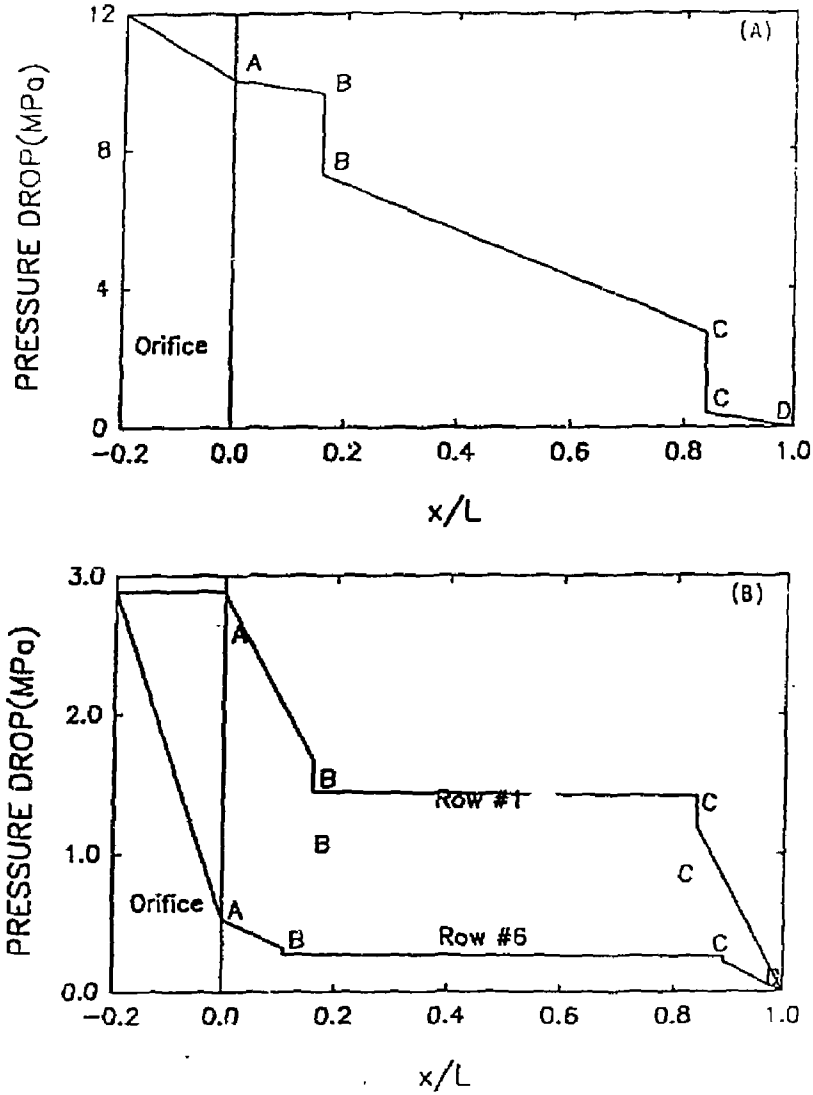

Figure 3. Pressure drop in coolant circuits: (A) first wall; (B) blanket. (AB and CD are the inlet and outlet ducts. There are 90 deg. bends at B and C. BC is the length of the channel.)

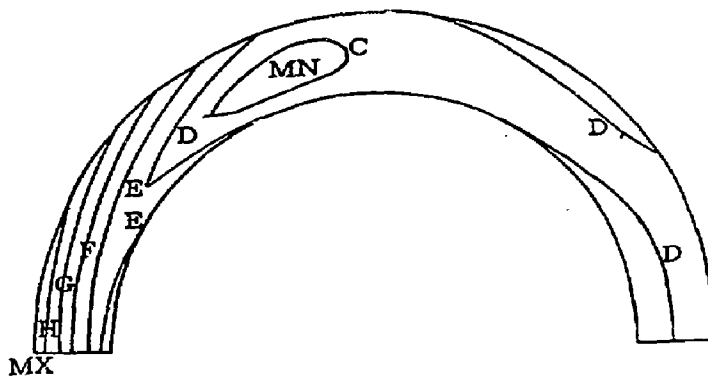

Figure 4. Contours of total equivalent stress (pressure plus thermal)(MPa) in the FW coolant channel. (MX=279, MN=11.8, C=40, D=80, E=120, F=160, G=200, and H=240).

AN OPTIMUM RANKINE POWER CYCLE FOR THE LITHIUM-COOLED TITAN-I REVERSED-FIELD-PINCH REACTOR

Mohammad Z. Hasan and D. K. Sze[1] for
The TITAN Research Group

Department of Mechanical, Aerospace and Nuclear Engineering
and Institute for Plasma and Fusion Research
University of California, Los Angeles
Los Angeles, CA 90024-1597, USA
[1]Argonne National Laboratory, Argonne, IL 60439, USA

ABSTRACT

A thermal power cycle for the TITAN-I fusion reactor is presented. The TITAN is a compact, high-power-density (neutron wall loading 18 MW/m^2) reactor based on the reversed-field pinch (RFP) confinement concept. The TITAN-I incorporates a fusion power core design with liquid-lithium as the coolant and breeder and vanadium alloy (V-3Ti-1Si) as the structural material. The total thermal power of TITAN-I is 2918 MW_t. Of this total thermal power, 736 MW_t is removed by the first-wall coolant, 29 MW_t by the divertor coolant and the rest 2153 MW_t by the blanket coolant. The primary coolant inlet temperature is 320°C. The exit temperatures are 440°C, 540°C and 700°C for the first-wall, divertor and blanket coolants, respectively. Coolants from the first wall and divertor are mixed upon exit which gives the first-wall/divertor mixed exit temperature of 442°C. The blanket coolant is kept separate. The coolant flow rates in the first-wall, divertor and blanket circuits are 1464, 31 and 1350 Kg/sec, respectively. Liquid-lithium is also chosen as the secondary coolant in the intermediate heat exchangers. Several power-cycle modifications are considered. The selected power cycle has two components—one for the conversion of the thermal power in the first wall and divertor coolants, and the other for conversion of the thermal power in the blanket coolant which is at much higher thermal potential. The power cycle for the first wall and divertor is a non-reheat, superheat Rankine cycle with 4 stages of regenerative feed water heating. The pressure and temperature of the throttle steam are 1500psia and 396°C, respectively. This results in a gross thermal efficiency of 37%. The power cycle for blanket is a Rankine cycle with 2-stage reheat and 7 stages of regenerative feed water heating. The throttle steam conditions are 562°C and 3100psia. The gross thermal efficiency for this cycle is 46.5%. The overall gross thermal efficiency of the lithium-cooled TITAN reactor is 44%. All the power cycle analyses are done by the code PRESTO developed at Oak Ridge National Laboratory in the United States.

1. INTRODUCTION

The TITAN study is a multi-institutional effort to investigate the potential of Reversed-Field Pinch (RFP) confinement concept as a high-power-density fusion reactor [1,2]. Two TITAN designs have emerged. TITAN-I is a self-cooled lithium design with vanadium structure [3] and TITAN-II is an aqueous salt-solution, loop-in-pool design with ferritic steel as the structural material [4]. The use of liquid lithium as the coolant for TITAN-I allows the removal of the thermal energy from the reactor at a suitably high thermal potential so that higher power cycle efficiency can be realized. Details of thermal-hydraulic design of the first wall and blanket are presented in a paper in this symposium [5].

In the thermal-hydraulic design of the first-wall and blanket for TITAN-I, the coolant circuits for the first wall and blanket are separated. This separation is necessary for dealing with high heat flux on the first wall. The maximum heat flux on the first wall of TITAN is 4.6 MW/m^2. It is even higher on the divertor plate. As a result of this separation, the exit temperature of the first-wall coolant can be made lower than that of the blanket coolant. This helps to remove higher heat flux on the first wall without exceeding the structure temperature limit. The same is also true for the divertor .Thermal design of the divertor is discussed in another paper in this symposium [6]. The divertor coolant has a different exit temperature from those of the first-wall and blanket coolants. Therefore, TITAN-I has three separate circuits for primary lithium—the first wall, divertor and blanket coolant circuits— each with different coolant exit temperatures. The inlet temperature is kept the same. The outlet temperatures of the three circuits were then obtained by optimizing the thermal-hydraulic design. The exit temperature of the blanket coolant is made as high as possible to increase the temperature potential of the thermal power in the blanket coolant.

One of the reasons for keeping the inlet temperature same is simplicity. Single inlet temperature allows the use of a single pump for the coolant circulation

pumps and one pump for more than one coolant circuits. TITAN-I uses the same coolant circulation pump for the first-wall and divertor. The pumps for the first-wall/divertor and blanket circuits draw lithium from the same sump. Maximum possible inlet temperature is used for the first wall and divertor. Higher inlet temperature is possible for the blanket circuit from thermal design point of view. The IBC [1] (Integrated Blanket Coil) section of the blanket carries electrical current for producing the toroidal magnetic field. Therefore, to keep the electrical resistance of lithium in the blanket and hence the joule loss small, higher coolant inlet temperature is not used for the blanket.

The total thermal power, coolant temperatures and flow rates in these three circuits are furnished in Table 1. In this paper, the power cycle for TITAN-I is disc ;sed.

2. INTERMEDIATE HEAT EXCHANGER AND SECONDARY COOLANT

Both the inlet and exit temperatures of the primary coolant affect the power cycle efficiency. The inlet temperature affect the pinch point and hence the maximum permissible steam pressure in a Rankine power cycle. In a steam generator, the pinch point is the location at which the temperature of the water reaches the boiling point. At the pinch point in a steam generator, the temperature of the hot fluid must be higher than the boiling point of water at the desired pressure by a minimum amount for efficient heat transfer. Otherwise, large heat transfer surface area, which corresponds to large steam generator, will be required. Suitably high inlet temperature of the primary/secondary coolant is, therefore, necessary for obtaining high steam pressure.The exit temperature determines the maximum steam temperature. Both high steam pressure and high steam temperature are essential for obtaining a high cycle efficiency.

The main purpose of an intermediate heat exchanger is to act as a barrier so that the primary coolant which may contain radioactive products does not come in

contact with water or steam of the steam cycle. From the consideration of power cycle efficiency, an intermediate heat exchanger is undesirable since it degrades the thermal potential of the thermal power in the coolant. In TITAN-I, it has been decided to have a barrier against tritium permeation and leakage of radiation products from the primary lithium into the steam cycle. Therefore, an intermediate heat exchanger is used in the power cycle.

Both liquid lithium and sodium were considered as the secondary coolant. Liquid lithium is preferable to sodium for several reasons. With lithium as the primary and secondary coolant, only one coolant is used in the plant. As a result, storage and handling of the coolant will be easier. Also the heat capacity of lithium is about twice that of sodium, thus the total amount of coolant will be much less with lithium than with sodium. Lithium is also less reactive with water than sodium.

The solubility of tritium in sodium is much lower than that in lithium. Therefore, when sodium is used as the secondary coolant, one desirable and one undesirable effects may result. The desirable one is that the tritium inventory in the secondary loop will be much smaller, by about two orders of magnitude. The other, possibility of higher tritium permeation to the steam cycle. The reason is that lower solubility is accompanied by higher tritium partial pressure which drives the permeation. However, if salt-extraction method is used to remove tritium from the primary lithium, then the amount of tritium permeation to the steam side is the same for both lithium and sodium as the secondary coolant. This is because the tritium concentration in the primary lithium can be reduced to less than 1 ppm by using salt-extraction process [7]. This corresponds to a tritium partial pressure of about 10^{-9} torr in the primary lithium which is much less than that obtainable by cold trap in sodium at $115^{o}C$ [8]. Therefore, the maximum tritium partial pressure in the secondary coolant (sodium or lithium), and hence tritium permeation to the steam side will be fixed by the tritium pressure in the primary lithium when salt-extraction method is used to remove tritium from the primary lithium. The only

benefit in using sodium seems to be that the tritium inventory will be much lower in the secondary coolant. However, it is assessed [1] that the added safety concern due to the higher tritium inventory in the secondary lithium is not significant.

Another potential advantage with sodium as the secondary coolant is the availability of sodium technology from the fast breeder fission reactors. However, this advantage is not significant for TITAN since the heat exchanger technology with lithium, in any case, needs to be developed for TITAN-I because the primary coolant is lithium. Therefore, it is decided to use liquid lithium as the secondary coolant for TITAN-I.

3. SELECTION OF POWER CYCLE(S)

The total thermal power of the TITAN-I reactor is removed by three primary coolant circuits— first-wall, divertor and blanket coolant circuits. The inlet temperature of lithium for all the three circuits is the same but the exit temperatures are different. Of the total thermal power, only 1% is removed by the divertor coolant, about 25% by the first-wall coolant and the remaining 74%, by the blanket/shield coolant. If the first-wall and divertor coolants are mixed upon exit, the mixed exit temperature becomes $442°C$. This leads to two amounts of the primary lithium removing 765 MW_t and 2153 MW_t of thermal power and having the exit temperatures of $442°C$ and $700°C$, respectively.

There could be three possible variations of power cycles for TITAN-I. These are shown in Fig. 1. Economics and simplicity will dictate the selection of a particular variation of power cycle. The case (a) in Fig. 1 is for mixing of the first-wall/divertor and blanket coolants upon exit and the use of a single power cycle. This is the simplest case. The mixed exit temperature of lithium in this case is $556°C$. The next case, case (b), allows partial mixing of the first-wall/divertor and blanket coolants in a special intermediate heat exchanger. This case will have higher steam temperature and pressure compared to the case (a), and will use one

steam generator/turbine set. The third case, case (c), is for two separate power cycles— one for the first-wall/divertor thermal power and the other for the blanket thermal power. Each power cycle will have a set of intermediate heat exchanger, steam generator, steam turbine and electric generator. Detailed discussion about Rankine power cycles for a high-power-density, liquid-metal-cooled fusion reactor is provided by Hasan and Sze [9].

The power cycle for case (a) in Fig. 1 is the simplest and least costly, but the thermal efficiency will be lower than those for the cases (b) and (c). The reason is the lower primary coolant exit temperature. New and complicated design of the intermediate heat exchanger and steam generator are necessary for the case (b). Consequently, the capital cost will be higher than that for case (a). Since the maximum steam temperature can be higher in this case, the thermal efficiency is higher than that for case (a). The total capital cost of the power cycles in case (c) is likely to be the highest among the three variations under consideration. The reason is that the cost of a power cycle goes down with the increase of thermal power for a single unit. The power cycles in case (c) are as simple as that in case (a). The only difference is the use of two power cycles. The overall thermal efficiency for this case will be higher than those for cases (a) and (b), because mixing in the latter two cases decreases the temperature potential at which the thermal power is utilized by the power cycle. In case (c), the maximum possible thermal power cycle efficiency can be realized for the thermal powers from both the first-wall/divertor and blanket coolants. The cost of the thermal power conversion system is a small fraction of the total capital cost of TITAN and, therefore, has less effect on the cost of electricity compared to that of thermal cycle efficiency. Therefore, the power cycle corresponding to the case (c) in Fig. 1 has been selected as the reference power cycle for TITAN-I. In the next section, results of analysis of this power cycle are presented.

4. ANALYSIS OF THE REFERENCE POWER CYCLE

A schematic of the flow diagram for the reference power cycle is shown in Fig. 2. The blanket power cycle is shown explicitly in this figure. The fusion power core of TITAN-I is divided into three sectors separated by divertor modules. For each sector, there is an intermediate heat exchanger and a steam generator for both the first-wall/divertor and blanket power cycles. The steam from the three steam generators of the first-wall/divertor power cycle are combined to run a single turbine-generator set, and similarly for the blanket power cycle.

The power cycle analysis is performed by the code PRESTO [10]. The pinch-point temperature difference in the steam generators of each of these power cycles are kept above $20°C$. For both of the first-wall/divertor and blanket power cycles, the temperature drops in the intermediate heat exchangers are taken to be $20°C$. The temperature-energy diagram for the first-wall/divertor power cycle is shown in Fig. 3. The first-wall/divertor power cycle is a superheat Rankine cycle with four stages of regenerative feed water heating. There is no reheat of the steam. The temperature and pressure of the throttle steam for this cycle are 396 $°C$ and 10.7 MPa, respectively. The blanket power cycle is a superheat Rankine cycle with two-stage reheat and 7 stages of regenerative feed water heating. The maximum steam temperature is limited to $565.6°C$ ($1050°F$) although higher temperature is reported. The throttle steam pressure is 21.4 MPa. The superheater and the reheaters are arranged in series. Figure 4 shows the temperature-energy diagram for the blanket power cycle. These two figures are drawn from the results of analysis by the code PRESTO. As shown in Figs. 3 and 4, more than 50% of the thermal energy is consumed in the boiler for phase change in the power cycle for first wall/divertor and less than 10% in the blanket power cycle. The reason is the difference in steam pressure.

With the inlet/outlet temperatures of the blanket/shield coolant of 320/700 $°C$, a supercritical Rankine cycle could be operated. However, the design of a steam

generator with supercritical pressure is complicated. Therefore, a subcritical cycle has been selected. The temperature difference at the pinch point for the blanket power cycle is 34 ^{o}C which is considerably higher than 20 ^{o}C. Again, the maximum steam temperature is considerably lower than the secondary coolant temperature in the superheater. Both of these will make the design of the steam generator and the superheater/reheater for the blanket power cycle compact. This will somewhat reduce the cost of the power cycle.

Other particulars for the two power cycles are as follow. For both power cycles, the generator power factor is assumes 0.9, the turbine-generator rotational speed is taken 3600 rpm and the feedwater pump turbine efficiency is assumed 0.8. There are one high-pressure (HP), one intermediate-pressure (IP) and four parallel, low-pressure (LP) turbines in each of the two power cycles. The number of regenerative feedwater heaters and the extraction pressures are obtained by optimizing the thermal efficiency. Of the four regenerative feedwater heaters in the first-wall/divertor power cycle, one is heated by steam extraction from the IP turbine and the remaining three by extractions from the LP turbines. The extraction pressures are 120, 35, 14.7 and 6 *psia*. In the blanket power cycle, the seven regenerative feedwater heaters are heated by one steam extraction from HP turbine, two from IP turbine and four from the LP turbines. The extraction pressures are 680, 320, 165, 70, 35, 14.7 and 6 *psia*.

The main results and parameters of the first-wall/divertor and blanket power cycles for TITAN-I are provided in Table 2. This table shows the inlet and outlet temperatures of the primary and secondary coolants, the throttle steam conditions, steam flow rate, the temperature difference at the pinch point, the condenser back pressure, inlet temperature of the feed water and the gross thermal efficiency. The overall gross thermal efficiency for TITAN-I, by combining the efficiencies of the first-wall/divertor and blanket power cycles, is 44%.

5. SUMMARY AND CONCLUSIONS

The total thermal power of TITAN-I removed from the reactor core by the primary lithium is divided into two groups at different temperature potentials. The mixed exit temperature of the first-wall/divertor coolant is $442°C$ and the exit temperature of the blanket coolant is $700°C$. In order to maximize the thermal efficiency, two separate Rankine power cycles— one for the first-wall/divertor and the other for the blanket— are used to convert the thermal energy into electrical energy. Intermediate heat exchangers are used to act as barriers for radioactive products and tritium permeation to the steam side. Liquid lithium is also used as the secondary coolant in the intermediate heat exchangers mainly for the reason of simplicity of storage and handling.

The power cycle for conversion of the thermal power in the first-wall/divertor coolant is a superheat Rankine cycle with no reheat and 4 stages regenerative of feed water heating. The gross efficiency of this cycle is 37.29%. The power cycle for conversion of the thermal power in the blanket coolant is a two-stage reheat, superheat Rankine cycle with 7 stages of regenerative feed water heating. This power cycle has a gross thermal efficiency of 46.52%. The resulting overall gross thermal efficiency of TITAN-I is 44%.

The maximum gross thermal efficiency that can be realized using water as the primary coolant is about 35%. The use of liquid metal as the primary and secondary coolant for TITAN-I has resulted in an increase of about 9% in thermal efficiency.

ACKNOWLEDGEMENT

This work was supported by the United States Department of Energy, Office of Fusion Energy, Grant No. DE-FG03-86ER52126.

REFERENCES

1. F. Najmabadi, R. W. Conn, *et al.*, "The TITAN Reversed-Field Pinch Fusion Reactor Study: Final Report," joint report of UCLA, GAT, LANL and RPI, UCLA-PPG-1200, 1988.
2. F. Najmabadi, R. W. Con., *et al.*, "The TITAN Reversed-Field Pinch Fusion Reactor Study: Scoping Phase Report," joint report of UCLA, GAT, LANL and RPI, UCLA-PPG-1100, 1987.
3. S. P. Grotz, N. M. Ghoniem, *et al.*, "Overview of the TITAN-I Fusion-Power Core," in these proceedings.
4. C. P. C. Wong, R. L. Creedon, *et al.*, "Overview of the TITAN-II Reversed-Field Pinch Aqueous Fusion Power Core Design," in these proceedings.
5. M. Z. Hasan, J. P. Blanchard and N. M. Ghoniem, "Thermal-Hydraulic and Structural Design for the Lithium-Cooled TITAN-I Reversed-Field Pinch Reactor," in these proceedings.
6. P. I. H. Cooke, *et al.*, "Engineering Design of the TITAN-II Divertor," in these proceedings.
7. K. Natesen, "Influence of Nonmetallic Elements on the Compatibility of Structural Materials with Liquid Alkali Metals," J. Nucl. Mater., **115** (1983) 251.
8. K. Natesen and D. L. Smith, "Effectiveness of Tritium Removal from a CTR Lithium Blanket by Cold Trapping Secondary Liquid Metals Na, K and NaK," Nuclear Technology, **22** (1974) 138.
9. M. Z. Hasan and D. K. Sze, "Optimum Rankine Cycle for a High-Power-Density Fusion Reactor Using Liquid Metal as Primary Coolant," UCLA-ENG-8801/PPG-1109, 1988.
10. L. C. Fuller and T. K. Stovall, "User's Manual for PRESTO: A Computer Code for the Performance of Regenerative Superheated Steam-Turbine Cycles," Oak Ridge National Laboratory Report ORNL-5547, NASA CR-159540, June 1979.

Table 1

THERMAL POWER REMOVED BY THE

THREE COOLANT CIRCUITS IN TITAN-I.

First-wall coolant circuit:	
Thermal power removed, P_{FW}	736 MW_{th}
Lithium inlet temperature, $T_{in,FW}$	320 ^{o}C
Lithium exit temperature, $T_{ex,FW}$	440 ^{o}C
Lithium flow rate, $\dot{M}_{FW}$	1464 Kg/s
Divertor coolant circuit:	
Thermal power removed, P_{DIV}	29 MW_{th}
Lithium inlet temperature, $T_{in,DIV}$	320 ^{o}C
Lithium exit temperature, $T_{ex,DIV}$	540 ^{o}C
Lithium flow rate, $\dot{M}_{DIV}$	31 Kg/s
Blanket coolant circuit:	
Thermal power removed, P_{BL}	2153 MW_{th}
Lithium inlet temperature, $T_{in,BL}$	320 ^{o}C
Lithium exit temperature, $T_{ex,BL}$	700 ^{o}C
Lithium flow rate, $\dot{M}_{BL}$	1352 Kg/s

Table 2

SUMMARY OF THE RESULTS OF POWER

CYCLE ANALYSIS FOR TITAN-I.

First-wall/divertor power cycle:	
Total thermal power in the primary coolant	765 MW_t
Primary lithium inlet/exit temperatures	320/442 $°C$
Secondary lithium inlet/exit temperatures	300/422 $°C$
Throttle steam temperature/pressure	396/10.69 $°C/MPa$
Steam flow rate	326 Kg/sec
Temperature difference at pinch point	21.6 $°C$
Condenser back pressure	2 $"Hg$
Stages of feed water heating	4
Feed water inlet temperature	169 $°C$
Gross thermal efficiency	37.29 %
Blanket power cycle:	
Total thermal power in the primary coolant	2153 MW_t
Primary lithium inlet/exit temperatures	320/700 $°C$
Secondary lithium inlet/exit temperatures	300/680 $°C$
Throttle steam temperature/pressure	565.6/21.38 $°C/MPa$
Steam temperature after 1st reheat	565.6 $°C$
Steam temperature after 2nd reheat	550 $°C$
Total steam flow rate	698 Kg/sec
Temperature difference at pinch point	34 $°C$
Condenser back pressure	2 $"Hg$
Stages of feed water heating	7
Feed water inlet temperature	258 $°C$
Gross thermal efficiency	46.52 %
Overall gross thermal efficiency	44 %

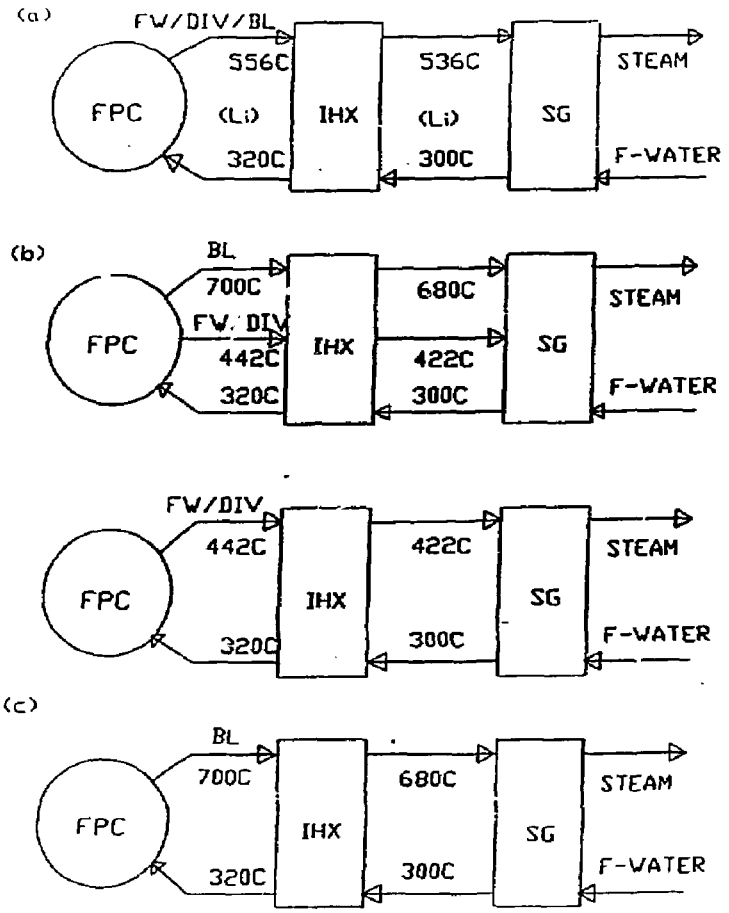

Figure 1. Schematics of the possible variations of power cycles for TITAN-I. (FPC=fusion power core, FW=first wall, DIV=divertor, BL=blanket, IHX=intermediate heat exchanger, SG=steam generator)

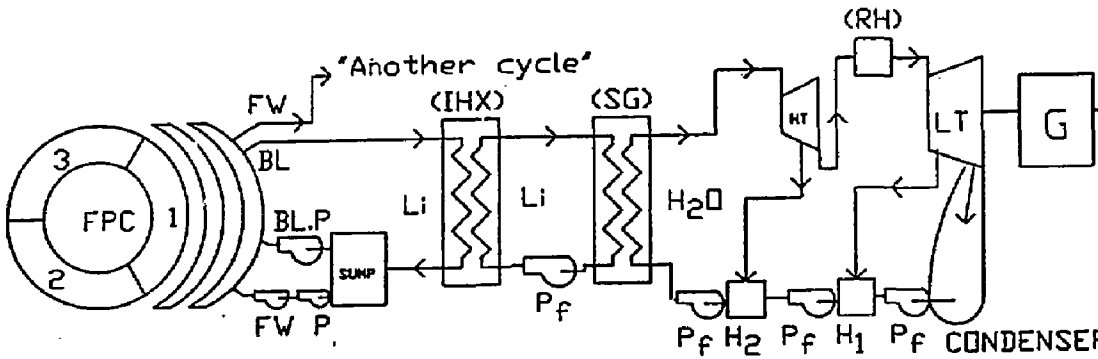

Figure 2. A schematic of the flow diagram of the power cycle for TITAN-I. The figure shows explicitly the blanket power cycle with one reheater and two regenerative feedwater heaters. (FPC=fusion power core, FW=first wall, DIV=divertor, BL=blanket, P=coolant pump, IHX=intermediate heat exchanger, SG=steam generator, HT=high-pressure turbine, RH=reheater, LT=low-pressure turbine, G=electric generator, P_f=feed-water pump)

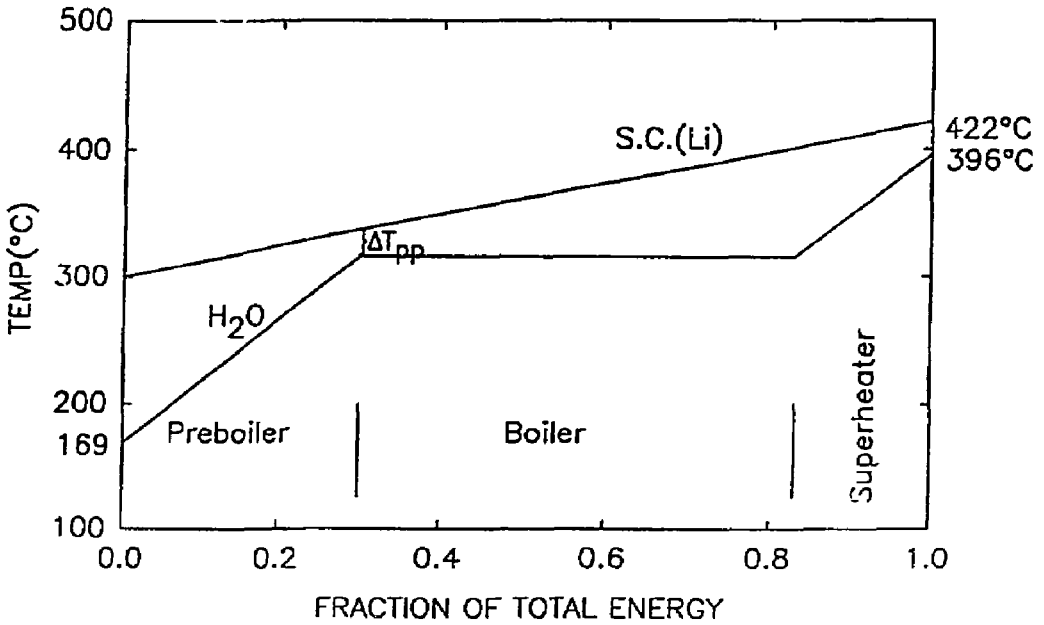

Figure 3. Temperature-energy diagram for the first-wall/divertor power cycle. ΔT_{pp} is the temperature difference at the pinch point.

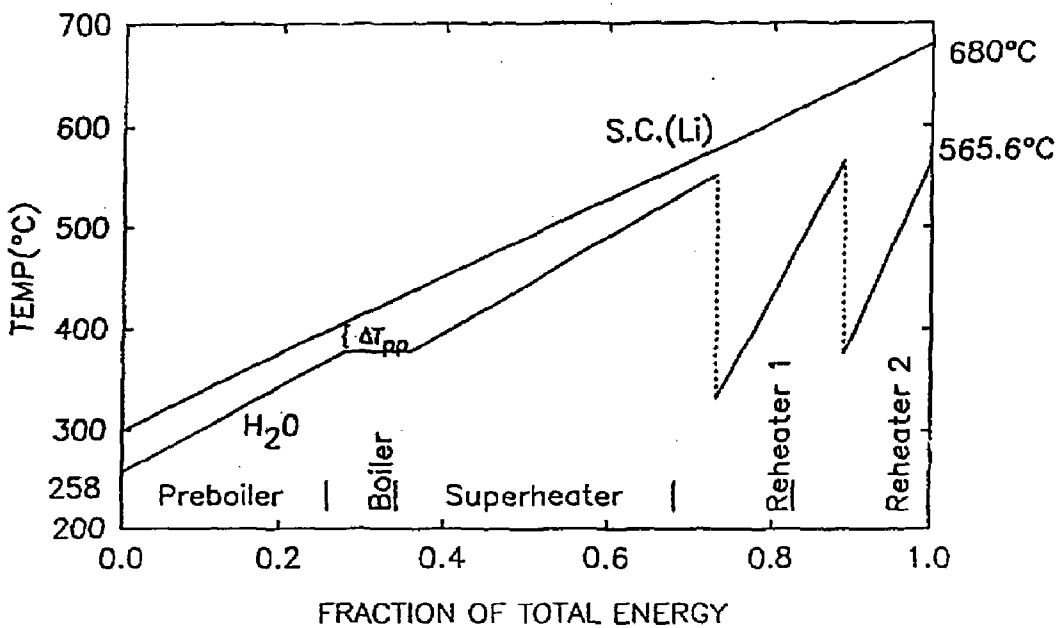

Figure 4. Temperature-energy diagram for the blanket power cycle. ΔT_{pp} is the temperature difference at the pinch point.

ENGINEERING DESIGN OF THE TITAN-II DIVERTOR

P. I. H. Cooke[1], C. G. Bathke[2], J. P. Blanchard, S. P. Grotz,
M. Z. Hasan, and S. Sharafat, for the TITAN Research Group,

Department of Mechanical, Aerospace and Nuclear Engineering
and Institute for Plasma and Fusion Research,
University of California at Los Angeles,
Los Angeles, CA 90024-1597, USA.

ABSTRACT

The design of the toroidal-field divertor for the TITAN-II reversed-field-pinch reactor is described. Strong radiation from the core and edge plasma spreads the heat load over the first wall and divertor areas of the high-power-density reactor, and careful shaping of the divertor target plate restricts the maximum heat flux to $\sim 7.5\,MW/m^2$. *A further feature leading to manageable heat fluxes is the "open" configuration for the divertor, in which the target plate is located close to the null point to take advantage of the expansion of magnetic flux. The divertor target is constructed from a single material, a tungsten-rhenium alloy, for both the armor and coolant tubes, to avoid stress concentrations which arise at the interface between different materials. This alloy was chosen for its high ductility and good thermal and mechanical properties, which are retained at high temperatures, and for its excellent resistance to erosion by sputtering in the anticipated divertor plasma conditions. Detailed finite-element modeling of the divertor target indicates a peak equivalent thermal stress in the armor of* $\sim 500\,MPa$. *Fabrication of the divertor plate is based on brazing the bank of coolant tubes to the armor, all components being manufactured using powder metallurgy techniques. The coolant for the divertor plate is an aqueous* $LiNO_3$ *solution, with a lithium atomic percentage of 6.4%, as used throughout the fusion power core. Consideration of the thermal and physical properties of this solution allows coolant conditions to be chosen such that an adequate safety margin for critical heat flux is provided.*

---

[1] *Permanent address: UKAEA Culham Lab., Abingdon, Oxon OX14 3DB, UK.*
[2] *Los Alamos National Laboratory, Los Alamos, New Mexico 87545, USA.*

1. INTRODUCTION

The TITAN reversed-field-pinch (RFP) reactor study [1] was undertaken to determine the technical feasibility and key developmental issues of a high-power-density, compact RFP fusion reactor. Two detailed designs for the fusion power core were studied, each having broadly the same plasma parameters, with major and minor radii of 3.9 m, and 0.6 m respectively, and a neutron wall loading of 18 MW/m^2. TITAN-I uses liquid lithium as the coolant and tritium breeding material, with a vanadium-alloy structure. The TITAN-II design is an aqueous loop-in-pool concept with a dissolved Li salt as the breeder and coolant, and a reduced-activation, high-strength ferritic steel (9-C) as the structural material.

For each design the impurity control and particle removal system consists of three toroidal-field divertors, and the background behind this choice is described in reference [2]. The design of the TITAN-I divertor is reported in references [1] and [2], while this paper concentrates on the TITAN-II design.

The design of the impurity control system poses some of the most severe problems of any component of a DT fusion reactor. For a high-power-density device like TITAN, the design of a system which simultaneously satisfies constraints on heat loadings and sputtering damage can be particularly challenging. In the early phases of the study [3] the heat load on the divertor target was found to be too high without radiating a large fraction of the plasma power. This result has led to the injection of xenon impurity to produce a strongly-radiating plasma. In the global plasma power balance, $\sim$ 93% of the plasma power is radiated in the core plasma and scrape-off layer, 4% in the high-density plasma near the divertor target and only 3% is deposited on the plate by the plasma. This high-radiation régime of operation, which appears to be an essential element for a high-power-density reactor, may be more easily achieved in a RFP than in a tokamak, because experimental evidence suggests that RFPs operate with a soft β-limit. In an experiment on ZT-40M [4] trace quantities of krypton impurity were added; as the radiative losses increased,

the non-radiative losses decreased to maintain a constant total confinement time and an unchanged operating point. Analysis of the edge plasma, including estimates of the erosion rate on the first wall and divertor target, is reported in reference [5].

Earlier work [6] showed that the poloidal asymmetries in the field-line density inherent in a toroidal-field divertor can yield a large peaking factor in a "closed" divertor configuration (in which the coils produce a "pinching" of the field lines and the divertor target is located in the shadow of the nulling coil). To minimize the poloidal asymmetry effect, the TITAN designs incorporate "open" divertors, with the target located close to the null point to take advantage of the magnetic flux expansion which occurs in that region. Neutral transport calculations [5] indicate that a negligibly small fraction of particles released from the target re-enters the core plasma, despite the proximity of the target to the null point.

A cross-section through the equatorial midplane of one divertor is given in Figure 1. This figure shows the location of the divertor coils and toroidal-field coils, and gives a two-dimensional tracing of the field lines near the separatrix on the inboard and outboard sides of the plasma.

2. MATERIALS

Estimates of sputtering erosion for various candidate plasma-facing materials led to the specification that a high atomic number (Z) material must be used for the surface of the divertor plate. These calculations showed that only for high Z materials is the threshold energy for sputtering high enough such that the erosion rate of the divertor target under the conditions expected for TITAN is acceptably low.

The material finally chosen for the divertor target was an alloy of tungsten and rhenium. Tungsten has good thermal and mechanical properties which are retained at high temperatures, and also has a very low sputtering rate. The use of pure tungsten was rejected because of its high ductile-to-brittle transition temperature

(DBTT) ($\sim$ 300°C) and resulting low ductility at low temperatures. Rhenium is added as an alloying element to improve ductility and lower the DBTT, and to avoid the loss of strength after recrystallization. The 26% rhenium alloy is used in this case to give the maximum improvement in performance, although this choice does entail a significant increase in cost. A further disadvantage of the use of rhenium is its activation and the subsequent rad-waste problem [4], but as the total mass of the divertor armor for the whole reactor is only $\sim$ 30 kg, this was only a minor consideration in the materials selection.

Because the use of different materials for the armor and substrate of the divertor plate creates stress concentrations at the interface [1,2], it is desirable to fabricate the divertor from a single material. For TITAN-I, MHD concerns associated with the liquid-lithium cooling preclude the use of high-conductivity tungsten-alloy coolant tubes, so a two-material divertor is necessary. In TITAN-II, though, the aqueous coolant allows the use of tungsten as both the plasma- and coolant-facing material, leading to a single-material design. The complex geometry of the target plate does not allow the structure to be fabricated from one piece, so the sputtering-resistant armor plate is produced separately and subsequently bonded to the coolant tubes, as described in Section 5.

An aqueous $LiNO_3$ solution, as proposed for the blanket, is to be used for the divertor target coolant for TITAN-II. Pure water was also considered, because of the eased corrosion and radiolysis problems, but these questions appear to have been satisfactorily accounted for in the blanket coolant analysis [1]. There is a large uncertainty in the thermal and physical properties of the salt solution [7], but the indications are that the changes relative to water should improve the thermal performance, by allowing operation at a lower pressure, and increasing the critical heat flux, for example. The $LiNO_3$ solution was therefore chosen for the divertor coolant to allow an assessment of its potential to be made, but it is recognized that certain issues cannot be fully resolved until more experimental data are available.

The concentration of the coolant is the same as for the blanket (Li atomic percentage 6.4%), but because of the higher loadings on the divertor, different inlet and outlet conditions have to be used. In particular, as described below, the higher pressure used for the divertor coolant allows a higher outlet temperature. This permits the heat deposited into the divertor target coolant to be extracted via a heat exchanger with the primary blanket inlet coolant, and avoiding the need for a complete separate cooling circuit.

3. TARGET DESIGN

Despite the intense radiation arising from the impurities injected into the plasma, careful shaping of the divertor target is required to maintain the heat flux at acceptable levels at all points on the plate. The shaping problem is highly complex because of the varying flux expansion factor (as the field lines converge or diverge) and the plasma and radiation heat fluxes, which depend in a non-linear way on the location in the scrape-off layer and the angle with respect to the core plasma. An iterative procedure has therefore been developed, in which the heat flux distribution corresponding to a possible shaping is calculated and then used to perform a thermal-hydraulics analysis, converging to an acceptable design. If any constraint imposed on the design is violated, then the shaping is adjusted until an acceptable solution is obtained. This involved iteration was simplified by writing a computer code to automate the thermal analysis. The final geometry for the outboard midplane of the TITAN-II divertor, is shown in Figure 2. The geometry for the inboard side is similar, but more compressed, because of geometrical effects and the $1/R$ dependence of the toroidal field, leading to somewhat higher heat fluxes on the inboard target.

For TITAN-II, the divertor target coolant flows in the toroidal/radial direction, as opposed to the poloidal direction which was mandated for TITAN-I to avoid an excessive MHD pressure drop. A disadvantage of the poloidal coolant routing (or, in general, if the coolant is directed along the majority magnetic field) is that the

heating rate can vary considerably from one tube to another. If the plasma should move slightly from its expected position, this can result in a coolant tube receiving a much greater heat load than it was designed for. With the coolant flowing in the direction perpendicular to the majority field, the total heat deposited on each tube is the same, and plasma motion will only alter the heat flux distribution along the tube's length. However, with the toroidal/radial flow proposed for TITAN-II, the length of the tubes is rather short, which can lead to a large volume flow rate of the coolant and a small inlet-to-outlet temperature rise. This problem is avoided here by the use of poloidal ring headers and a multi-pass coolant flow.

Because of the double curvature of the divertor plate, the cross-section of the coolant tubes must vary along their length in order for the tubes to remain touching. As this would impose difficulties in the fabrication of the tungsten-rhenium tubes, the tubes are designed to touch only at the apex of the target (the location of minimum minor radius), with a slight gap between adjacent tubes at other points. The effect of these gaps on the thermal and stress analysis is discussed in detail in the following section, but the results of this more sophisticated analysis were incorporated into the overall design described here.

The coolant tube diameter was chosen to be as large as possible (to minimize the number of tubes, and, hence, the likelihood of failure at the ends of the tubes where they are brazed to the headers), without requiring so large a wall thickness that thermal stresses became a problem. This process led to a diameter of 10 mm and a wall thickness of 1 mm.

To accommodate the high heat loads on the divertor target, advantage is taken of the high heat transfer coefficients possible in the sub-cooled flow boiling régime, as used in the first-wall cooling. In the absence of any correlations specifically for high-temperature aqueous solutions, general water-derived correlations for heat transfer and critical heat flux (CHF) have been used to assess the cooling performance of the TITAN-II divertor target. At any point along the coolant tube, the heat transfer

coefficient is taken as the greater of the values predicted by the Dittus-Boelter (forced convection) correlation and the Thom correlation [8] for sub-cooled flow boiling. For CHF, the correlation derived by Jens and Lottes [9] was used.

An important factor in considering critical heat fluxes is the conduction of heat from the surface of the target into the coolant. As discussed below, the heat flux tends to be concentrated from the value on the surface to a smaller area of the inner tube wall. This peaking, which is augmented by the gap between the coolant tubes, is included in the analysis, by using an approximate fit to the concentration factor given by the results of the finite element thermal analysis.

Figure 3 shows the distribution of heat flux along the divertor target for the inboard location where the highest loadings occur. The distance along the target is measured in the direction of the coolant flow; the center of the figure, where the heat flux drops, is at the apex of the target, facing directly into the core plasma. The figure shows the plasma and radiation components of heat flux, yielding a maximum surface heat flux of $7.5\,\mathrm{MW/m^2}$ on the inboard target and $5.8\,\mathrm{MW/m^2}$ on the outboard. An estimate is also shown of the concentration in the heat flux which occurs between the values on the surface and at the tube inner wall.

With the heat loadings evaluated, the coolant conditions are determined by the requirements of obtaining an adequate safety factor on critical heat flux, and allowing the heat deposited into the divertor target cooling loop to be removed via a heat exchanger with the inlet coolant for the blanket. Additional constraints were that the coolant velocity should not exceed 20 m/s and that its composition should be the same as for the blanket, namely, a lithium atom percentage of 6.4%. These considerations led to the selection of the following outlet conditions: temperature 345°C, pressure 14 MPa. At this pressure the 6.4% $LiNO_3$ solution boils at 405°C [7], yielding a sub-cooling at the outlet conditions of 60°C, and a critical heat flux of $16.2\,\mathrm{MW/m^2}$ as predicted by the Jens and Lottes correlation. The curve of critical heat flux on Figure 3 indicates that the CHF exceeds the

estimated heat flux into the coolant by a factor of more than 1.4 (the typical design safety factor for water-cooled systems) at all points on the target. On the outboard target, where the heat fluxes are lower, the minimum safety factor is $\sim$ 1.8. The slight fall in the CHF is due to the reduction in sub-cooling as the coolant temperature rises along the tube.

The inlet-to-outlet coolant temperature rise is about 7°C. To maintain a minimum temperature difference of 20°C in the heat exchanger between the divertor coolant and the 298°C inlet blanket coolant, the divertor coolant inlet temperature must be not less than 318°C. This permits four passes of the divertor coolant across the target.

4. THERMAL AND STRUCTURAL ANALYSIS

4.1 Thermal Analysis

A detailed finite element thermal analysis was performed for one half of a coolant tube and the associated armor using the model shown in Figure 4. This should be accurate because the thickness of the divertor is much less than the distance over which the surface heat flux changes appreciably (Figure 3). The heat flux was assumed to be uniform over the plasma-facing surface and the lines of symmetry or the sides were taken to be adiabatic. As for the global analysis, the heat transfer coefficient at the interface between the tube wall and the coolant was taken to be the greater of the two coefficients calculated from subcooled flow boiling and forced flow convection correlations.

The results of this analysis showed that for the case when tubes are touching, the peak temperature, located at the surface, midway between two neighboring tubes, is 762°C. A crucial aspect of this thermal analysis is the maximum local heat flux into the coolant, which must be well below the critical heat flux of $\sim 16\,\mathrm{MW/m^2}$. The maximum local heat flux is greater than the nominal surface heat flux of $7.5\,\mathrm{MW/m^2}$ for two reasons:

1. The area available for transfer into the coolant is less than the area facing the plasma. Assuming that only about 65° of the inner wall on either side of the apex actually conducts heat into the coolant (as indicated by the finite element calculations), this effect would amplify the peak heat flux to over $8\,MW/m^2$.

2. The heat tends to flow into the coolant along radial paths, rather than flowing perpendicular to the plasma-facing surface, thus concentrating the heat flux towards the apex of the tube.

   These factors lead to a peak heat flux into the coolant of $10.7\,MW/m^2$.

At the point of maximum heat flux, there is a small gap of about 0.4 mm between neighboring tubes, because of the curvature of the divertor plate. This increases the maximum heat flux into the coolant to $10.9\,MW/m^2$ and the peak temperature to 779°C.

4.2 Stress Analysis

As with the thermal analysis, the boundary conditions and global deformations have little effect on the pressure stresses in the divertor. Hence, the detailed model used previously can be used to calculate the primary stresses induced by the 14 MPa coolant pressure. The peak stress is 83 MPa and there is some bending in the tube wall, thus increasing the peak primary stress above the expected value of 56 MPa ($\sigma \approx pr/t$). Also, the primary stress in the plasma-facing surface, which will be shown to be the location of the peak thermal stress, is essentially zero.

Because the coolant flow in TITAN-II is toroidal, there is no poloidal axisymmetry in the structures and the detailed model used for the thermal analysis cannot be used for the analysis of thermal stresses, which depend dramatically on the imposed boundary conditions. Fortunately, the coolant tubes themselves have little effect on the thermal stress distribution, as indicated by preliminary analyses, so an axisymmetric model can be used to approximate the structural behavior of the

divertor. This allows accurate treatment of the boundary constraints using a two-dimensional, axisymmetric model, without a prohibitive loss of detail.

One half of the divertor target length was modeled for the finite element analysis of the thermal stresses, with 600 axisymmetric quadrilateral elements, and using symmetry conditions to model the other half. The heat flux was distributed along the surface of the divertor according to Figure 5, and a constant heat transfer coefficient of 200 kW/m^2 was assumed along the entire inner surface. The coolant bulk temperature was assumed to be 345°C.

The surfaces stresses, which represent the peak equivalent stresses along the arc-length, are shown in Figure 5. The maximum equivalent stress, which occurs at the same location as the peak temperature, is 505 MPa. Since the pressure stress at this point is zero, the allowable stress at this location is $3\,S_{mt}$, which is estimated to be 600 MPa for the W-26Re alloy [10]. This indicates that the TITAN-II divertor can withstand the very high heat fluxes expected during normal operation.

5. FABRICATION

Various procedures have been considered for the fabrication of the divertor target. As mentioned above, the toroidal/radial orientation of the coolant flow results in tubes of constant cross-section touching only at one location. Methods of manufacturing tubes of varying cross-section, by hydroforming, or by chemical vapor deposition on to specially-shaped mandrels [1], have been examined, but the reference design is based on the use of tubes of constant cross-section, as the thermal penalties associated with this approach appear manageable.

Powder metallurgy techniques are used to manufacture a 1 mm thick W-26Re plate, which is then bent into the desired shape. A numerically-controlled milling procedure is used to form grooves in the plate for the coolant channels. The W-26Re coolant tubes (which are themselves manufactured using powder metallurgy) are then brazed into the grooves, using a CuPd18 braze alloy [10] (application

temperature $\sim$ 1100°C). The ends of the W-26Re tubes are then interconnected by brazing them to poloidal headers at the inlet and outlet.

An alternative procedure is to use chemical vapor deposition (CVD) to deposit the armor on to the bank of coolant tubes. The resulting surface must be ground to produce the necessary smooth surface. This method of fabrication requires the development of large CVD furnaces which allow uniform deposition rates to be retained.

6. CONCLUSIONS

At the present level of analysis, the TITAN toroidal-field divertor design appears to represent a feasible design approach for the impurity control and particle removal system for a high-power-density RFP reactor. Operation in the radiation-dominated régime with an "open" divertor geometry and careful shaping of the divertor target surface are necessary features to limit the peak heat flux on the divertor plate to $\sim 7.5\,\mathrm{MW/m^2}$.

The TITAN-II divertor target plate is constructed from a single material, a tungsten-rhenium alloy, for both the armor and coolant tubes, to avoid stress concentrations which arise at the interface between different materials. Careful shaping of the target restricts the peak equivalent thermal stress to $\sim$ 500 MPa. The coolant is an aqueous $LiNO_3$ solution, as used for the blanket, which appears to offer the advantage of high critical heat fluxes, because of the changed physical and thermal properties compared with pure water.

ACKNOWLEDGEMENT

Work supported in part by the United States Department of Energy under Contract No. DE-FG03-86ER52126.

REFERENCES

1. F. Najmabadi, R. W. Conn, S. P. Grotz, N. M. Ghoniem, *et al.*, "The TITAN Reversed Field-Pinch Fusion Reactor Study : Final Report", Joint Report of UCLA, GA Technologies Inc., Los Alamos National Laboratory and Rensselaer Polytechnic Institute, UCLA-PPG-1200 (March 1988).

2. P. I. H. Cooke *et al.*, "Divertor Design for the TITAN Reversed-Field-Pinch Reactor", Proc. 12th Symposium on Fusion Engineering, Monterey, CA, October 1987, to appear.

3. F. Najmabadi, N. M. Ghoniem, R. W. Conn *et al.*, "The TITAN Reversed Field-Pinch Fusion Reactor Study : Scoping Phase Report", Joint Report of UCLA, GA Technologies Inc., Los Alamos National Laboratory and Rensselaer Polytechnic Institute, UCLA-PPG-1100 (January 1987).

4. M. M. Pickrell, J. A. Phillips, C. J. Buchenauer, T. Cayton, J. N. Downing *et al.*, "Evidence for a Poloidal Beta Limit on ZT-40M", *Bull. Am. Phys. Soc.*, **29**, (1894) 1403.

5. A. K. Prinja, P. I. H. Cooke, E. L. Vold *et al.*, "Edge Plasma Analysis for the TITAN Reversed-Field-Pinch Reactor", Proc. 12th Symposium on Fusion Engineering, Monterey, CA, October 1987, to appear.

6. C. Copenhaver, R. A. Krakowski, N. M. Schnurr, R. L. Miller, C. G. Bathke, R. L. Hagenson *et al.*, "Compact Reversed-Field-Pinch Reactors (CRFPR) — Fusion Power Core Integration Study", Los Alamos National Laboratory Report, LA-10500-MS (August 1985).

7. P. I. H. Cooke, S. P. Grotz, M. Z. Hasan, R. Martin, S. Sharafat, D. K. Sze, C. P. C. Wong *et al.*, "Properties of Concentrated Aqueous Lithium Nitrate Solutions and Applications to Fusion Reactor Design", Proc. International Symposium on Fusion Technology, Tokyo, April 1988, to appear.

8. J. G. Collier, "Convective Boiling and Condensation" (McGraw-Hill, London, 1972) pp.159-160.

9. W. H. Jens and P. A. Lottes, "Analysis of Heat Transfer, Burnout, Pressure Drop and Density Data for High Pressure Water", USAEC Report, ANL-4627 (1951).

10. Metallwerk Plansee GmbH, "Tungsten-Rhenium Alloys", in *Refractory Metals and Special Metals*, PLANSEE, 1987.

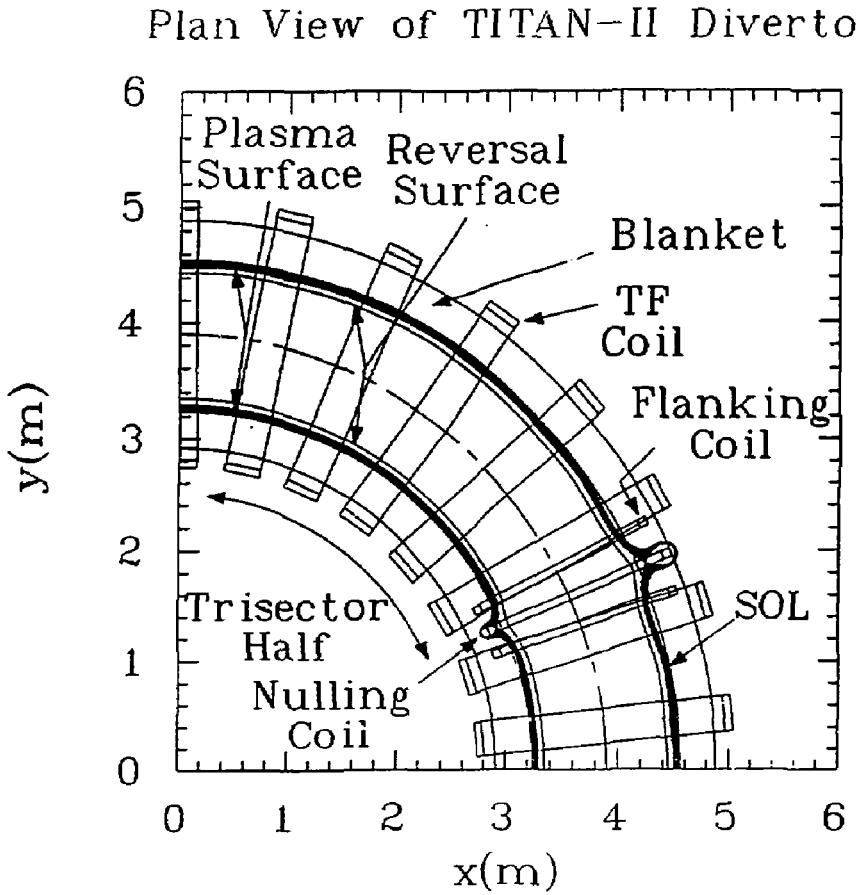

Figure 1. Equatorial plane view of divertor coils and magnetic field lines for TITAN-II.

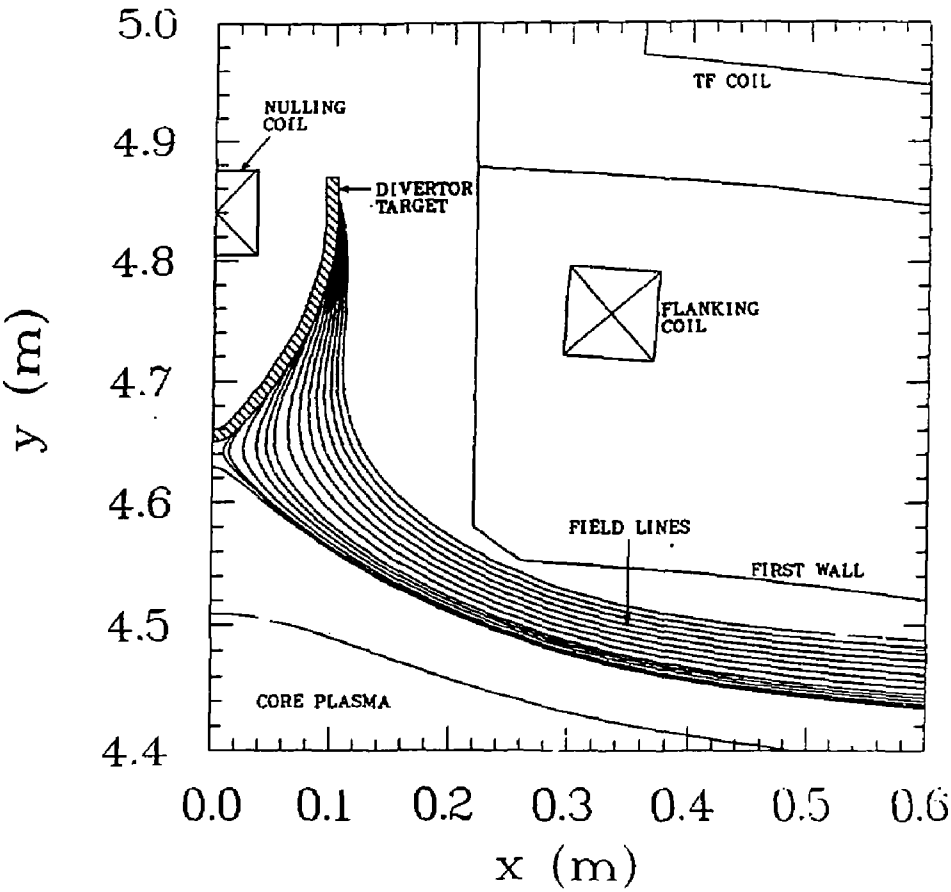

Figure 2. Equatorial plane view of outboard divertor region for TITAN-II.

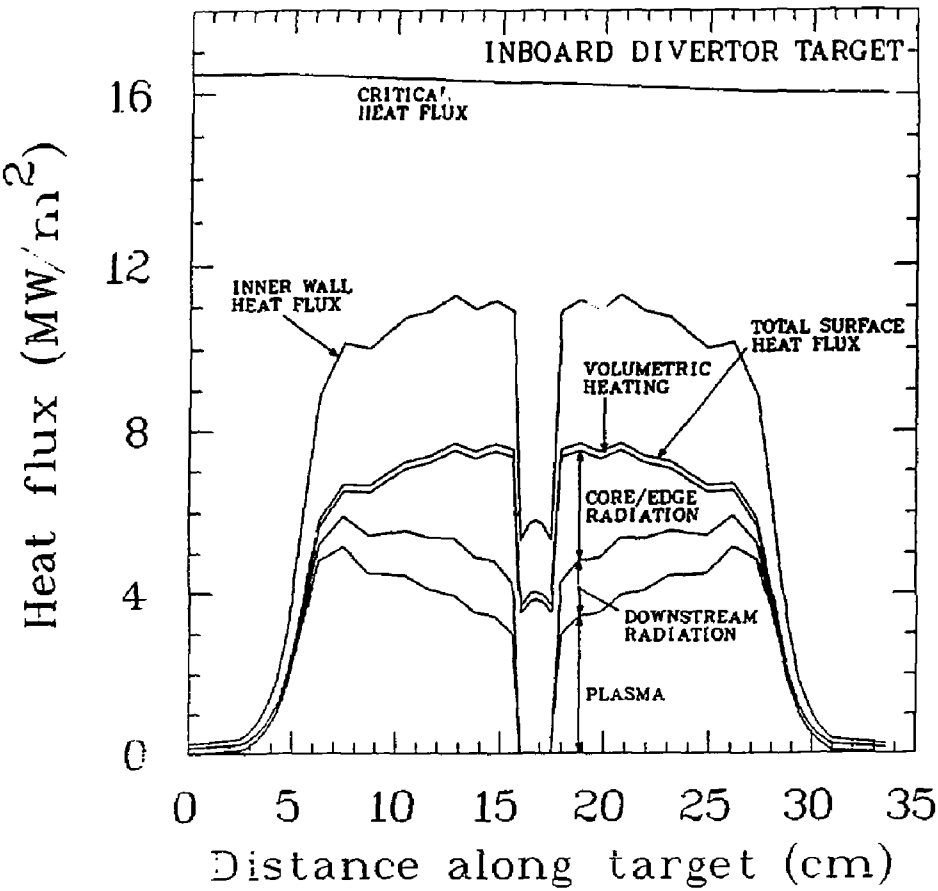

Figure 3. Heat flux distribution on inboard section of divertor target. Distance along target is measured in the direction of coolant flow.

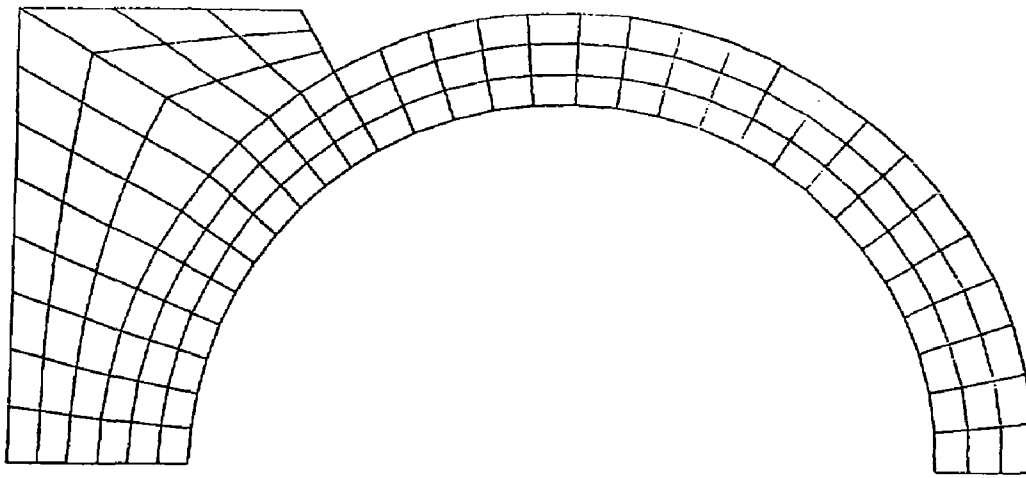

Figure 4. Model used for finite element analysis of temperatures and pressure stresses.

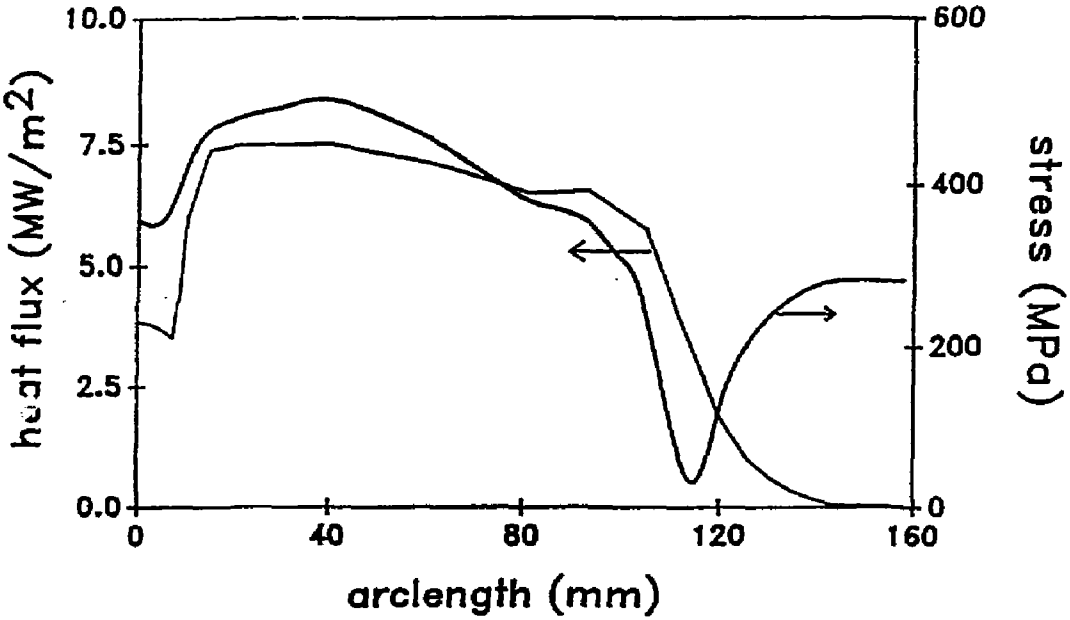

Figure 5. Heat flux and peak equivalent thermal stress distributions along the arc-length of the divertor.

PROPERTIES OF CONCENTRATED AQUEOUS LITHIUM NITRATE SOLUTIONS AND APPLICATIONS TO FUSION REACTOR DESIGN

P. I. H. Cooke[1], S. P. Grotz, M. Z. Hasan, R. Martin, S. Sharafat, D.-K. Sze[2] and C. P. C. Wong[3] for the TITAN Research Group,

Department of Mechanical, Aerospace and Nuclear Engineering
and Institute for Plasma and Fusion Research,
University of California at Los Angeles,
Los Angeles, *CA 90024-1597, USA.*

ABSTRACT

Aqueous solutions of Li-containing compounds have been proposed to serve as the combined tritium breeding material and coolant for fusion reactors. The salt used for the TITAN-II reversed-field-pinch reactor design is $LiNO_3$, which was chosen for its good neutronics properties, relatively good corrosion characteristics, and for its high solubility in water. An extensive literature survey has shown that the physical and thermal properties of high-temperature, concentrated aqueous $LiNO_3$ solutions are markedly different from the pure water properties at similar conditions. These changes alter the heat transfer performance of the coolant, and the critical heat flux is estimated to rise for sub-cooled flow boiling, while the heat transfer coefficient for forced convection falls. Another important result is the elevation in boiling point, which may allow the operating pressure of the primary coolant to be reduced to a value below that of the secondary steam circuit, preventing leakage of the tritiated coolant into the steam circuit. Further research is needed into corrosion and radiolysis issues, but the available data imply that careful control of the coolant chemistry can minimize the problems.

---

[1] *Permanent address: UKAEA Culham Lab., Abingdon, Oxon OX14 3DB, UK.*
[2] *Argonne National Lab., 9700 South Cass Avenue, Argonne, Illinois 60439, USA.*
[3] *GA Technologies Inc., P. O. Box 85608, San Diego, CA 92138 USA.*

1. INTRODUCTION

The use of aqueous solutions of Li-containing compounds as the combined tritium-breeding material and coolant was proposed by Steiner [1]. Since that time, various studies [2-6] of the concept have been made, examining such issues as the neutronics and tritium-breeding performance of such a blanket, and the corrosion and compatibility of structural materials with the solution. The simplicity of this concept led to its selection as one of the two blanket designs considered for the TITAN Reversed-Field Pinch reactor [7]. The salt used for the TITAN-II design is $LiNO_3$, which was chosen for its good neutronics properties, relatively good corrosion characteristics compared with other candidate salts, and for its high solubility in water. To allow an efficient energy conversion cycle, the blanket coolant operating temperature is around 300°C, similar to that in present-day Pressurized-Water Reactors (PWR). A relatively high salt concentration is used to reduce the amount of beryllium required for neutron multiplication purposes, and to reduce the required enrichment in ^{6}Li. This paper examines the changes in the physical and thermal properties of the salt solution compared with those of pure water.

2. THERMAL AND PHYSICAL PROPERTIES

In order to estimate the thermal and physical properties of $LiNO_3$ solutions at high temperatures, an extensive literature survey was made to find any relevant experimental data. Where such data were not available, and reasonable extrapolations were not possible, corresponding data for NaCl solutions were used, as the NaCl–H_2O system has been much more widely studied than any other solution, and many solutions of 1-1 electrolytes (such as NaCl, KBr, and $LiNO_3$) have similar properties at the same concentrations. It is expected that such estimates should be accurate to about 20% [8], which is adequate to allow a reasonable assessment of the thermal performance of the blanket to be made.

Results from this work are given in the following sections, with figures of the various properties as a function of temperature and salt concentration. While the

blanket design was being optimized, it proved convenient for the neutronics analysis to specify the salt concentration as the atomic percentage of Li atoms present, and the properties are presented in that manner here. A more detalied report of the properties of these solutions, including correlations as a function of temperature and concentration, is given in reference [7].

2.1 Density

Experimental data are available for the density of $LiNO_3$ solutions for temperatures up to 350°C and for concentrations from pure water to pure $LiNO_3$ [9,10]. These data are given in the form of a polynomial fit as a function of temperature and concentration for lower temperatures and concentrations, with tables of experimental results to cover the rest of the range. Figure 1 shows the density as a function of temperature for various values of the lithium atom percentage. A significant increase in density over the pure water value is apparent for the higher concentrations, the difference being a factor of about two for a lithium atom percentage of 8%.

One point of note arising from these papers is that the authors state that $LiNO_3$ and H_2O are completely miscible at temperatures above the melting point of $LiNO_3$ (253°C). This implies that there is effectively no upper limit to the salt concentration for high temperatures from solubility considerations.

2.2 Viscosity

Measurements of the viscosity of $LiNO_3$ solutions for temperatures up to 275°C and for concentrations up to 10 mol/kg ($\sim$ 4.5% Li) have been made [11,12]. A correlation for the viscosity of the solution relative to that of pure water as a function of concentration, with temperature-dependent constants, was also given. The fit was said to be valid only for mole fractions up to 0.1 ($m \sim 6$ mol/kg, or $A_{Li} \sim 3\%$), although it reproduces the experimental data well up to 10 mol/kg. The relative viscosity at a given concentration is almost constant with varying temperature at the high temperatures of relevance here. The correlation has therefore been applied

throughout the concentration and temperature ranges of interest, with the values of the temperature-dependent constants evaluated at 250°C. The results are given in Figure 2 and show a large increase in the relative viscosity for higher concentrations; the viscosity compared with that of pure water is larger by a factor of ~ 6 for the 8% $LiNO_3$ solution.

2.3 Specific Heat Capacity

No experimental measurements have been reported for the specific heat capacity of $LiNO_3$ solutions at high temperatures. Moreover, it is difficult to correlate this quantity simply with temperature because the specific heat capacity of pure water becomes infinite as the critical point (374°C and 22.1 MPa) is approached. As the addition of even small quantities of a salt changes the critical temperature and pressure quite significantly, the specific heat capacity of the solution can vary markedly from that of pure water at the same conditions. Wood and Quint have proposed a very simple and accurate way of estimating the specific heat capacity for aqueous salt solutions, using a "corresponding-states" method [13], in which the properties of the solution are approximated by the properties of water at the same "relative" conditions with respect to the critical points. This method requires knowledge of the critical temperature and pressure of the solution as a function of concentration, and as no measurements for $LiNO_3$ solutions are available, the extensive dataset for NaCl solutions [14] has been used, although a large extrapolation has been made from the NaCl data (≤ 6 mol/kg) for the most concentrated $LiNO_3$ solutions proposed. Measurements of critical values for various salt solutions [15] have shown that many 1-1 electrolytes have very similar critical temperatures at the same molality.

Figure 3 shows the estimated critical temperature and pressure for $LiNO_3$ solutions; these values have then been used to yield specific heat capacities as illustrated in Figure 4. A rapid increase in the critical temperature and pressure with increasing salt concentration is evident from Figure 3, although the large extrapolation

made for the higher concentrations makes these values rather uncertain. The possibility of operating an aqueous blanket at high temperatures (greater than 400°C) is suggested by the increase in critical temperature, if the higher pressures can be tolerated and if suitable materials can be found for these conditions.

Figure 4 shows an initial dramatic reduction in specific heat capacity as the salt is added to pure water, although there is little additional effect as the concentration is increased. The uncertainty associated with these estimates is high, especially for the higher concentrations. This is due not only to the extrapolation made for the critical properties of the solution, but also because the contribution due to the dissolved salt, which may be significant at high concentrations, has been ignored.

2.4 Boiling Point

Reference [16] reported measurements of the vapor pressure of $LiNO_3$ solutions for concentrations up to 24 mol/kg and for temperatures up to 110°C. The results showed that the relative vapor pressure (the ratio of the vapor pressure of the solution to that of pure water) for a given concentration remained approximately constant independent of changes in temperature. It has been assumed that this relationship is valid for higher temperatures, in the absence of relevant experimental data. Figure 5 shows these results for pressures ranging from 4 to 16 MPa, which indicate that the boiling point of the $LiNO_3$ solution should be significantly higher than for pure water. For a lithium atom percentage of 5% the increase is 40–50°C, which can have a major effect on the thermal design of the blanket as described below.

2.5 Discussion

Other properties of $LiNO_3$ solutions have also been examined, but the changes in properties relative to pure water tend to be smaller. The thermal conductivity of the solution is predicted to fall by about 10–15% compared with pure water, for the highest concentrations considered, based on data for NaCl solutions. These

properties indicate that the Prandtl number of the solution is higher than for pure water, the increase being a factor of $\sim$ 1.8 for a 5% lithium concentration. Room temperature data on the surface tension of $LiNO_3$ solutions suggest a relative increase of about 15–20% for a lithium atom percentage of 5%.

The above estimates of the properties of $LiNO_3$ solutions at high temperatures clearly show the need to consider the exact coolant conditions proposed in designing the blanket, because of the marked differences from the properties of pure water. However, many of the estimates are extrapolations from experimental data or have been obtained from the results for other salt solutions. Although these predictions should give good indications of the trends to be expected for the various properties, a much expanded experimental database is required for the salts and conditions proposed before the thermal performance of an aqueous salt blanket at high temperature can be confidently predicted.

3. APPLICATIONS TO REACTOR DESIGN

3.1 Heat Transfer

The differences in the properties of the $LiNO_3$ solution compared with pure water affect the heat transfer performance of the coolant. The TITAN-II design, which uses a $LiNO_3$ solution with a 6.4% lithium concentration as the primary coolant will be used to illustrate some of the changes.

The Dittus-Boelter correlation was used to assess the effect on the forced convection régime of heat transfer. For the TITAN-II concentration, and a coolant temperature of 300°C, the heat transfer coefficient is lower by about 50% for the aqueous solution than for water. The main factor in this reduction is the increase in viscosity, as the changes in density and specific heat capacity largely cancel out. This implies that the film temperature drop will be higher with the aqueous solution which will lead to higher channel-wall temperatures.

A potentially more important effect of the salt addition is on heat transfer in the subcooled flow boiling (SFB) régime. In the high-heat-flux components of a fusion reactor, such as the first wall, limiter and divertor plate, SFB heat transfer will be highly efficient and may be essential when water or an aqueous solution is used as the coolant. Experimental data on boiling heat transfer with aqueous solutions are extremely limited, but because of the elevation of boiling point, the incipience of boiling may be delayed for aqueous solutions. The heat transfer coefficient for SFB is thus expected to be somewhat reduced, but since the film temperature drop in SFB is small, this effect will not be of major consequence to the thermal-hydraulic design.

A significant improvement in SFB is expected to be in the form of an increase in the critical heat flux (CHF). Sources cited in reference [17] report that the CHF increases by as much as 40% for an aqueous solution of ethanol as compared with water. In the absence of a correlation for the critical heat flux for aqueous $LiNO_3$ solutions, the correlation by Jens and Lottes [18] for water was used for TITAN-II. This correlation is of the form

$$q''_{CHF} = K(\rho v)^m \Delta T_{sub}^{0.22}$$

where the constants K and m are functions of pressure, ρ and v are the coolant density and velocity, respectively, and ΔT_{sub} is the sub-cooling. For the same coolant velocity, sub-cooling, and pressure, the increase in CHF over the pure water value ranges from $\sim$ 15% to 25%, for pressures of 7 to 14 MPa. However, if the coolant inlet and outlet temperature are kept fixed to match to a given steam cycle, then the velocity of the aqueous solution coolant must be greater than that for pure water, because of the reduction in thermal capacity. With this increase in coolant velocity, which was included for TITAN-II, the CHF increases further, to 30% to 60% above the water value. The higher values of CHF provide a greater safety margin and allow higher heat fluxes to be tolerated in the design.

To take advantage of the elevation in boiling point of the aqueous salt solution, a higher exit temperature can be used at the same pressure as that for water, or, if the exit temperature is kept the same, the pressure of the aqueous solution coolant can be greatly reduced. The implications of the latter approach for the power cycle are discussed in the next section. If the same temperature rise is used for water and the aqueous solution, the volume flow rate and flow velocity will be higher for the aqueous solution because of its lower thermal capacity, as observed above. As a result, the pressure drop and pumping power for coolant circulation will be higher with the aqueous salt solution as the primary coolant.

3.2 Primary Coolant Conditions

One of the problems associated with the PWR arises from the large pressure difference between the primary coolant and the steam. Since the primary coolant has to have a higher temperature than the steam, this large pressure difference (about 7 MPa) cannot be avoided, and can cause leaks of the activated primary water across the steam generator tubing. Also, stress corrosion is potentially a serious problem in the steam generator. For an aqueous solution blanket, the leakage can be particularly troublesome because of the high tritium concentration in the primary coolant.

As discussed in Section 2.4, the presence of the $LiNO_3$ increases the boiling point of the solution at a constant pressure. If the coolant temperature is maintained constant, then the operating pressure can be reduced, and it is possible that the steam pressure can become slightly higher than that of the primary coolant. For typical PWR conditions, the water exit temperature is 330°C and the steam pressure is 7.3 MPa. To equalize the pressure of the primary coolant and the steam, a lithium atom percentage of 6.4% is required, as can be seen from Figure 5. This concentration is not unreasonable as tritium breeding considerations suggest a concentration of about 5%. The primary benefit for such a system is that all leakage at the steam generator can be made inward, *i.e.*, from the steam side to the primary

coolant side. The tritium leakage problem can thus be substantially alleviated, and the requirement for an intermediate heat exchanger is avoided, although tritium permeation is not affected. Another important gain is that the steam generator can be stress free, improving its reliability.

Another possible operational scenario is to operate the aqueous solution at a higher temperature. For a pressure of 16.5 MPa and a lithium concentration of 5%, the saturation temperature of the solution is about 400°C, allowing superheated steam of 16.5 MPa and 380°C to be generated. This steam condition can yield a gross thermal efficiency of 38.5%, which is 3.5 points higher than the PWR technology, without a significant increase in pressure on the primary side. Further, the coolant temperature rise of the primary coolant can be about 120°C, compared with 40°C for a PWR. Therefore, the coolant flow rate will be reduced by a factor of three, significantly reducing the cost of the primary loop, as well as the size and the capacity of the pump.

3.3 Corrosion and Radiolysis

Steels in contact with aqueous solutions can suffer from two forms of corrosion attacks. One is a uniform or localized corrosion process which may leave the surface clean or coated with corrosion products, the other is stress-corrosion cracking (SCC). During SCC a metal is virtually unaffected over most of its surface while fine cracks progress through it. Corrosion processes are electrochemical in nature and thus strongly depend on the choice of material and characteristics of the medium.

Investigations of SCC in ferritic steels in boiling nitrate solutions [19] indicate that the potency of $LiNO_3$ lies between that of NH_4NO_3 and that of $NaNO_3$. There is a marked reduction in the threshold stress to failure as the concentration of the solution increases. Crack initiations appear to be accelerated under acidic conditions, and additions of NaOH to $NaNO_3$ solutions increase the time to failure [19–22]. However, for $Ca(NO_3)_2$ solutions, the time to failure is maximized

at a pH of about 4 [19]. It is clear that careful control of the pH, perhaps by adding LiOH, is necessary for $LiNO_3$ solutions.

Oxidizing agents tend to accelerate crack formation while compounds, such as Na_2CO_3, H_3PO_2, Na_2HPO_4 and $CO(NH_2)_2$, that form insoluble iron products retard failure [21]. Since oxidizing agents reduce the formation of radiolytic decomposition products, an optimum level of oxidizer additions may exist.

No specific corrosion problems have been reported for austenitic stainless steels in the presence of nitrate solutions [6]. The threshold stress to cause failure decreases with increasing nitrate concentration, and the time to failure decreases with increasing temperature. The aggressiveness of nitrates with choice of cation decreases in the order NH_4, Ca, Li, K and Na, and at a pH above 7 to 8 the susceptibility of steel to SCC diminishes.

Radiolytic decomposition of water molecules arises under high levels of ionizing radiation, such as γ-rays, neutrons, α-particles and tritium recoil ions (from (n,α) reactions with lithium). For gamma-irradiation of highly-concentrated $LiNO_3$ solutions, the H_2 yields are very small and the H_2O_2 yield decreases by a factor of about 3 relative to pure water [23,24]. The oxygen production due to α-particle radiation increases, while the yields of H_2, H_2O_2, H, OH, HO_2 all decrease with increasing salt concentration [25]. The limited data suggest that neither the light nor the heavy particle radiation of a highly concentrated $LiNO_3$ salt solution leads to high levels of radiolytic decomposition products, except for the formation of oxygen. In fact, an increase of salt concentration leads to a decrease in the production of H_2O_2, H_2, H, OH, and HO_2 and a slight increase in NO_2^- yields relative to highly diluted salt solutions [6]. Experience gained in the fission industry with pure water suggests that the stability of non-boiling water to radiolysis improves at elevated temperatures, due to an increase in the recombination rates of radicals [26].

In conclusion, although many uncertainties remain and much research is required in the area of radiolysis, the use of a highly concentrated aqueous $LiNO_3$

salt solution should not lead to the formation of volatile or explosive gas mixture. The effects of radiolytic decomposition products on corrosion, however, will remain a subject of great uncertainty until an experimental data base in a fusion environment becomes available.

4. CONCLUSIONS

An extensive literature survey has shown that the physical and thermal properties of high-temperature, concentrated aqueous $LiNO_3$ solutions, which have been proposed for the coolant and tritium breeding medium of fusion reactors, are markedly different from the pure water properties at similar conditions. For a lithium atom percentage of 5% and a temperature of 300°C, it is estimated that the density increases by $\sim$ 50%, the viscosity increases by a factor of more than 3, and the specific heat capacity falls by about 55%, while the boiling point at a pressure of 10 MPa increases by $\sim$ 45°C, compared with the values for pure water. As there is a large uncertainty associated with many of these estimates, because of the lack of data for the conditions of interest, an experimental program to provide this information would be of value.

The changes in properties compared with pure water lead to differences in the heat transfer performance, in particular, the critical heat flux is estimated to rise for sub-cooled flow boiling, while the heat transfer coefficient for forced convection falls. Again experimental data are required for heat transfer in aqueous solutions of lithium salts. The elevation in boiling point of the solution may allow the operating pressure of the primary coolant to be reduced to a value below that of the secondary steam circuit, without adjusting the temperature in either loop. Leakage of the tritiated coolant into the secondary circuit through the steam generator should thus be prevented, avoiding the requirement for an intermediate heat exchanger. More data are required for a complete assessment of corrosion issues for structural materials exposed to the $LiNO_3$ solutions, but no specific problems have been observed, and careful control of the pH should minimize attack. Further research

is also needed on radiolysis problems, but the available data imply that high levels of decomposition products should not occur.

ACKNOWLEDGEMENT

Work supported in part by the United States Department of Energy under Contract No. DE-FG03-86ER52126.

REFERENCES

1. D. Steiner *et al.*, "A Self-Cooled, Heavy Water Breeding Blanket", Proc. 11th Symp. on Fus. Eng., Austin, Texas, November 1985, pp. 539–543.

2. D. Steiner *et al.*, "Applications of the Aqueous Self-Cooled Blanket Concept", *Fus. Tech.* **10** (1986) 641–646.

3. M. J. Embrechts *et al.*, "Neutronics Analysis for Aqueous Self-Cooled Blankets", *Fus. Tech.* **10** (1986) 1443–1448.

4. D. A. O'Brien *et al.*, "First Wall Structural Analysis for Aqueous Self-Cooled Blanket Concept", *Fus. Tech.* **10** (1986) 1611–1616.

5. M. J. Embrechts *et al.*, "Tritium Breeding Performance of a Self-Cooled Water Based Blanket", *Nucl. Eng. & Des.* **4** (1987) 211–222.

6. W. F. Bogaerts, M. J. Embrechts and R. Waeben, "Application of the Aqueous Self-Cooled Blanket Concept to a Tritium Producing Shielding Blanket for NET", NET Report No. 75 (October 1987).

7. F. Najmabadi, R. W. Conn, S. P. Grotz, N. M. Ghoniem, *et al.*, "The TITAN Reversed Field-Pinch Fusion Reactor Study : Final Report", Joint Report of UCLA, GA Technologies Inc., Los Alamos National Laboratory and Rensselaer Polytechnic Institute, UCLA-PPG-1200 (March 1988).

8. R. H. Wood, University of Delaware, Newark, personal communication, August 1987.

9. L. V. Puchkov and V. G. Matashkin, "Densities of $LiNO_3$–H_2O and $NaNO_3$–H_2O Solutions at Temperatures in the Range 25 – 300°C", *J. Appl. Chem. USSR* **43**, (1970) 1848.

10. L. V. Puchkov, V. G. Matashkin and R. P. Matveeva, "Density of Aqueous Lithium Nitrate Solutions at High Temperatures (up to 350°C) and Concentrations", *J. Appl. Chem. USSR* **52**, (1979) 1167.

11. L. V. Puchkov and P. M. Sargaev, "Viscosities of Lithium, Sodium, Potassium, and Ammonium Nitrate Solutions at Temperatures up to 275°C", *J. Appl. Chem. USSR* **46**, (1973) 2367.

12. L. V. Puchkov and P. M. Sargaev, "Dependence of Viscosity of Electrolyte Solutions on Temperature and Concentration", *J. Appl. Chem. USSR* **47**, (1974) 280.

13. R. H. Wood and J. R. Quint, "A Relation between the Critical Properties of Aqueous Salt Solutions and the Heat Capacity of the Solutions near the Critical Point using a Single-Fluid Corresponding-States Theory", *J. Chem. Thermodynamics* **14**, (1982) 14.

14. S. Sourirajan and G. C. Kennedy, "The System H_2O–NaCl at Elevated Temperatures and Pressures", *Am. J. Sci.* **260**, (1962) 115.

15. W. L. Marshall and E. V. Jones, "Liquid-Vapor Critical Temperatures of Aqueous Electrolyte Solutions", *J. Inorg. Nucl. Chem.* **36**, (1974) 2313.

16. G. A. Sacchetto, G. G. Bombi and C. Macca, "Vapor Pressure of very Concentrated Electrolyte Solutions", *J. Chem. Thermodynamics* **13**, (1981) 31.

17. R. D. Boyd, C. P. C. Wong and Y. S. Cha, "Technical Assessment of Thermal Hydraulics for High-Heat-Flux Fusion Components", Sandia National Labortory Report, SAND84-0159, (1985).

18. W. H. Jens and P. A. Lottes, "Analysis of Heat Transfer, Burnout, Pressure Drop and Density Data for High Pressure Water", USAEC Report, ANL-4627 (1951).

19. R. N. Parkins,"Environmental Aspects of Stress Corrosion Cracking in Low Strength Ferritic Steels", in Stress Corrosion Cracking and Hydrogen Embrittlement of Iron Base Alloys, Conference held at Unieux-Firminy France, June 12-16, 1973.

20. P. L. Andresen, " The Effects of Aqueous Impurities on IGSCC of Sensitized Type 304 Stainless Steel", EPRI Contract T115-3, Final Report N. NP-3384, Electric Power Research Institute, Palo Alto, California, November 1983.

21. R. N. Parkins and R. Usher, Proc. 1st Int. Congr. Metallic Corrosion, 1961, p.289, (London, Butterworths).

22. Z. Szklarska-Smialowski, *Corrosion*, 20, 198t, 1964.

23. M. Daniels,"Radiolysis and Photolysis of the Aqueous Nitrate System",in *Radiation Chemistry*, Vol. 1, Ed. R. F. Gould, *Am. Chem. Soc.*, Washington D. C., 1968.

24. J. T. Kiwi and M. Daniels, "On the radiolysis of concentrated alkaline and calcium-nitrate solutions", *J. Inorg. Nucl. Chem.*, Vol. 40, 1978, pp.576-579,

25. M. Burton and K. C. Kurien, *J. Phys. Chem.* 63 (1959) 899.

26. P. Cohen, in "Water Coolant Technology of Power Reactors", American Nuclear Society, 1980.

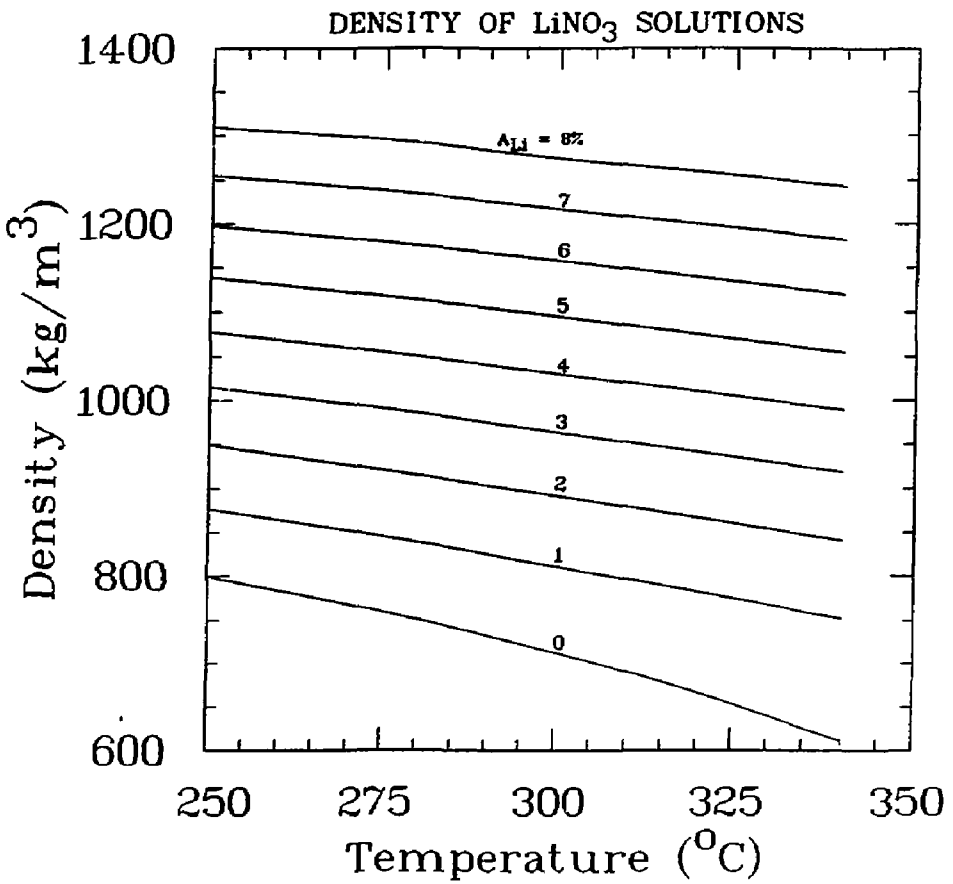

Figure 1. Density of $LiNO_3$ solutions at various temperatures and for a range of lithium atom percentages.

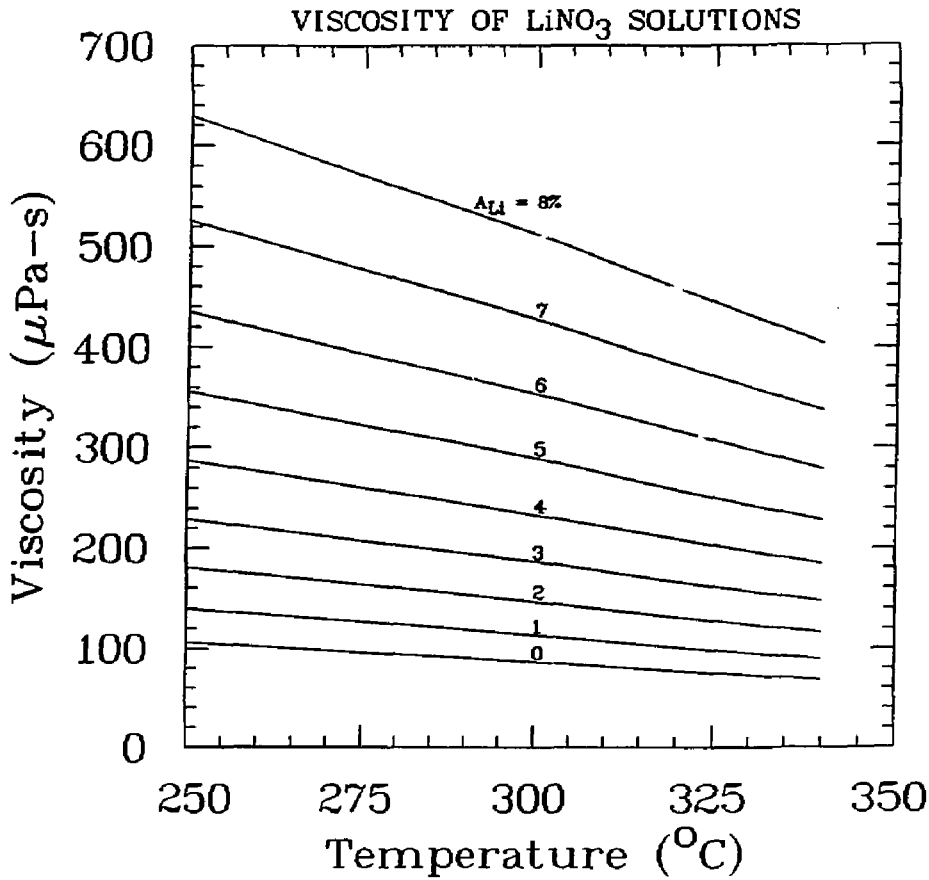

Figure 2. Viscosity of $LiNO_3$ solutions at various temperatures and for a range of lithium atom percentages.

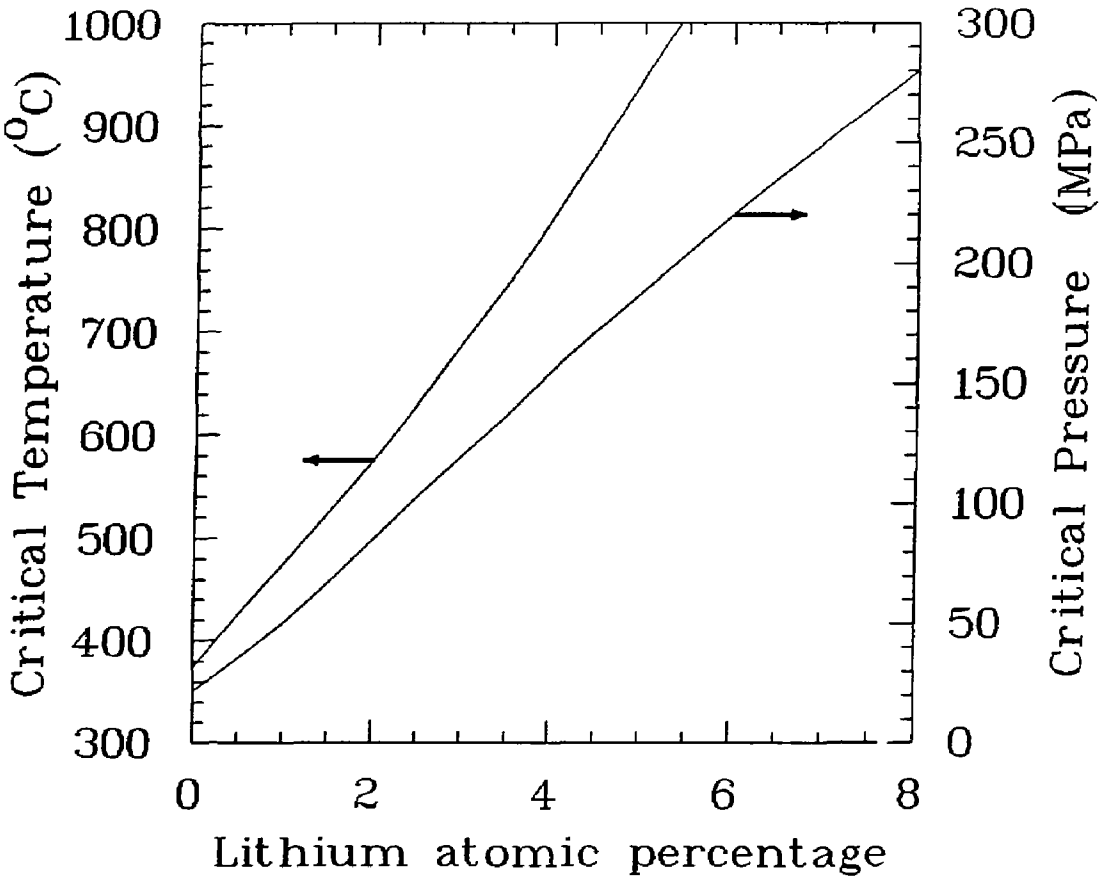

Figure 3. Critical temperature and pressure for $LiNO_3$ solutions as estimated from measurements for NaCl solutions.

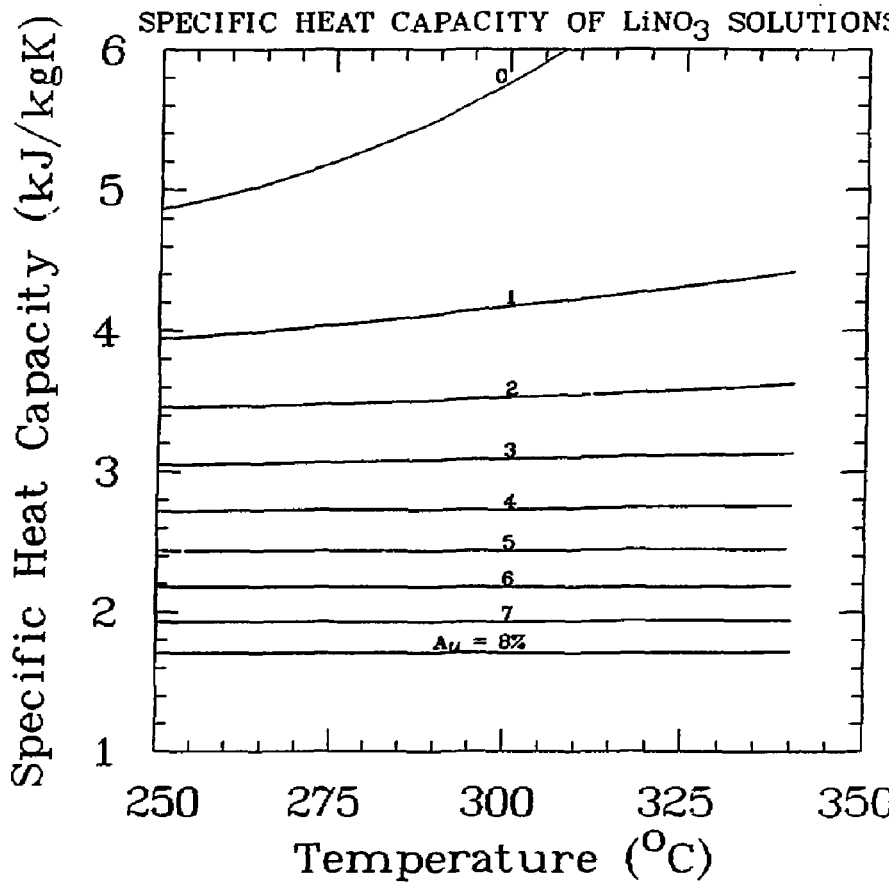

Figure 4. *Specific heat capacity of $LiNO_3$ solutions at various temperatures and for a range of lithium atom percentages.*

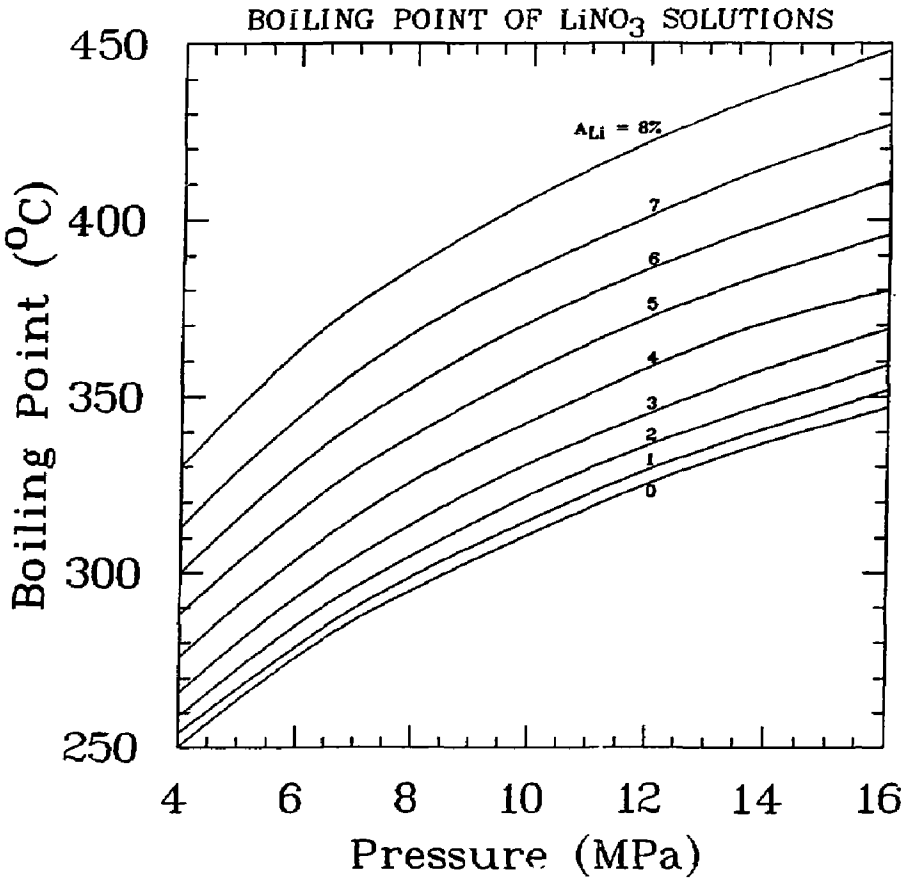

Figure 5. Boiling temperatures of $LiNO_3$ solutions at various pressures and for a range of lithium atom percentages.